



AMERICAN UNIVERSITY OF BEIRUT

BODY COOLING METHODS FOR IMPROVING ENDURANCE  
IN HOT ENVIRONMENTS AT MINIMAL ENERGY

by  
MARIAM MOUNIR ITANI

A dissertation  
submitted in partial fulfillment of the requirements  
for the degree of Doctor of Philosophy  
to the Department of Mechanical Engineering  
of the Maroun Semaan Faculty of Engineering and Architecture  
at the American University of Beirut


Beirut, Lebanon  
September 2018

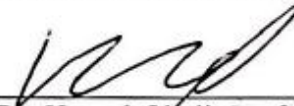
AMERICAN UNIVERSITY OF BEIRUT

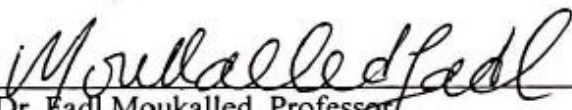
BODY COOLING METHODS FOR IMPROVING ENDURANCE  
IN HOT ENVIRONMENTS AT MINIMAL ENERGY

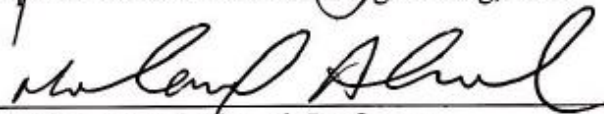
by  
MARIAM MOUNIR ITANI

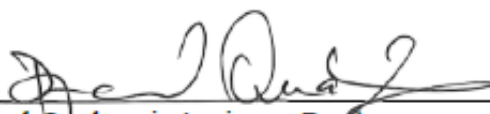
Approved by:

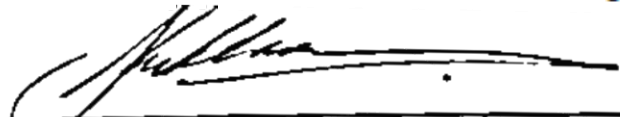
  
\_\_\_\_\_  
Dr. Nesreen Ghaddar, Professor  
Department of Mechanical Engineering, AUB  
Advisor

  
\_\_\_\_\_  
Dr. Kamel Ghali, Professor  
Department of Mechanical Engineering, AUB  
Member of Committee

  
\_\_\_\_\_  
Dr. Fadl Moukalled, Professor  
Department of Mechanical Engineering, AUB  
Member of Committee

  
\_\_\_\_\_  
Dr. Mohammad Ahmad, Professor  
Department of Chemical and Petroleum Engineering, AUB  
Member of Committee

  
\_\_\_\_\_  
Dr. Djamel Ouahrani, Assistant Professor  
Department of Architecture and Urban Planning, Qatar University  
Member of Committee

  
\_\_\_\_\_  
Dr. Kalev Kuklane, Associate Professor  
Department of Design Sciences, Lund University  
Member of Committee

Date of dissertation defense: September 12, 2018



## ACKNOWLEDGMENTS

I would like to thank my advisor Dr. Nesreen Ghaddar and co-adviser Dr. Kamel Ghali for their guidance and support throughout my research work. I had the chance to benefit from their research experience and critical thinking. I would also like to thank the members of my dissertation committee: Dr. Fadl Moukalled, Dr. Mohammad Ahmad, Dr. Djamel Ouahrani and Dr. Kalev Kuklane, for their valuable comments and recommendations and the faculty members and staff of the Mechanical Engineering Department at the American University of Beirut for their help in the achievement of this work. Furthermore, I would also like to thank the co-authors of this work Dr. Beatrice Khater and Dr. Walid Chakroun.

I would also like to acknowledge the support of my colleagues and friends at the American University of Beirut who motivated me to achieve my goal: Douaa Al Assaad, Nagham Ismail, Albert Touma, Rana Bachnak, Manar Younis, Asmaa Jrad, Rasha Seblany, Farah Mneimneh, Safaa Khalil, Jinane Charara, Hanin Hamdan, Jessica Daaboul, Hussein Daoud, Mohamad Mahdi Allouche, Abed El Kader Saidi, Ragheb Raad, Walid Abou Hweij, Mohammad Hout.

Special thanks to my family; my sisters and my parents. Your presence has always been a source of joy and inspiration in my life. Words cannot express how appreciative I am for your help and care. Mom and Dad, thank you for always being there by my side and thank you for all the sacrifices that you have made on my behalf.

## AN ABSTRACT OF THE DISSERTATION OF

Mariam Mounir Itani for Doctor of Philosophy  
Major: Mechanical Engineering

Title: Body Cooling Methods for Improving Endurance in Hot Environments at Minimal Energy

Personal cooling vests that incorporate phase change material (PCM) have been used to improve thermal sensation of people working outdoors in different fields (firefighting, construction, military, police, etc.). It is proposed in this study to investigate by modeling and experimentation the effect of applying different strategies to enhance the cooling effect of PCM vests and comfort of workers through: 1) targeting torso sensitive areas that trigger comfort; 2) using two PCM melting temperatures in one cooling vest and the possibility of reducing vest weight and 3) applying a two-bout strategy while reducing energy use, carried weight and material cost. A fabric-PCM model is developed and integrated with a bio-heat model to predict human thermal responses and comfort levels. Experiments on human subjects are done to validate the predictions of the integrated model and perform simulations to improve the PCM vest performance and apply the different proposed strategies.

Since the PCM cooling vests have some disadvantages that involve the risk of condensation at their low temperature surface and the hindrance of moisture transport from the microclimate air near the skin to the environment, a PCM-Desiccant packet is proposed for use in cooling vests. A fabric-PCM-Desiccant model is developed and validated with experiments on a wet clothed heated cylinder. The different vest models are integrated with a bio-heat model to assess at which ambient conditions and human activity the different systems would provide enhanced cooling.

## LIST OF PUBLICATIONS AND CONTRIBUTIONS

This thesis is based on the following papers, which will be referred to in the text.

### Paper

- I Itani, M., Ouahrani, D., Ghaddar, N., Ghali, K., & Chakroun, W. (2016). The effect of PCM placement on torso cooling vest for an active human in hot environment. *Building and Environment*, 107, 29-42.
- II Itani, M., Ghaddar, N., Ghali, K., Ouahrani, D., & Chakroun, W. (2017a). Cooling vest with optimized PCM arrangement targeting torso sensitive areas that trigger comfort when cooled for improving human comfort in hot conditions. *Energy and Buildings*, 139, 417-425.
- III Itani, M., Ghaddar, N., & Ghali, K. (2017b). Innovative PCM-desiccant packet to provide dry microclimate and improve performance of cooling vest in hot environment. *Energy Conversion and Management*, 140, 218-227.
- IV Itani, M., Ghaddar, N., Ouahrani, D., Ghali, K., & Khater, B. (2017c). An Optimal Two-Bout Strategy with Phase Change Material Cooling Vests to Improve Comfort in Hot Environment. *Journal of Thermal Biology*, 72, 10-25.
- V Ouahrani, D., Itani, M., Ghaddar, N., Ghali, K., & Khater, B. (2017). Experimental study on using PCMs of different melting temperatures in one cooling vest to reduce its weight and improve comfort. *Energy and Buildings*, 155, 533-545.
- VI Itani, M., Ghaddar, N., Ghali, K., Ouahrani, D., & Khater, B. (2018). Significance of PCM Arrangement in Cooling Vest for Enhancing Comfort at Varied Working Periods and Climates: Modeling and Experimentation. Accepted for publication in *Applied Thermal Engineering Journal* on September 11.

The following journal and conference papers are additional work done but not included in the thesis.

### Paper

- I Hamdan, H., Ghaddar, N., Ouahrani, D., Ghali, K. and Itani, M., (2016). PCM cooling vest for improving thermal comfort in hot environment. *International Journal of Thermal Sciences*, 102, pp.154-167.
- II Bachnak, R., Itani, M., Ghaddar, N., & Ghali, K., (2018). Performance of Hybrid PCM-Fan Vest with Deferred Fan Operation in Transient Heat Flows from Active Human in Hot Dry Environment. *Building and Environment*, 144, 334-348.

- III Itani, M., Ghaddar, N., Ouahrani, D., Ghali, K. and Chakroun, W., (2016). Mathematical Modeling of PCM Cooling Vest for Workers in Hot Climates. 6th International Conference on Energy Research and Development, State of Kuwait, March 14-16.
- IV Itani, M., Ghaddar, N., Ouahrani, D., Ghali, K. and Chakroun, W., (2016). Effect of PCM Packet Mass and Melting Temperature on Cooling Vest Performance. Presented at the 2nd International Conference Efficient Building Design: Materials and HVAC Equipment Technologies, Beirut, Lebanon September 22-23.
- V Itani, M., Ghaddar, N., Ghali, K., Ouahrani, D. and Chakroun, W, (2017). Improving Comfort and Productivity of Workers at Moderate Activity and Hot Environment by Means of a PCM Cooling Vest. Presented at the 2nd International Conference on Energy and Indoor Environment for Hot Climates, Doha, Qatar February 26-27.
- VI Itani, M., Ghaddar, N., Ghali, K., Khater, B., Ouahrani, D., & Chakroun, W. (2017). Experimental study on effective placement of PCM packets in cooling vest to improve performance in warm environment, no. HT2017-4756, July 9–14. In Proceedings of the 2017 ASME Summer Heat Transfer Conference, Bellevue, Washington.
- VII Itani, M., Ghaddar, N., Ghali, K., Khater, B., Ouahrani, D., & Chakroun, W. (2018). PCM Cooling Vests of Different Melting Temperatures in a Two-Bout Strategy to Enhance Comfort and Sensation: An Experimental Study. Presented at the 2018 ASHRAE Annual Conference, Houston, Texas.



# CONTENTS

ACKNOWLEDGEMENTS .....	v
ABSTRACT.....	vi
LIST OF PUBLICATIONS AND CONTRIBUTIONS.....	vii
LIST OF ILLUSTRATIONS.....	xi
LIST OF TABLES.....	xiv
ABBREVIATIONS.....	xv
Chapter	
I. INTRODUCTION.....	1
II. BACKGROUND.....	9
III. MATERIALS AND METHODOLOGIES.....	17
A. Cooling Vest Modeling.....	17
1. Fabric-PCM Model.....	17
2. Fabric-PCM-Desiccant Model.....	23
B. Bio-Heat and Comfort Modeling.....	29
C. Integration of Fabric-PCM and Bio-Heat.....	32
D. Experimental Methods.....	35
1. Validation of Integrated Fabric-PCM and Bio-Heat model with Human Subject Testing.....	36
a. Validation Applying Two-Bout Strategy.....	36
b. Validation with Placement of PCM Packets on Torso Segments that Trigger Comfort.....	45
2. Testing on a Thermal Manikin and on Human Subjects of PCM Packets of Different Melting Temperatures Used in One Cooling Vest.....	48

3. Validation of Fabric-PCM-Desiccant on a Wet Clothed Heated Cylinder.....	54
<b>IV. RESULTS AND DISCUSSIONS.....</b>	<b>59</b>
A. Integrated Fabric-PCM and Bio-Heat model simulations and Human Subject Testing.....	59
1. Applying Two-Bout Strategy.....	59
a. Physiological responses of skin and core temperatures, heart rate and body weight loss.....	59
b. Thermal comfort and sensation.....	65
2. Placement of PCM Packets on Torso Segments That Trigger Comfort.....	68
a. Physiological responses of heart rate, skin and core temperatures and body weight loss.....	69
b. Thermal comfort and sensation.....	73
B. Testing on a Thermal Manikin and on Human Subjects of PCM Packets of Different Melting Temperatures Used in one Cooling Vest.....	76
1. Results of manikin testing.....	76
2. Results of human subject experiments.....	78
a. PCM different states during exercise.....	79
b. Heart rate and local skin temperatures.....	80
c. Mean skin and core temperatures and body weight loss...	83
d. Thermal comfort and sensation.....	86
e. Discussion.....	88
C. Fabric-PCM-Desiccant on a Wet Clothed Heated Cylinder Vest.....	92
<b>V. CONCLUSIONS AND RECOMMENDATIONS.....</b>	<b>99</b>
<b>BIBLIOGRAPHY.....</b>	<b>103</b>

## ILLUSTRATIONS

Figure		Page
1.	Schematics showing (a) a human body with the torso covered with PCM packets (b) side view of the PCM packet in a cooling vest sandwiched between the human skin and environment and (c) top view of cooling vest with PCM packets covering different segments and the radii of the corresponding layers.....	18
2.	A 3D schematic of the PCM-Desiccant packet placed in a cooling vest	24
3.	Schematic of the (a) cooling vest side view with different fabric and air layers sandwiching the PCM-Desiccant packet and (b) area fraction of PCM and desiccant in the packet.....	24
4.	Schematic of (a) mass transfer and (b) heat transfer at different layers of the cooling vest.....	25
5.	Flowchart of the integrated bio-heat and fabric-PCM model.....	35
6.	Flowchart of the experimental methodology.....	36
7.	Pictures showing (a) a participant at QU doing exercise while wearing a cooling vest and (b) PCM packets of 28 °C and PCM packets of 18 °C melting temperatures.....	38
8.	Schematic showing the PCM placement cases (a) 4UF-0LF-10B, (b) 2UF-2LF-10B, (c) 0UF-4LF-10B, (d) 4UF-2LF-8B, (e) 4UF-4LF-6B and (f) 6UF-4LF-4B.....	48
9.	Picture showing Newton thermal manikin clothed with the PCM cooling vest.....	51
10.	Pictures showing (a) one participant doing exercise while wearing a vest at QU and (b) skin temperature sensor locations on body segments.....	52
11.	Schematic of the experimental setup of the wet clothed inner heated cylinder.....	56
12.	Simulation and experimental data (mean $\pm$ SD) of (a) local torso skin temperature during exercise for 50 min and (b) body weight loss after exercise for the different cases.....	61

13.	Transient variation of the (a) experimental (mean $\pm$ SD) heart rate and simulated and experimental (mean $\pm$ SD) (b) core temperature and (c) mean skin temperature during 50 min exercise for the different cases.....	63
14.	Simulation and experimental data (mean values $\pm$ SD) of (a) torso thermal sensation and (b) thermal comfort for the different cases during exercise.....	66
15.	Experimental (mean values $\pm$ SD) and simulation results of (a) front local skin temperature, (b) back local skin temperature during 45 min exercise and (c) back skin temperature at the end of experiment for the different cases.....	71
16.	Mean experimental values and SD (solid fill bars) and predicted values by simulation (hatched bars) of sweat production after exercise.	72
17.	Experimental (mean values $\pm$ SD) and simulation results of (a) torso thermal sensation, (b) thermal comfort during exercise and (c) thermal comfort at end of exercise.....	74
18.	Mean values of heart rate during 45 minutes exercise (dotted lines represent the reference cases of no vest and vests with uniform packets of 28 °C and 18 °C melting temperature).....	81
19.	Frontal local skin temperature for the different cases during exercise for 45 min (dotted lines represent the reference cases of no vest and vests with uniform packets of 28 °C and 18 °C melting temperature)...	82
20.	Back local skin temperature for the different cases during exercise for 45 min (dotted lines represent the reference cases of no vest and vests with uniform packets of 28 °C and 18 °C melting temperature).....	82
21.	Sweat production or body weight loss after exercise (Mean values and SD) (with hatched columns representing the reference cases of no vest and vests with uniform packets of 28 °C and 18 °C melting temperature).....	85
22.	Experimental mean ratings of overall thermal comfort showing (a) front and back cases & (b) upper and lower cases (hatched columns represent reference cases of no vest and vests with uniform packets of 28 °C and 18 °C melting temperature).....	86
23.	Experimental mean ratings of torso thermal sensation during exercise showing (a) front and back cases & (b) upper and lower cases (hatched columns represent reference cases of no vest and vests with uniform packets of 28 °C and 18 °C melting temperature).....	87

24.	Plots showing the variation with time of the (a) experimental and simulation results of the PCM temperature and simulated PCM melted fraction and (b) the microclimate air temperature corresponding to the experiment on the PCM packet only.....	93
25.	Plot showing the variation with time of experimental and simulation results of the PCM and desiccant temperature as well as the PCM melted fraction corresponding to the experiment on the PCM-Desiccant packet.....	95
26.	Plot showing the variation with time of experimental and simulation results of the microclimate and macroclimate temperatures corresponding to the experiment on the PCM-Desiccant packet.....	95
27.	Plot showing the time variation of the experimental and predicted microclimate air relative humidity when using only the PCM packet and when using the PCM-Desiccant packet.....	97

## TABLES

Table	Page
1. Clothing characteristics used in experiments.....	39
2. Thermo-physical properties of PCM packets (Swedish Emergency & Disaster Equipment AB, 2017; All Safe Industries, 2017).....	40
3. Different PCM experiments tested on human subjects.....	42
4. PCM arrangements of the different experiments on the UF, LF and back.....	47
5. Different PCM arrangements tested on thermal manikin.....	51
6. Different PCM arrangements tested on human subjects.....	53
7. Change in mean skin, core and body temperatures from the start of the experiment for single-bout cases and for every bout of two-bout case (bout 1: $T$ (at $t = 25$ min) - $T$ (at $t = 0$ min) and bout 2: $T$ (at $t = 50$ min) - $T$ (at $t = 25$ min)).....	64
8. Results of the thermal manikin experiments.....	78
9. Experimental results for PCM initial and final states (mean $\pm$ SD) during exercise and the time melting started for the different PCM arrangements.....	80
10. Change in mean skin, core and body temperatures from initial state (mean $\pm$ SD) and heat storage reported every 15 min during exercise for the different cases.....	84

## ABBREVIATIONS

<i>A</i>	area (m <sup>2</sup> )
<i>B</i>	Back torso segment
<i>BW</i>	body weight per unit area (kg/m <sup>2</sup> )
<i>C<sub>p</sub></i>	specific heat (J/kg·K)
<i>d</i>	gap width (m)
<i>e</i>	thickness (m)
<i>Exp</i>	experimental results
<i>f</i>	volume fraction
<i>g</i>	gravitational acceleration (m/s <sup>2</sup> )
<i>h<sub>ad</sub></i>	heat of adsorption (J/kg)
<i>h<sub>c</sub></i>	convective heat transfer (W/m <sup>2</sup> ·K)
<i>h<sub>des</sub></i>	mass transfer coefficient (m/s)
<i>h<sub>f</sub></i>	heat transfer coefficients (kg/m <sup>2</sup> ·kPa·s)
<i>h<sub>fg</sub></i>	heat of evaporation (J/kg)
<i>h<sub>m</sub></i>	mass transfer coefficient (kg/m <sup>2</sup> ·kPa·s)
<i>h<sub>sf</sub></i>	latent heat of fusion (J/kg)
<i>HR</i>	heart rate (beats/min)
<i>ISO</i>	International Organization for Standardization
<i>IRTT</i>	infrared tympanic thermometer
<i>j</i>	index indicating the PCM packet number
<i>k</i>	thermal conductivity (W/m·K)
<i>l</i>	width of the PCM packet (m)
<i>LF</i>	lower front torso segment
<i>m</i>	mass (kg)
<i>MET</i>	Metabolic Equivalent for Task
<i>m<sub>a</sub></i>	mass flow rate triggered by buoyancy forces (kg/s)
<i>m<sub>sw</sub></i>	sweat mass flow rate per unit area (kg/m <sup>2</sup> ·s)
<i>M<sub>h</sub></i>	metabolic rate at hot ambient conditions (W)
<i>M<sub>p</sub></i>	metabolic rate prior to hot exposure (W)
<i>n</i>	number of phase change material packets
<i>No vest</i>	no vest is worn by the participant

<i>P</i>	vapor pressure (kPa)
<i>PCM</i>	phase change material
<i>q</i>	heat flux (W/m <sup>2</sup> )
<i>Q</i>	desiccant heat of adsorption (J/kg)
<i>QU</i>	Qatar University
<i>r</i>	radius (m)
<i>R<sub>d</sub></i>	dry thermal resistance of the fabric (m <sup>2</sup> ·K/W)
<i>R<sub>e</sub></i>	evaporative resistance of the fabric (m <sup>2</sup> ·kPa/W)
<i>R<sub>if</sub></i>	inner fabric regain
<i>R<sub>tot</sub></i>	total thermal resistance (m <sup>2</sup> ·K/W)
<i>RH</i>	relative humidity (%)
<i>S</i>	change in body heat storage (W)
<i>SD</i>	standard deviation
<i>Sim</i>	simulation results
<i>T</i>	temperature (°C)
<i>TC</i>	thermal comfort
<i>TTS</i>	torso thermal sensation
<i>TWL</i>	thermal work limit (W/m <sup>2</sup> )
<i>t</i>	time (s)
<i>t<sub>adh</sub></i>	thickness of adhesive tape (m)
<i>t<sub>DM</sub></i>	thickness of desiccant membrane (m)
<i>UF</i>	upper front torso segment
<i>w</i>	humidity ratio (kg <sub>w</sub> /kg <sub>air</sub> )
<i>WBGT</i>	wet bulb globe temperature (°C)
<i>18F-18B</i>	PCMs of 18 °C melting temperature cover front and back
<i>18F-28B</i>	PCMs of 18 °C melting temperature cover front and 28 °C melting temperature cover back
<i>28F-18B</i>	PCMs of 28 °C melting temperature cover front and 18 °C melting temperature cover back
<i>28F-28B</i>	PCMs of 28 °C melting temperature cover front and back
<i>28U-18L</i>	PCMs of 28 °C and 18 °C melting temperature cover upper torso and lower torso, respectively



<i>18U-28L</i>	PCMs of 18 °C and 28 °C melting temperature cover upper torso and lower torso, respectively
<i>All-V18</i>	vest with PCMs of 18 °C melting temperature worn for 50 min
<i>All-V28</i>	vest with PCMs of 28 °C melting temperature worn for 50 min
<i>V28 → V18</i>	vest with PCMs of 28 °C melting temperature worn in first bout for 25 min then vest with PCMs of 18 °C melting temperature worn in second bout for 25 min

### Greek Symbols

$\alpha$	fraction of melted PCM
$\beta$	volumetric thermal expansion( $^{\circ}\text{C}^{-1}$ )
$\Delta$	change
$\lambda$	condensation rate ( $\text{kg}/\text{m}^2 \cdot \text{s}$ )
$\nu$	kinematic viscosity of air ( $\text{m}^2/\text{s}$ )
$\rho$	density ( $\text{kg}/\text{m}^3$ )
$\Psi$	condensation coefficient

### Subscripts

<i>a</i>	microclimate air
<i>adh</i>	adhesive tape
<i>air</i>	macroclimate air
<i>avg</i>	average
<i>b</i>	body
<i>con</i>	conduction
<i>cr</i>	core
<i>des</i>	desiccant
<i>DM</i>	desiccant membrane
<i>dp</i>	dew point
<i>env</i>	environment
<i>f</i>	fabric
<i>final</i>	final state
<i>i</i>	body segment index
<i>in</i>	inner

<i>initial</i>	initial state
<i>if</i>	inner fabric
<i>j</i>	PCM packet index
<i>liq</i>	liquid
<i>mean</i>	mean
<i>out</i>	outer
<i>of</i>	outer fabric
<i>PCM</i>	phase change material
<i>sat</i>	saturated
<i>skin</i>	skin layer
<i>Tot</i>	total

# CHAPTER I

## INTRODUCTION

The need to provide comfortable working spaces in warm or hot conditions requires cooling these spaces and thus consuming energy. In the presence of global warming, the ability to provide comfort is becoming more challenging and the need for cooling is increasing leading to an increase in energy consumption (Pallubinsky et al., 2016). Outdoor workers in some countries are exposed to very hot environmental conditions and to the direct sun, while performing their physically demanding tasks. Consequently, the ability of the active human body to dissipate heat to the ambient is hindered and heat accumulation happens subjecting workers to heat stress. In other words, the rate of body heat gain becomes higher than that of heat loss and the human's thermoregulatory mechanisms would fail in regulating the body temperature (Haldane, 1905). Different types of personal and local cooling methods have been used in previous studies to reduce thermal stresses on outdoor workers (Barr et al., 2010; Holmér et al., 2006; Zander et al., 2015) and improve comfort of indoor workers in office and commercial buildings (He et al., 2017). Local cooling allows for having elevated macroclimate air temperatures, since the microclimate of the workers is cooled and thus less energy is required by space air conditioning systems (Pallubinsky et al., 2016).

One type of local cooling includes phase change material (PCM) cooling vests, which incorporate ice packets, paraffin or even salt-based packets used to cool the human torso (Gao et al., 2010; House et al., 2012; Itani et al., 2016). In addition, PCM have been incorporated in textiles in the form of microcapsules to improve the clothing thermal performance (Mondal, 2008; Sarier and Onder, 2012). The PCM cooling vest popularity increased in such applications since it is portable, does not hinder mobility as

long as its weight is not excessive or require installation cost (Chan et al., 2016; Chan et al., 2017). Such a system allows for exploiting the latent heat storage effect without consuming additional energy unlike active refrigeration systems that cool the whole occupied space and unlike active cooling vests with ventilation fans. The PCM cooling vests among other microclimate cooling systems are known to be the cheapest, most portable, and the easiest to be worn (Coleman, 1989; Kamon et al., 1986; Kenny et al., 2011).

Most studies on PCM cooling vests were based on empirical work to examine the performance of the vests in hot dry and in hot humid environments (Reinertsen et al., 2008; Schlader et al., 2010; Zhao et al., 2012). It was concluded that the PCM vest was effective in hot and humid environments compared to hot and dry environments, where body heat can be dissipated by evaporative cooling; a mechanism of body cooling that is not applicable in humid environments. Researchers considered improving vest performance by varying the PCM melting temperature, the PCM mass in the vest, and the PCM covering area of the torso (Gao et al., 2010; House et al., 2012). The empirical results in literature show that the PCM vests with the lowest melting temperatures had the greatest cooling power. Also, the vests with higher mass of PCMs had longer cooling durations while those with higher PCM covering area of the torso had higher cooling rates (Gao et al., 2010; House et al., 2012). Adding more PCM packets results in additional weight to be carried by the worker which might hinder the ease of movement during activity and increase metabolic rate (Dorman and Havenith, 2009; Yazdi et al., 2015). Different types of activity, such as walking or going over an obstacle course, as well as the location of the carried weight affect differently the metabolic rate (Dorman and Havenith, 2007; Dorman and Havenith, 2009). As per the recommendation of Dorman et al. and Havenith (2009), a 2.7 % increase in the

metabolic rate is adopted for each kg increment in carried weight taken to account for the additional load on the human body while performing a certain activity and wearing protective clothing. If the carried weight was distributed on the torso part of the human body, then a 1 % increase in the metabolic rate is adopted for each kg increment in carried weight (Dorman and Havenith, 2007; Dorman and Havenith, 2009; Givoni and Goldman, 1971). Moreover, increasing the number of PCM packets in the vest could impede water vapor transmission to the environment and increase the risk of condensation. Once condensation occurs, heat will be released to the PCM vest and might thus counteract the cooling effect of the PCM. Therefore, there is a need to minimize the weight of the vest, which can be achieved by focusing on body regions that are more sensitive to cooling for placement of the PCM in the vest. To the authors' knowledge, the effect of the PCM packets' arrangement in the vest has not been investigated in literature empirically or by modeling while taking into consideration human thermal comfort and sensation when subject to local cooling.

Manikin testing and bio-heat modeling integrated with cooling vest models have been previously employed to predict human subject physiological and psychological responses (Gao et al., 2012; Hamdan et al., 2016; Itani et al., 2016). There are many bio-heat models that are capable of predicting thermal response of clothed humans with associated thermal sensation and comfort based on skin and core temperatures (Al-Othmani et al., 2008; Fiala et al., 2012; Huizenga and Hui, 2001; Karaki et al., 2013; Salloum et al., 2007). These models are based on theories of physiology, thermodynamics and transport processes and were reported to accurately predict core and skin temperatures of the entire human body or a part of it. The core and skin temperatures as well as their rate of change were also used by researchers (Al-Assaad et al., 2017; Hatoum et al., 2017; Holopainen, 2012; Itani et al., 2016) to

estimate accurately local and overall comfort and sensation in transient environments based on Zhang et al. (2004) empirical correlations. Hence, integrated bio-heat and comfort models of clothed human could be used as tools to perform testing on different cooling vest scenarios to optimize PCM performance. Modeling the PCM cooling vest and integrating it with a segmental bio-heat model has been recently introduced by Hamdan et al. (2016) who was first to use modeling approach for cooling vests. Although, their model predicted the temperatures of the air layers in the cooling vest and heat loss from the human body for given environmental conditions and PCM and clothing properties but it did not consider the effect of added PCM weight and hot environments on human metabolism and the possible occurrence of condensation at the inner surface of the PCM packets facing the human skin. In addition, no comparisons have been done between actual human subject testing and an integrated bio-heat and cooling vest model (Hamdan et al., 2016; Itani et al., 2016) to validate physiological and comfort predictions, while working in hot environments with temperature exceeding that of human skin and where productivity is significantly affected. Moreover, the literature is lacking the analysis of the best placement of PCM packets on the upper trunk or on both the upper and lower trunk. Such placements and considerations will affect the overall thermal sensation and comfort of the humans particularly for workers in hot environment.

Previous studies have investigated the performance of PCM cooling vests under a wide range of PCM melting temperatures (Gao et al., 2010; Gao et al., 2011; Hamdan et al., 2016; Itani et al., 2016). Some manufacturers of salt-hydrate PCMs (Climator Sweden AB; Teappcm; Rubitherm Technologies GmbH) and researchers in previous studies (Gao et al., 2010; Zalba et al., 2003), reported ranges of PCM melting temperatures from 6 °C to 32 °C, with an increasing trend in the latent heat of fusion as

the melting temperature increases (Farid et al., 2004; Itani et al., 2017a; Marks, 1982). As the environment gets warmer, it is advantageous to use lower PCM melting temperature rather than higher ones because they result in higher body cooling rates due to the significant temperature gradient between the human skin and the PCM surface (Gao et al., 2010; Gao et al., 2011; House et al., 2012). However, there are some shortcomings of the low melting temperature salt-hydrate PCM used in such applications: i) it can last for a short period of time before complete melting due to its low latent heat of fusion (Marks, 1980; Marks, 1983) at higher body cooling rate and ii) it requires storage at low temperature which consumes energy and requires adequate transport for end use. On the other hand, PCM packets with higher melting temperatures have relatively high latent heat of fusion so they can last for longer durations when worn, if the same temperature gradient exists between the PCM melting temperature and the skin and the environment. Moreover, higher PCM melting temperature would result with a longer cooling effect as a consequence of a lower temperature gradient between the PCM melting temperature and the skin and environment. In addition, they can be regenerated or solidified at room temperatures or in conditioned spaces without the need for refrigeration, thus providing local cooling without consuming any additional energy. Conversely, they have lower cooling rates due to the lower temperature gradient as reported in previous studies (Gao et al., 2010; Gao et al., 2011; House et al., 2012). Combining two different melting temperatures in the same vest is an interesting research question, however, it would have to be in such a manner that is responsive to human physiology to target body areas that are sensitive to cooling. Therefore, there is a viable option of using two different melting temperatures of PCM packets, a relatively low and a relatively high one, in the same vest to result in a significant, fast, and lasting cooling effect at lower mass of the vest and regeneration

energy use. The research question would then be: Is it possible to combine the advantage of the low melting PCM temperature (more comfort) and the advantage of higher melting temperature (larger heat of fusion and lower regeneration energy consumption)?

Post-exercise cooling was also used to shorten the recovery period and rest in between working bouts for long working durations and strenuous work in hot conditions (Yi et al., 2017). Outdoor work is highly intermittent in nature, thus, applying work-rest programs and dividing the long work periods and shifts into short bouts, especially in hot conditions, are effective ways of preventing heat stress and protecting workers. Moreover, dividing the working duration into two equally-timed bouts, would decrease the required PCM weight to at least half of that needed in the single-bout case. Thus, at hot environmental conditions, the possibility of using intermittent work periods while wearing light good-fitting PCM cooling vests, might enhance the working performance and prevent excessive body heat storage. However, the PCM melting temperature used in the two bouts need not be the same. Using low PCM melting temperature for initial cooling in the first bout would cause discomfort sensation when the body skin temperature is still close to thermo-neutrality. In addition, besides the initial discomfort, there is an energy saving incentive to use higher melting temperature PCMs in the first bout. The research question that is posed to overcome the problem of deteriorated cooling performance of the vest: Would it be possible to sustain good cooling performance by using a two-bout strategy during which a cooling vest with high melting temperature PCM (with lower mass) is worn first followed by the low melting temperature PCM (fast cooling effect)?

In humid ambient conditions, cooling the body by sweat evaporation is restricted and thus the presence of the PCM cooling vest was shown to be effective in



cooling the human body. However, in situations where the ambient conditions are dry and the metabolic rate of the worker is high enough to cause sweat secretion from the human skin, the PCM cooling vest performance have been shown to deteriorate and cause discomfort due to skin wettedness. Recent solutions to overcome the deterioration of the PCM performance due to condensation and sweat accumulation on the skin layer have been proposed, including a PCM-Fan hybrid vest (Lai et al., 2017; Song and Wang 2016) and a PCM-Desiccant cooling vest introduced in this study. Keeping the skin and microclimate air dry can be done by: 1) supplying dry ambient air in the space between the PCM packets via ventilation fans placed in the vest, which enhance cooling by sweat evaporation or 2) utilizing a thin solid desiccant packet covering part of the PCM packet surface. The solid desiccant such as silica gel can decrease the moisture content of the microclimate air between the PCM packet and the inner fabric layer of the cooling vest through an adsorption process. However, the released heat of adsorption might increase the temperature of the microclimate air if the PCM mass is insufficient for absorbing both the generated heat by the desiccant and the heat lost from the torso of the human body. In addition, the use of ventilation fans can cause faster melting of the PCM packets due to heat gains from the ambient air. It is of interest to determine whether the PCM-Desiccant packet combination is capable of enhancing the cooling performance of the vest and at which ambient conditions and activity levels. The placement of the PCM-Desiccant packet in the cooling vest could target torso areas that contain high distribution of sweat glands like the chest and upper back segments (Arens and Zhang, 2006; Havenith et al., 2008; Herrmann et al., 1952; Randall, 1946; Smith and Havenith, 2011). The combination of PCM and desiccant for use in the cooling vest has not been modeled or tested in previous studies. Moreover, it is of interest to assess

at what ambient conditions and activity levels such cooling vests can be used to achieve enhanced cooling performance.

The aim of this thesis is to improve the performance of the PCM cooling vest while taking into consideration the human physiology at high metabolic rates in hot environments, and some negative effects related to added PCM weight and condensation. A predictive model that integrates bio-heat and fabric-PCM models is developed to improve the PCM vest performance. In addition, a fabric-PCM-Desiccant model is developed to investigate the ability of enhancing the microclimate conditions near the human skin and at what ambient conditions and activity levels these systems are recommended. Different methods are used to validate the developed models, including human subject testing, thermal manikin testing and clothed wet heated cylinder. Different PCM arrangements are considered to optimize the arrangement of the PCM packets targeting torso sensitive areas that trigger comfort. Under extreme heat stress, targeting torso sensitive area to improve comfort might dampen the awareness of the wearer to the heat load on the body. Thus, the cooling vest has to sufficiently cool the body even though comfort might be improved when targeting torso sensitive areas.

## CHAPTER II

### BACKGROUND

Workers performing tasks in hot environmental conditions are subjected to high heat stress that limits the duration for continuous work and affect the productivity of the worker (Wong et al., 2014). To avoid any risk to the worker's health, many standards and safety protocols have recommended combinations of work and rest periods at different environmental conditions. At the very hot environmental conditions, a reduced working duration is recommended which means less economic productivity during heat exposure. At the long run, the individual, local, national and regional economic productivity will be affected (Kjellstrom et al., 2009; Kosonen and Tan, 2004; Lundgren et al., 2013).

A widely used indicator for the presence of heat stress is the core temperature of the human body and the level it rises to (Elson and Eckels, 2015). For example, based on the wet bulb globe temperature (WBGT) index, the maximum allowable core temperature over an 8-hour shift is 38 °C as adopted by ISO standard 7243 (ISO, 7243:1989). Another heat stress index for continuous safe working durations is the Thermal Work Limit (TWL), which takes into consideration the dry bulb temperature, wet bulb temperature, wind speed, radiation as well as the type of clothing and acclimatization state of the worker (Bates and Schneider, 2008; Miller and Bates, 2007). The ISO 5151 (ISO, 5151:2010) sets test conditions for rating the performance of non-ducted air conditioners and heat pumps, which include the cool (27 °C), moderate (35 °C) and hot (46 °C) climate. At relatively cool and moderate ambient conditions of 28 °C and 35 °C, prevailing in the Mediterranean countries, with a WBGT index around 28 °C, a 2-hour working duration is recommended followed by a recovery period of 15

minutes (Chan et al., 2012; Yi and Chan, 2013). Performing outdoor work at moderate intensity in such a WBGT index of 28 °C might result in low levels of thermal comfort when working continuously for two hours. At the very hot ambient temperature of 45 °C, in the Gulf Cooperation Council countries (Kingdom Saudi Arabia, Kuwait, Qatar, United Arab Emirates etc.) for example, a working duration of 45 minutes is recommended followed by a recovery period of 15 minutes based on the TWL thermal stress index (Bates and Schneider, 2008; Miller and Bates, 2007). Thus, there exists a need to use cooling systems and to optimize them in a way that would enable extending the working duration in the hot environmental conditions to be comparable to that in the moderate environmental conditions and to improve the thermal comfort at cool and moderate environmental conditions.

Previous experiments done on human subjects in the study of Gao et al. (2011) and House et al. (2012) showed relatively high core temperatures of 38.40 °C and 38.25 °C when performing activity while wearing a firefighting ensemble of 2.78 clo for 0.4 hours at 55 °C and for 0.75 hours at 40 °C, respectively. It can be deduced from the results of the core temperature that as the environmental conditions get hotter, the core temperature reaches relatively high values faster and during shorter working periods. Therefore, in order to combat the heat stress, local cooling and passive personal cooling systems have been used (Ghaddar et al., 2011; Pallubinsky et al., 2016). The PCM cooling vest is a personal cooling system (Chou et al., 2008; Sharma and Sagara, 2005) that can be worn by workers while performing their tasks outdoors. One type of a PCM cooling vest comprises of packets of phase change material of certain weight and surface area that can be placed inside pockets on the inner layer of the vest (Bendkowska et al., 2010; Yazdi and Sheikhzadeh, 2014). The PCM packets adjacent to

the human skin absorb the heat released by the torso in hot environments and thus maintain a lower skin temperature (Hamdan et al., 2016).

The PCM cooling vests used in previous studies came in different designs and the PCM packets had different properties to meet the body cooling requirements. The major properties that were considered by researchers to affect the performance of the cooling vest were the PCM melting temperature and the PCM weight in the vest (House et al., 2012; Gao et al., 2010). Modeling methods that do not involve comprehensive human physiology have been used for comparing PCM cooling vest performances and were based on simple energy balances like finding the change in the body heat storage,  $S$ , after wearing the cooling vest, where  $S$  depended on obtaining the mean skin and core temperatures at the end of the work period and the change in the mean body temperature from the start of the work period till its end (Elson and Eckels, 2015; House et al., 2012). Since safety of workers is a critical factor to be considered when designing cooling vests, this simplified energy balance,  $S$ , is found to be inadequate for optimizing cooling vests. In addition, previous studies have considered optimizing and assessing the cooling performance of the PCM vest via experiments done on human subjects (Gao et al., 2011; Reinertsen et al., 2008). However, literature is lacking simulation tools with comprehensive modeling that can be used for optimization purposes and hence limit the number of experiments to be conducted on human subjects to achieve optimal performance.

Thermal comfort and sensation have been previously recorded for subjects performing work at different activity levels and subjected to different environmental conditions. For example, McNall et al. (1967) performed experiments on subjects at three activity levels (1.7, 2.3 and 2.9 MET) and environmental conditions ranging between 15.6 °C and 25.6 °C, then recorded their thermal sensation votes after three

hours of activity. Gao et al. (2012) performed experiments on human subjects in order to investigate if a PCM cooling vest can improve thermal comfort and sensation while the subjects performed office work at an ambient temperature of 34 °C. The results showed that after wearing the vest, the overall thermal sensation and that of the torso improved while the thermal comfort improved slightly at the given activity level and ambient conditions. The results also indicate that local cooling is an interesting field of research due to the ability of controlling a human's local environment in an office space to save energy and improve comfort. In the study of Holopainen (2012), it was reported that Zhang's thermal sensation and comfort model (Zhang, 2003) which was originally developed for sedentary activities predicted well the thermal sensation and comfort at high activity levels (at about 3 MET). It is known that cooling different parts of the human body results in different thermal comfort and sensation levels (Stevens, 1979; Zhang, 2003), thus placing the PCM packets on the back and upper and lower front segments of the torso can result in different comfort levels. The ability to improve comfort by targeting the different torso segments needs to be combined with reduced body heat storage, so that masking of the warning signals of the human body does not happen in hot climates and in applications such as firefighting.

The nervous system of the human body consists of nerves or sensors located within its brain, skin, spine and abdomen (Arens and Zhang, 2006; Pan and Gibson, 2006) which sense if a certain organ or region of the human body is being cooled or heated and act upon it to regulate the human thermal state (Heller and Schiff, 1991; Stevens, 1979). Zhang et al. (2010) reported that the back was the main segment affecting the overall sensation of the human and that during transient experiments of back cooling, the overall sensation followed the local sensation of the back. Zhang et al. (2010) reported that the brain tends to give more attention to cooling changes in the

segments near the body core than to changes in the extremities. Thus this study using a modeling approach will take into consideration the human sensation and physiology to improve the distribution of PCM packets on the different torso segments for an active human while alleviating some negative effects related to added PCM weight and condensation.

Cooling vests have been used as pre-cooling techniques to improve the working performance, however, it was found unfeasible to many applications (Chan et al., 2017). In addition, cooling vests have been proved to significantly improve working performance while doing continuous exercise in hot conditions (Bongers et al., 2014). However, continuous cooling was not favored and had some lack of interest in situations where ergonomic problems arise due to the added PCM weight for prolonged work periods and the likely hindrance of movement (Chan et al., 2013; Tyler et al., 2013). Researchers have shown that as the environment gets hotter and with the increase of the WBGT, the ability of workers to carry loads decreases as well as their productivity (Dorman and Havenith, 2009; Snook and Ciriello, 1974; Weng et al., 2014). Moreover, improving the thermal state and comfort of workers wearing PCM cooling vests in hot conditions requires the use of low PCM melting temperatures, such as 10 °C, since higher melting temperatures such as 24 °C and 28 °C were found ineffective at 55 °C (Gao et al., 2011; House et al., 2012). The recommended work duration for moderate activity at very hot ambient conditions with WBGT of 32 °C is about 45 to 50 min (Bates and Schneider, 2008; ISO 7243, 1989). During that period, the amount of heat stored in the human body,  $S$ , would be about 150 W with a 1.49 °C increase in the body temperature,  $T_b$  (House et al., 2012). The estimated salt-hydrate PCM weight required to remove the heat stored after working continuously for 50 min, without considering the effect of the hot ambient condition, is about 3.8 kg with 18 °C

PCM melting temperature and 113 kJ/kg heat of fusion (All Safe Industries, 2017; Swedish Emergency & Disaster Equipment AB, 2017). On the other hand, dividing the working duration into two equally-timed bouts, would decrease the required PCM weight to at least half of that needed in the single-bout case. Thus, at hot environmental conditions, the possibility of using intermittent work periods while wearing light well-fitting PCM cooling vests, might enhance the working performance and prevent excessive body heat storage.

Cooling vests with PCM packets at low melting temperatures would trigger more heat losses due to the high temperature gradient between the human skin and the PCM temperature (Gao et al., 2011; House et al., 2012). However, there would be several disadvantages with using low melting temperatures: i) discomfort sensation, as reported by House et al. (2012) when using ice-vests to cool subjects performing stepping in 40 °C ambient temperature, ii) additional PCM weight due to condensation if present, high temperature gradients and lower heat of fusion when using salt-hydrates of low melting temperatures (Marks, 1980; Marks, 1983), which increases the metabolic rate of the worker and incurs higher material cost (Dorman and Havenith, 2009; Snook and Ciriello, 1974), iii) energy consumption for cooling/solidifying the PCM during storage at low temperatures, iv) the risk of condensation at the PCM surface with more use of packets that hinder moisture transport (Reinertsen et al., 2008) and v) the reduction in the cooling efficiency of the low melting temperature PCMs due to heat gains from the high temperature gradients between the packets and the hot environment, as reported by Yazdi et al. (2015). Thus, dividing the work period into two bouts established a decrease in the carried weight, while using the same low PCM melting temperature in the two bouts. However, besides the initial discomfort, there is an energy saving incentive to use higher melting temperature PCMs in the first bout.



However, PCM cooling vest effectiveness is constrained in hot humid environment due to reduced moisture transport from the vest and the consequent risk of sweat and condensation on the PCM packet surface. In a study by Dotti et al. (2016), three back protectors were evaluated for comfort through experiments done on human subjects performing intermittent physical activity. They reported that the back protector with the highest breathability and lowest microclimate humidity ranked the first among other protectors in terms of thermal sensation and that moisture management played the major role in the acceptance of back protectors. Houshyar et al. (2015) also indicated that using clothing that prevent air and water vapor transport would result in saturation of the microclimate humidity near the skin layer and condensation of water vapor due to sweating leading to heat stress and reduction of the work efficiency. Wang and Hu (2016) also showed that the mean thermal sensation of humans in hot conditions was related to sweating sensation.

Reinertsen et al. (2008) assessed experimentally the effect of covering the whole trunk or part of it with PCM packets on sweat evaporation through the vest in hot environment. They reported that thermal sensation was better when decreasing the number of PCM packets in the vest due to improved sweat transport through the vest. However, reducing the number of PCM packets in the vest may decrease the vest cooling duration. Zhao et al. (2012) performed experiments on a thermal manikin in a hot and humid environment and in a hot and dry environment to test the PCM vest cooling performance when sweat evaporation from the manikin skin is restricted. Results showed that the PCM cooling capability in the hot humid environment did not compensate for the restricted cooling by evaporation and led to lower torso heat losses.

This thesis work aims to improve the performance of the PCM cooling vest while taking into consideration the human physiology at moderate metabolic rates in hot

environments, and some negative effects related to added PCM weight and condensation. Moreover, this work aims to enhance comfort levels and cooling performance of the PCM vest by integrating desiccants with the PCM packets. More specifically, this thesis focuses on the following objectives:

- (1) To develop and validate with human data a predictive model consisting of a fabric-PCM model and a bio-heat model. The integrated model incorporates the effect of condensation if it happens in the vest and the effect of the vest carried weight and the hot ambient conditions on human metabolism.
- (2) To enhance comfort of outdoor workers by improving the cooling performance of torso cooling PCM vests through targeting torso sensitive areas.
- (3) To investigate the effect of using two PCM melting temperatures in one cooling vest on thermal comfort and the possibility of reducing vest weight.
- (4) To assess whether applying a two-bout strategy would improve comfort and sensation of workers while reducing energy use, carried weight and material cost.
- (5) To develop and validate on a wet clothed heated cylinder a fabric-PCM-Desiccant model. The PCM-Desiccant packet would provide dry microclimate air conditions that would enhance comfort of workers performing high activity levels and producing sweat.

In the following chapters of this dissertation, the methodology of developing the mathematical models of the cooling vests will be first presented. Then, the bio-heat modeling and the integration with the fabric-PCM model will be provided. In addition, the development of PCM-Desiccant model to improve the cooling vest performance in providing dry microclimate air conditions will be presented. After that, the different experimental methods will be described followed by the results and discussions and finally the conclusions and recommendations of the current work.

# CHAPTER III

## MATERIALS AND METHODOLOGIES

### **A. Cooling Vest Modeling**

In this section the mass and energy balance equations that constitute the fabric-PCM model, followed by those of the fabric-PCM-Desiccant model will be introduced. After that, the integration of the fabric-PCM model with the bio-heat model and the solution methodology will be introduced.

#### **1. *Fabric-PCM Model***

The cooling vest covering the human torso, shown in Fig. 1(a), was made up of an inner and outer fabric layer that were exposed to the human skin and environment, respectively, as shown in a side view of a part of the cooling vest in Fig. 1(b). The vest has 20 pockets that can hold 20 PCM packets covering the front and back torso segments. The fabric-PCM model divided the vest into four layers; inner fabric layer near the skin, microclimate air layer behind each PCM packet, macroclimate air layer in front and in between the packets and the outer fabric layer exposed to the environment. The PCM packet was closer to the inner fabric layer due to the Velcro fasteners and thus, a thin microclimate region was present. The PCM packet would directly affect the microclimate air region and would allow vertical buoyancy motion to happen in the thin microclimate layer (Bejan, 1994). In addition, the fabric-PCM model took into account the increase in the resistance due to the dissimilarity in the areas of the different vest layers (Ghali et al., 2009). This dissimilarity was caused by the cylindrical geometry and is represented by a ratio of the radii shown in a top view of the cooling vest in Fig. 1(c). The PCM packets, prior to wearing the vest, would be in a solid state and are affected by the heat gained from the hot environment and the microclimate air near the

skin. The macroclimate air layer in front of the PCM packets and in between the packets was considered to be lumped for each torso segment, as shown in Fig. 1(b).

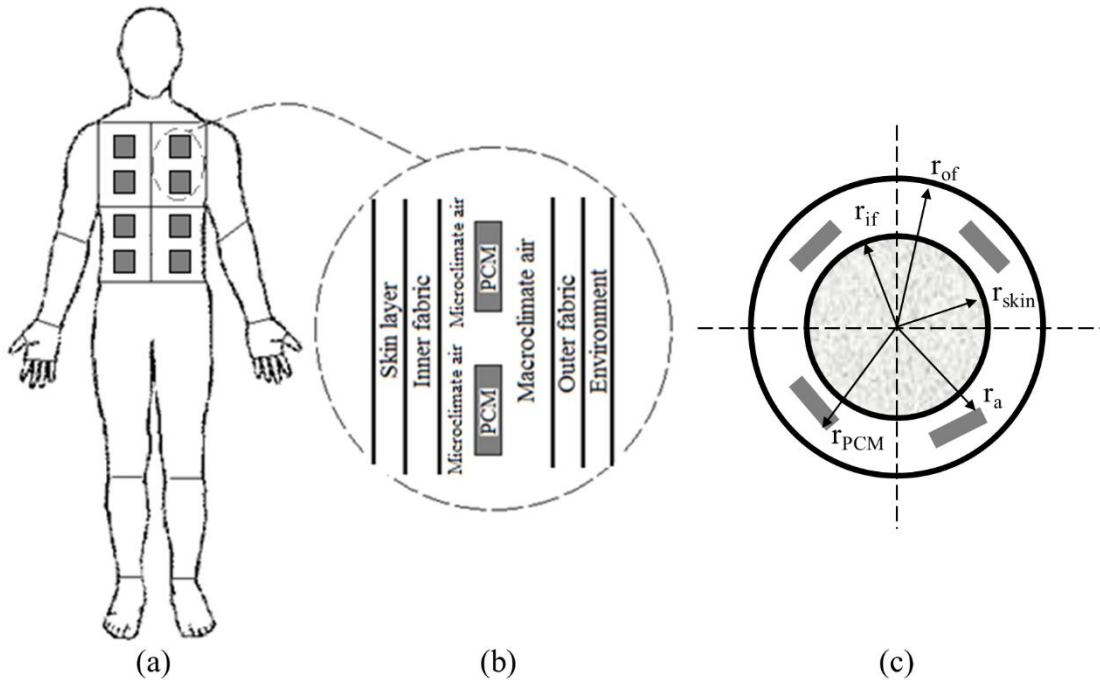


**Fig. 1:** Schematics showing (a) a human body with the torso covered with PCM packets (b) side view of the PCM packet in a cooling vest sandwiched between the human skin and environment and (c) top view of cooling vest with PCM packets covering different segments and the radii of the corresponding layers

The fabric-PCM model considered mass and energy balances for each fabric and air layer as well as an energy balance for the PCM packet and its melted fraction. The mass balances considered water vapor transport only in the horizontal direction between the skin and the inner fabric, and between the inner fabric and the micro and macro climate air layers as well as the moisture loss due to condensation. The energy balances considered heat exchange between the skin and the inner fabric and between the inner fabric and the micro and macro climate air layers as well as heat loss due to condensation. Moreover, an energy balance was used to predict the PCM temperature during the non-melting phase and the melted fraction during melting of the PCM packet.

During melting, the PCM temperature is constant and is equal to its melting temperature. The PCM packets exchanged heat with the micro and macro climate air layers and would be affected if condensation happens at the relatively cool surface of the PCM. The highest possibility for condensation to occur is at the surface of the PCM packet, since it has the lowest temperature in the microclimate region. Condensation causes the release of latent heat that would decrease the performance of the PCM packet. The mass and energy balances for the different layers and PCM packet are as follows:

Energy balance of inner fabric layer:

$$\begin{aligned} \rho_{if} e_{if} \left( C_{if} \frac{dT_{if,i}}{dt} - h_{ad} \frac{dR_{if,i}}{dt} \right) &= \frac{T_{skin,i} - T_{if,i}}{\frac{R_{d,if}}{2}} \times \frac{r_{skin,i}}{r_{if,i}} + \frac{T_{air,i} - T_{if,i}}{\frac{R_{d,if}}{2} + \frac{1}{2 \times h_{f,in}}} \times \frac{A_{f,i} - \sum_{j=1}^n A_{PCMi,j}}{A_{f,i}} \\ &+ \frac{T_{ai,j} - T_{if,i}}{\frac{R_{d,if}}{2} + \frac{1}{2 \times h_{f,in}}} \times \frac{\sum_{j=1}^n A_{PCMi,j}}{A_{f,i}} \end{aligned} \quad (1)$$

Mass balance of inner fabric layer:

$$\begin{aligned} \rho_{if} e_{if} \frac{dR_{if,i}}{dt} &= \frac{P_{skin,i} - P_{if,i}}{\frac{R_{e,if} \times h_{fg}}{2}} \times \frac{r_{skin,i}}{r_{if,i}} + \frac{P_{air,i} - P_{if,i}}{\frac{R_{e,if} \times h_{fg}}{2} + \frac{1}{2 \times h_{m,in}}} \times \frac{A_{f,i} - \sum_{j=1}^n A_{PCMi,j}}{A_{f,i}} \\ &+ \frac{P_{ai,j} - P_{if,i}}{\frac{R_{e,if} \times h_{fg}}{2} + \frac{1}{2 \times h_{m,in}}} \times \frac{\sum_{j=1}^n A_{PCMi,j}}{A_{f,i}} \end{aligned} \quad (2)$$

Energy balance of outer fabric layer:

$$\rho_{of} e_{of} \left( C_{of} \frac{dT_{of,i}}{dt} - h_{ad} \frac{dR_{of,i}}{dt} \right) = \frac{T_{env} - T_{of,i}}{\frac{R_{d,of}}{2} + \frac{1}{2 \times h_{f,out}}} + \frac{T_{air,i} - T_{of,i}}{\frac{R_{d,of}}{2} + \frac{1}{2 \times h_{f,in}}} \times \frac{r_{if,i}}{r_{of,i}} \quad (3)$$

Mass balance of outer fabric layer:

$$\rho_{of} e_{of} \frac{dR_{of,i}}{dt} = \frac{P_{env} - P_{of,i}}{\frac{R_{e,of} \times h_{fg}}{2} + \frac{1}{2 \times h_{m,out}}} + \frac{P_{air,i} - P_{of,i}}{\frac{R_{e,of} \times h_{fg}}{2} + \frac{1}{2 \times h_{m,in}}} \times \frac{r_{if,i}}{r_{of,i}} \quad (4)$$

In equations (1) through (4), the indices *if*, *of*, *skin*, *air*, *a*, *j* and *env* indicate the inner fabric, outer fabric, skin layer, macroclimate air layer, microclimate air layer, an index indicating the PCM packet number and the environment, respectively. The symbols  $\rho$ ,  $e$ ,  $C$ ,  $R_d$ ,  $R_e$ ,  $h_m$ ,  $h_f$  and  $h_{ad}$ , represent the fabric density, thickness, specific heat, dry thermal resistance, evaporative resistance, mass transfer coefficient, heat transfer coefficient and heat of adsorption, respectively. The heat transfer coefficient in the micro and macro climate air layers was taken from the experimental data on internal heat transfer coefficients with air gaps between 5 to 10 mm in the study of Danielsson (1996). The adopted microclimate gap thickness was about 5 mm and the macroclimate one about 7 mm, resulting with an internal convective heat transfer coefficient of about 3.1 W/m<sup>2</sup>.K for temperature differences ranging between 4 and 10 between the skin and clothing layer. The symbols  $r$ ,  $A$ ,  $P$ ,  $h_{fg}$ ,  $n$  and  $i$  represent the radius, area, vapor pressure, heat of evaporation, number of PCM packets and an index indicating the body segment number, respectively.

The PCM temperature,  $T_{PCM,i,j}$ , can be found if no melting is taking place by applying an energy balance (equation (5)) in which condensation effect is taken into

consideration through the symbol  $\Psi$ . In addition, the PCM melted fraction,  $\alpha_{i,j}$ , during melting can be found using equation (6), where  $\Psi$  is set to unity if condensation is present, otherwise, it is set to zero, as shown in equation (7). Condensation takes place on the surface of the PCM packets only when the PCM temperature is less than the microclimate air dew point temperature,  $T_{dp,a,i,j}$ , or the macroclimate one,  $T_{dp,air,i}$ .

PCM temperature during non-melting phase:

$$m_{PCMi,j} C_{PCMi,j} \frac{dT_{PCMi,j}}{dt} = h_c \times A_{PCMi,j} \times (T_{ai,j} - T_{PCMi,j}) \times \frac{r_{if,i}}{r_{PCMi,j}} + h_c \times A_{PCMi,j} \times (T_{air,i} - T_{PCMi,j}) + \Psi \times (\lambda_{ai,j} + \lambda_{air,i}) \times h_{fg} \times A_{PCMi,j} \quad (5)$$

PCM melted fraction during melting:

$$h_{sf} m_{PCMi,j} \frac{d\alpha_{i,j}}{dt} = h_c \times A_{PCMi,j} \times (T_{ai,j} - T_{PCMi,j}) \times \frac{r_{if,i}}{r_{PCMi,j}} + h_c \times A_{PCMi,j} \times (T_{air,i} - T_{PCMi,j}) + \Psi \times (\lambda_{ai,j} + \lambda_{air,i}) \times h_{fg} \times A_{PCMi,j} \quad (6)$$

$$\text{where } \Psi = \begin{cases} 1 & \text{if } T_{PCMi,j} < T_{dp,a,i,j} \text{ or } T_{dp,air,i} \\ 0 & \text{else} \end{cases} \quad (7)$$

The symbols  $m$ ,  $h_{sf}$ , and  $h_c$  represent the PCM mass, PCM latent heat of fusion and the convective heat transfer coefficient, respectively. The symbols  $\lambda_{ai,j}$  and  $\lambda_{air,i}$  represent the segmental condensation rates of the micro and macro climate air, respectively.

The microclimate air mass flow rate,  $\dot{m}_{ai,j}$ , in the small gap width between each PCM packet and the corresponding inner fabric layer can be found using equation (8), assuming a Poiseuille flow (Ghali et al., 2009), as follows:

$$\dot{m}_{ai,j} = \rho_{air} \times g \times \beta \times \frac{T_{air,i} - T_{ai,j}}{12\nu} \times d^3 \times l \quad (8)$$

The symbols  $g$ ,  $\beta$ ,  $d$ ,  $\nu$  and  $l$  represent the gravitational acceleration, the thermal expansion coefficient of air, the gap width, the kinematic viscosity of air and the width of the PCM packet, respectively.

Mass and energy balances are used to predict the segmental microclimate air humidity ratio,  $w_{ai,j}$ , condensation rate,  $\lambda_{ai,j}$ , and temperature,  $T_{ai,j}$ . as well as the segmental macroclimate air humidity ratio,  $w_{air,i}$ , condensation rate,  $\lambda_{air,i}$ , and temperature,  $T_{air,i}$ , as follows:

Mass balance of microclimate air:

$$\rho_{air} \times d \times \frac{dw_{ai,j}}{dt} = \sum \frac{P_{if,i} - P_{ai,j}}{\frac{R_{e,if} \times h_{fg}}{2} + \frac{1}{2 \times h_{m,in}}} \times \frac{r_{if,i}}{r_{ai,j}} + \dot{m}_{ai,j} \times (w_{air,i} - w_{ai,j}) \times \frac{1}{d \times l} - \psi \times \lambda_{ai,j} \quad (9)$$

Energy balance of microclimate air:

$$\rho_{air} \times d \times A_{PCMi,j} \times C \frac{dT_{ai,j}}{dt} = A_{PCMi,j} \times h_c (T_{PCMi,j} - T_{ai,j}) + A_{PCMi,j} \times h_c (T_{if,i} - T_{ai,j}) \frac{r_{if,i}}{r_{ai,j}} + \dot{m}_{ai,j} \times C_{air} \times (T_{air,i} - T_{ai,j}) - \psi \times \lambda_{ai,j} \times h_{fg} \times A_{PCMi,j} \quad (10)$$

Mass balance of macroclimate air:

$$\rho_{air} \times e_{air} \times \frac{dw_{air,i}}{dt} = \frac{P_{of,i} - P_{air,i}}{\frac{R_{e,of} \times h_{fg}}{2} + \frac{1}{2 \times h_{m,in}}} + \sum \dot{m}_{ai,j} \times (w_{ai,j} - w_{air,i}) \times \frac{1}{d \times l} + \frac{P_{if,i} - P_{air,i}}{\frac{R_{e,if} \times h_{fg}}{2} + \frac{1}{2 \times h_{m,in}}} \times \frac{A_{f,i} - \sum_{j=1}^n A_{PCMi,j}}{A_{f,i}} \times \frac{r_{if,i}}{r_{air,i}} - \psi \times \lambda_{air,i} \quad (11)$$



Energy balance of macroclimate air:

$$\begin{aligned}
\rho_{air} \times e_{air} \left( C \frac{dT_{air,i}}{dt} - h_{fg} \frac{dw_{air,i}}{dt} \right) &= h_c (T_{of,i} - T_{air,i}) + \sum \frac{A_{PCMi,j}}{A_{f,i}} \times h_c (T_{PCMi,j} - T_{air,i}) \\
+ \frac{A_{f,i} - \sum A_{PCMi,j}}{A_{f,i}} \times h_c (T_{if,i} - T_{air,i}) &+ h_{fg} \frac{P_{if,i} - P_{air,i}}{R_{e,if} h_{fg} + \frac{1}{2}} \times \frac{A_{f,i} - \sum A_{PCMi,j}}{A_{f,i}} \times \frac{r_{if,i}}{r_{air,i}} \\
+ h_{fg} \times \frac{P_{of,i} - P_{air,i}}{\frac{R_{e,of} \times h_{fg}}{2} + \frac{1}{2 \times h_{m,in}}} &+ \sum \dot{m}_{ai,j} C_{air} \times (T_{air,i} - T_{ai,j}) - \psi \times \lambda_{air,i} \times h_{fg} \quad (12)
\end{aligned}$$

More details on the modeling methods can be found in Itani et al. (2016).

## 2. *Fabric-PCM-Desiccant Model*

A model that predicts the conditions of the microclimate and macroclimate air in the presence of the PCM-Desiccant packet placed near the human skin, as shown in Fig. 2, would be a significant tool for improving the performance of a PCM cooling vest in situations where moisture transport is hindered. The presence of a solid desiccant will adsorb, through the water vapor permeable membrane holding the solid desiccant, moisture from the microclimate air layer released due to sweat secretion and prevent condensation from happening at the packet surface. Meanwhile, the PCM will absorb the heat of adsorption released by the desiccant so that no excess heat is released to the microclimate air. Thus, the fabric-PCM model developed by Hamdan et al. (2016) has been modified to include the effect of a solid desiccant added to the PCM packet as shown in Fig. 3(a). The solid desiccant in the model is considered to be lumped with a surface area  $A_{des}$ , which in addition to the surface area of the PCM,  $A_{PCM}$ , form the total area,  $A_{Tot}$ , of the PCM-Desiccant packet shown in Fig. 3 (b).

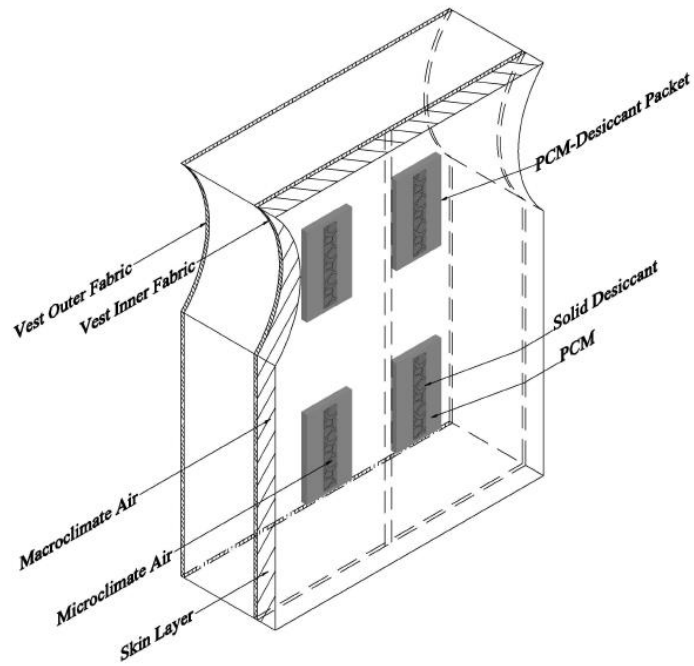


**Fig. 2:** A 3D schematic of the PCM-Desiccant packet placed in a cooling vest

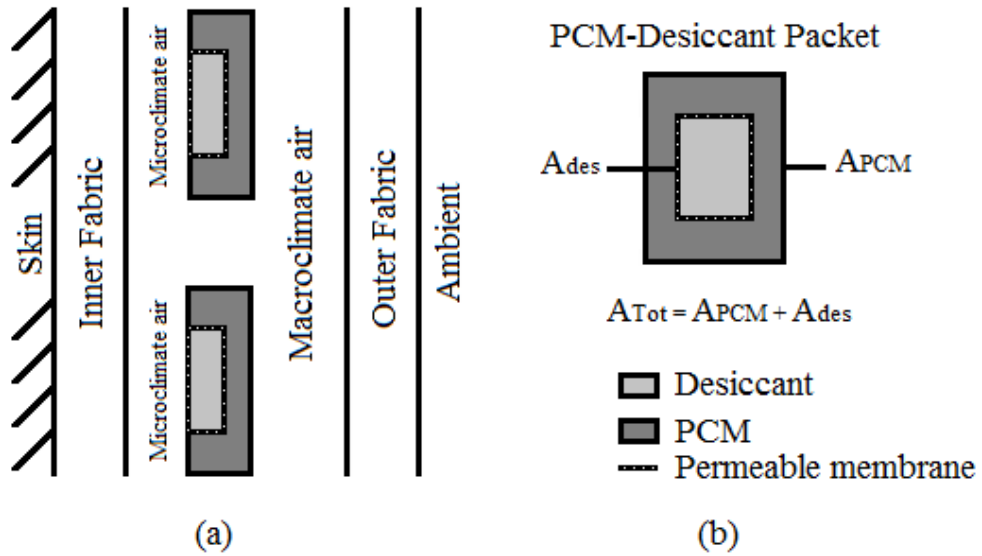


**Fig. 3:** Schematic of the (a) cooling vest side view with different fabric and air layers sandwiching the PCM-Desiccant packet and (b) area fraction of PCM and desiccant in the packet

The desiccant present between the microclimate air layer and the PCM will adsorb moisture from the microclimate air layer as shown in Fig. 4 (a). In addition, mass

transfer will take place between the different layers of the cooling vest due to the pressure differences between the different air and fabric layers and the environment. The PCM as well as the desiccant are both assumed to have a lumped temperature since the packet is thin. In addition, the thermal resistance between the PCM and the desiccant is assumed to be minimal due to the high thermal conductivity of the wrappings of the PCM and the desiccant and the thermally conductive double-sided tape used to join the PCM and the desiccant into one packet. Resistances to the aforementioned mass transfer are represented as evaporative resistances for the fabric layers and reciprocals of the mass transfer coefficients. Furthermore, the PCM in contact with the desiccant will exchange heat with the microclimate and macroclimate air layers and with the desiccant as shown in Fig. 4 (b). Heat transfer will also take place between the different layers of the cooling vest and the hot environment. Thermal resistances to heat flow are represented as dry resistances for the fabric layers and reciprocals of the convective heat transfer coefficients.

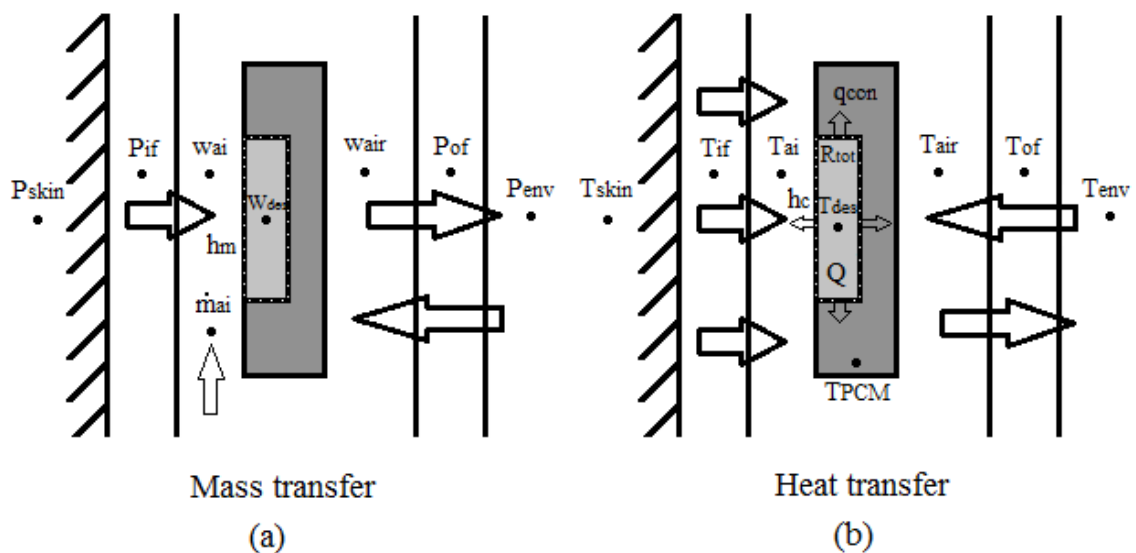


**Fig. 4:** Schematic of (a) mass transfer and (b) heat transfer at different layers of the cooling vest

The PCM and the solid desiccant, which are present in one packet, are considered to have distinct temperatures. The temperature of the PCM,  $T_{PCMi,j}$ , can be found using equation (13) if no melting is taking place, through an energy balance in which the PCM exchanges convective heat with the macroclimate and microclimate air layers and exchanges heat with the desiccant through a contact surface of thermal resistance,  $R_{tot}$ , found using equation (14). It is noted that the desiccant is placed in a water vapor permeable membrane that does not allow liquid water to pass, thus the effect of wicking in this case is neglected. During melting, the PCM melted fraction,  $\alpha_{i,j}$ , can be found as given in equation (15), where the PCM temperature is fixed at the melting temperature.

The PCM packet energy balance when there is no melting:

$$\begin{aligned} f_{PCMi,j} m_{PCMi,j} C_{PCMi,j} \frac{dT_{PCMi,j}}{dt} &= h_c A_{PCM,i,j} (T_{ai,j} - T_{PCMi,j}) \frac{r_{if,i}}{r_{PCMi,j}} \\ &+ A_{Tot,i,j} \frac{(T_{desi,j} - T_{PCMi,j})}{R_{tot}} + h_c A_{Tot,i,j} (T_{air,i} - T_{PCMi,j}) \frac{r_{air,i}}{r_{PCMi,j}} \end{aligned} \quad (13)$$

The thermal resistance between PCM and desiccant:

$$R_{tot} = \frac{t_{adh}}{k_{adh} \times A_{adh}} + \frac{t_{DM}}{k_{DM} \times A_{DM}} \quad (14)$$

The PCM packet energy balance during melting:

$$\begin{aligned} f_{PCMi,j} m_{PCMi,j} h_{sf} \frac{d\alpha_{i,j}}{dt} &= h_c A_{PCM,i,j} (T_{ai,j} - T_{PCMi,j}) \frac{r_{if,i}}{r_{PCMi,j}} + A_{Tot,i,j} \frac{(T_{desi,j} - T_{PCMi,j})}{R_{tot}} \\ &+ h_c A_{Tot,i,j} (T_{air,i} - T_{PCMi,j}) \frac{r_{air,i}}{r_{PCMi,j}} \end{aligned} \quad (15)$$

In addition, mass and energy balances are used to predict the segmental humidity ratio of the microclimate air,  $w_{ai,j}$  and the temperature of the lumped microclimate air,  $T_{ai,j}$ , using equation (16) and equation (17), respectively. The segmental macroclimate air humidity ratio,  $w_{air,i}$  and temperature,  $T_{air,i}$ , can also be found using the mass and energy balances developed by Hamdan et al. (2016). The mass balances consider water vapor transport between the fabric layers and the microclimate and macroclimate air layers as well as the moisture loss due to adsorption. The energy balances consider heat exchanges between the fabric layers, the desiccant, the PCM and the microclimate and macroclimate air layers, as follows:

Mass balance of microclimate air:

$$\rho_{air} d \frac{dw_{ai,j}}{dt} = \sum \frac{P_{if,i} - P_{ai,j}}{\frac{R_{e,if} \times h_{fg}}{2} + \frac{1}{2 \times h_m}} \frac{r_{if,i}}{r_{ai,j}} + \dot{m}_{ai,j} (w_{air,i} - w_{ai,j}) \frac{1}{d \times l} - \rho_{air} h_{des} (w_{ai,j} - w_{desi,j}) \frac{r_{ai,j}}{r_{des,i,j}} \quad (16)$$

Energy balance of microclimate air:

$$\rho_{air} \times d \times A_{Tot,i,j} \times \left( C \times \frac{dT_{ai,j}}{dt} - h_{fg} \times \frac{dw_{ai,j}}{dt} \right) = h_c A_{des,i,j} (T_{desi,j} - T_{ai,j}) \frac{r_{ai,j}}{r_{des,i,j}} + A_{PCM,i,j} h_c (T_{PCMi,j} - T_{ai,j}) \frac{r_{ai,j}}{r_{PCM,i,j}} + A_{Tot,i,j} h_c (T_{if,i} - T_{ai,j}) \frac{r_{if,i}}{r_{ai,j}} + \dot{m}_{ai,j} C_{air} (T_{air,i} - T_{ai,j}) \frac{r_{air,i}}{r_{ai,j}} \quad (17)$$

Mass and energy balance equations are also used to find the inner and outer fabric regains and temperatures (Hamdan et al., 2016).

The mass and energy balances of the desiccant are used to predict the moisture content,  $w_{desi,j}$  (kg water/kg dry desiccant) and the temperature of the desiccant,  $T_{desi,j}$ , using equation (18) and equation (19), respectively. The mass balance considers water vapor transport between the desiccant and the microclimate air layer due to adsorption. The energy balance considers heat exchanges between the desiccant, the microclimate air layer and the PCM. In addition to the heat released due to the adsorption process, as shown below:

Mass balance of solid desiccant:

$$\rho_{des} \times e_{des} \times \frac{dw_{desi,j}}{dt} = \rho_{air} h_{des} (w_{ai,j} - w_{desi,j}) \frac{r_{ai,j}}{r_{des,i,j}} \quad (18)$$

Energy balance of solid desiccant:

$$\begin{aligned} f_{des,i,j} \rho_{des} e_{des} A_{desi,j} (C_{p,des} + w_{desi,j} C_{p,liq}) \frac{dT_{desi,j}}{dt} = h_c A_{des,i,j} (T_{ai,j} - T_{desi,j}) \frac{r_{ai,j}}{r_{des,i,j}} \\ - A_{Tot,i,j} \frac{(T_{desi,j} - T_{PCMi,j})}{R_{tot}} + f_{des,i,j} \rho_{air} Q \times h_{des} A_{desi,j} (w_{ai,j} - w_{desi,j}) \frac{r_{ai,j}}{r_{des,i,j}} \end{aligned} \quad (19)$$

The mass and energy balance equations of the fabric-PCM-Desiccant model are solved using the explicit Euler forward method. Initial temperatures of the air layers, fabric layers and PCM-Desiccant packets are defined. The initial conditions of the pressures of the different clothing layers as well as the humidity ratios of the air layers are set. Initially, the inner and outer fabric regains are found at the new time step followed by finding their temperatures and values of the relative humidity (Hearle and Morton, 2008). Also, the new temperatures found are used to calculate the fabric saturation pressures (Hyland and Wexter, 1983) and the corresponding vapor pressures.

The mass flow rate of the microclimate air layer due to buoyancy is found and used to calculate the humidity ratios and temperatures of the microclimate and macroclimate air layers at the new time step. The temperature of the PCM and the desiccant can also be found, where the PCM temperature is compared to its melting temperature at each time step to check whether the PCM started melting and to find its corresponding melted fraction. It should be noted that the heat of adsorption of the desiccant is found using the formula developed by Pesaran and Mills (1987) which depends on the moisture content of the desiccant.

More details on the modeling methods can be found in Itani et al. (2017b).

## **B. Bio-Heat and Comfort Modeling**

The bio-heat and comfort model constituted of a multi-node segmental transient bio-heat model developed by Karaki et al. (2013) and a comfort and sensation model developed by Zhang et al. (2004). The multi-node bio-heat model developed by Karaki et al. (2013) is used in this study to obtain realistic skin temperatures, skin vapor pressures and human thermal responses. However, their model do not consider the effect of working in extremely hot conditions on the metabolism and heart rates. In addition, their models did not incorporate the effect of the clothing weight on the metabolic rate of the human.

In this study, the bio-heat model developed by Karaki et al. (2013) is corrected for use in hot environment and added weight. The bio-heat model divides the body into 27 segments (10 fingers, 2 palms, 2 forearms, 2 upper arms, head, 2 feet, 2 calves, 2 thighs, upper front of torso, lower front of torso, upper back of torso, lower back of torso). The torso is divided into 4 segments, where each segment has two skin nodes and a certain area that can be covered by a number of PCM packets of a given area (see Fig. 1a). Each torso segment has two skin nodes, thus, the bio-heat model was sensitive

to angular variations in the torso environment (Ghali et al., 2009). The bio-heat model was based on the multi-branched blood flow model of Avolio (1980) and was first published in the work of Salloum et al. (2007). Energy balances were performed on four nodes (core, skin, artery blood, and vein blood), while utilizing the circulatory system model to predict the blood flow in the arteries and veins and perfusion rates to the core and skin. The human body dissipates heat to the environment by means of radiation, convection, and evaporation to maintain its core temperature within a narrow range. Detailed description of the bio-heat model equations can be found in the study of Karaki et al. (2013) and Salloum et al. (2007) and will not be presented here. However, the bio-heat model required the following main input parameters:

- The initial thermal state of the human body.
- The clothed and unclothed segments and the clothing physical and thermal properties (thickness, density, dry thermal resistance, evaporative resistance).
- The metabolic rate of the human corresponding to the type of activity level.
- The environmental conditions surrounding the human (temperature, relative humidity and surrounding mean radiant temperature).

Three adjustments were done to the bio-heat model of Karaki et al. (2013) for better predictions of human thermal responses; two on the metabolic rate and one on the heart rate.

The first adjustment incorporates an increase in the metabolic rate of the human once the ambient temperature exceeds 39 °C (Weng et al., 2014) and the new metabolic rate at the hot conditions,  $M_h$ , is given by

$$M_h = M_p \times (1 + 0.13(T_{amb} - 39)) \quad (20)$$



where  $M_p$  is the metabolic rate of the human prior to being exposed to the hot ambient temperature of 39 °C and  $T_{amb}$  is the ambient temperature, respectively. It is noted that a correlation between the increase in metabolic rate or oxygen consumption and the body temperature was recently introduced by Kampmann and Bröde (2015) using experimental data of human subjects doing light work in warm environments.

The second adjustment to the bio-heat model is a correction on the metabolic rate to account for the additional weight of the PCM cooling vest carried by the human body. Different types of activity, such as walking or going over an obstacle course, as well as the location of the carried weight affect differently the metabolic rate (Dorman and Havenith, 2007; Dorman and Havenith, 2009). As per the recommendation of Dorman and Havenith (2009), a 2.7 % increase in the metabolic rate is adopted for each kg increment in carried weight taken to account for the additional load on the human body while performing a certain activity and wearing protective clothing. If the carried weight was distributed on the torso part of the human body, then a 1 % increase in the metabolic rate is adopted for each kg increment in carried weight (Dorman and Havenith, 2007; Dorman and Havenith, 2009; Givoni and Goldman, 1971).

The third adjustment to the bio-heat model is the increase in the heart rate,  $\Delta HR$ , when the ambient temperature reaches 31 °C and above (Weng et al., 2014) as follows:

$$\Delta HR = 4.75 \times \left( \frac{\dot{m}_{sw} \times t}{BW} \right) \quad (21)$$

The symbols  $t$ ,  $BW$ , and  $\dot{m}_{sw}$  represent the time, the body weight per unit area, and the sweat rate per unit area, respectively.

The bio-heat model was integrated with the comfort and sensation model of Zhang et al. (2004). The model of Zhang et al. (2004) included empirical correlations

that made use of the segmental core and skin temperatures and their rate of change to predict local and overall transient thermal sensation and comfort. The comfort and sensation scales vary from -4 (very uncomfortable or very cold) to +4 (very comfortable or very hot). Zhang et al.'s model (2004) was developed through experiments on sedentary people, however, Holopainen (2012) reported that thermal sensation and comfort were predicted well by Zhang et al.'s model at activity levels of about 3 MET.

### C. Integration of Fabric-PCM and Bio-Heat

The integration between the models was needed since the cooling vest performance is affected by the local torso skin temperatures. The average of the microclimate air temperatures and vapor pressures corresponding to the PCM elements covering one torso segment were found from the PCM-fabric model as shown in Fig. 1 (b). Then, their values were taken as inputs to find the skin temperature and skin vapor pressure of the torso segment in the bio-heat model, while ensuring continuity of fluxes and skin temperatures at any time (Hamdan et al., 2016). The procedure was followed for all the torso segments to find their corresponding skin temperatures. A mass balance was performed at the skin surface to find the segmental skin vapor pressure,  $P_{skin,i}$  (Jones and Ogawa, 1993), as follows:

$$P_{skin,i} = \left( \frac{P_{skin,i,sat}}{R_{e,skin}} + \frac{P_{a,j,avg}}{R_{e,a}} + \dot{m}_{sw,i} \times h_{fg} \right) / \left( \frac{1}{R_{e,skin}} + \frac{1}{R_{e,a}} \right) \quad (22)$$

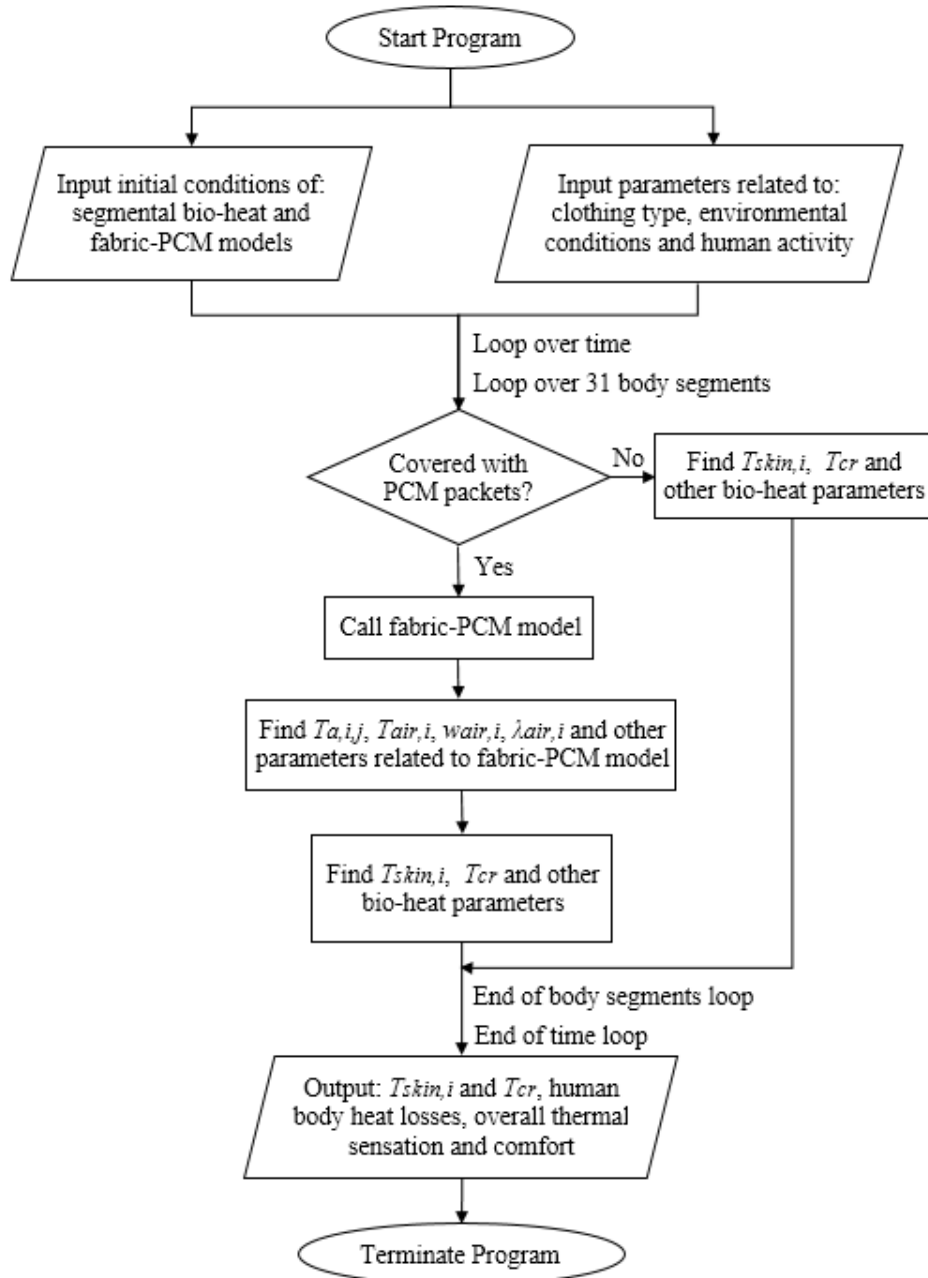
where  $P_{skin,i,sat}$ ,  $P_{a,j,avg}$ ,  $\dot{m}_{sw,i}$ ,  $R_{e,a}$  and  $R_{e,skin}$  represent the segmental skin saturated pressure, the average microclimate air vapor pressure, the local segmental sweat rate per unit area, the evaporative resistance of the microclimate air layer, and the skin evaporative resistance. If  $P_{skin,i}$  was greater than  $P_{skin,i,sat}$ , then  $P_{skin,i}$  was set to be equal to  $P_{skin,i,sat}$ .

Fig. 5 presents a flowchart of the numerical methodology summarizing the simulation steps of the integrated bio-heat and fabric-PCM model. Using the explicit Euler forward method and a time step of 0.02 s, the equations of the model were solved over the desired simulation period (working duration) while looping over all the body segments. The integrated fabric-PCM and bio-heat model requires to set the ambient environmental conditions as well as the clothing type, PCM properties and activity level of the human. In order to find the initial conditions for the unsteady simulations, the ambient conditions of the pre-conditioned environmental parameters (temperature, humidity, etc.), the activity level and clothing properties before wearing the vest are determined and the simulation model is run for a long period of time to reach steady state at the preconditioning environment. Then, the steady state results were used as initial conditions for the unsteady calculations of various segmental node skin and core temperatures and the sensible and latent heat losses from the skin (Hamdan et al., 2016; Karaki et al., 2013; Salloum et al., 2007).

The different parameters concerning the fabric layers, air layers and PCM packets were initialized. The fabric regains were also set based on correlations relating the regain to the relative humidity of the environment (Hearle and Morton, 2008). The initial conditions for the different layers of the temperature, humidity and pressure were set to be equivalent to the ambient environmental conditions. At the new time step, the model first solves for the inner and outer fabric regains, and then the corresponding temperatures can be found. Using the correlation relating the fabric regain and the relative humidity (Hearle and Morton, 2008), the relative humidity at the new time step can be found. After that, the fabric saturation pressures using psychrometric formulas (Hyland and Wexler, 1983) were found followed by the corresponding fabric vapor pressures.

Upon finding the mass flow rate of the microclimate air, the corresponding humidity ratio and temperature can be found as well as those of the macroclimate air. Regarding the PCM temperature, it was compared at every time step with the melting temperature of the PCM to check if the PCMs reached the melting temperature or not. Once the PCM melting temperature is reached, the melted fraction of the PCM can be found, while the PCM temperature is maintained constant. If condensation was present, then the condensation rates,  $\lambda$ , were found by setting equations (9) and (11) to be equal to zero and the condensation coefficients,  $\Psi$ , to be equal to unity; otherwise, the condensation rates and coefficients were zero.

Thus, the integrated model through the segmental skin vapor pressures and temperatures, which were associated with the average microclimate air vapor pressure and temperature of the fabric-PCM model, predicted at each time step the skin temperatures, sweat rate and heat losses. Finally, Zhang et al.'s model (2004) was used to predict thermal comfort and sensation.



**Fig. 5:** Flowchart of the integrated bio-heat and fabric-PCM model

#### D. Experimental Methods

The flowchart summarizing the experimental methodology is presented in Fig. 6. In this section we will describe how human subject testing was done to validate the integrated fabric-PCM and bio-heat model when: 1) applying the two-bout strategy and 2) placing PCM packets on torso segments that trigger comfort. In addition, the placement of PCM packets of different melting temperatures in one cooling vest will be

tested on a thermal manikin and human subjects. Finally, we will describe the validation of the fabric-PCM-Desiccant model on a wet clothed heated cylinder.

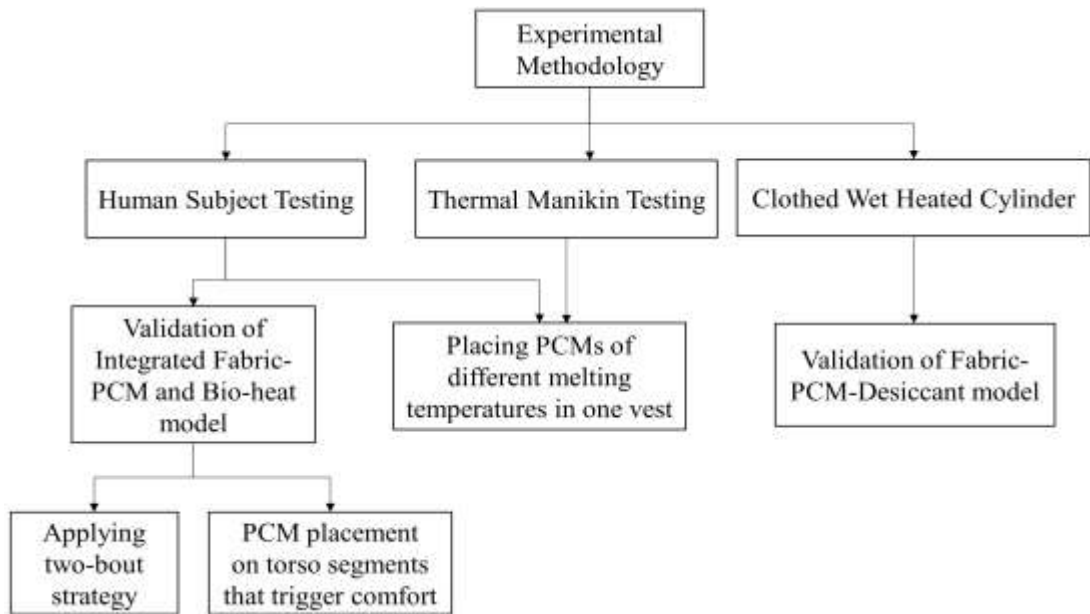


**Fig. 6:** Flowchart of the experimental methodology

## 1. Validation of Integrated Fabric-PCM and Bio-Heat model with Human Subject Testing

### a. Validation Applying Two-Bout Strategy

In this study (Itani et al., 2017c), the cooling vest cases tested on six human subjects at hot environment of 40 °C and 40 % *RH* were used for validating an integrated bio-heat and fabric-PCM model. The objective of this validation was to ensure proper predictions of physiological and subjective data when having a hot environment, moderate activity level (3 MET) and a working duration that was divided into two bouts with transient variation of torso skin temperatures. The ambient conditions of the experiments were equivalent to a *WBGT* of 32 °C, at which the recommended duration for moderate work is about 45 to 50 min (Bates and Schneider, 2008; ISO 7243, 1989). In the tested cases, fixed PCM coverage area over the whole trunk was considered, while varying the PCM melting temperature in the vest with two

trunk was considered, while varying the PCM melting temperature in the vest with two available PCM types of 28 °C and 18 °C melting temperatures. Testing first considered the effect of wearing one cooling vest for the whole duration of 50 min and second wearing in sequence two cooling vests starting first with the high PCM melting temperature followed by the lower one during the same working period, but divided into two 25-min bouts. Human subject testing was performed to record and assess both the physiological data and subjective votes on sensation and comfort.

Participants:

The Institutional Review Board at Qatar University approved to carry out this study on six male subjects, who were students at the university. The number of participants was found adequate for validating the predictions of the integrated model. The participants were acclimatized to the environmental conditions since they have been residents of Qatar for at least six months. In addition, they were healthy and used to working out outdoors in the heat. The average age, height and weight of the participants were  $22.2 \pm 1.1$  years (mean  $\pm$  SD),  $1.74 \pm 0.06$  m and  $75.8 \pm 12.1$  kg, respectively. The participants were asked not to drink alcohol or coffee for at least 24 hours before the experiment and eat or smoke for a minimum of two hours before the experiments. The participants arrived with their personal vehicles to the research laboratory. After briefing the participants about the experiments and signing the consent forms, the experiments were conducted under the supervision of a registered nurse. Fig. 7 (a) shows one participant at QU doing exercise while wearing a cooling vest. A total of four experiments; one without a cooling vest and three with a vest, were done by each of the six participants at a randomized order at the same time of the day (afternoon), with at least two days between the experiments. All the experiments were

conducted in the months May and June, where outdoor ambient temperature and  $RH$  were about  $35 \pm 1$  °C and  $45 \pm 3$  %, respectively.

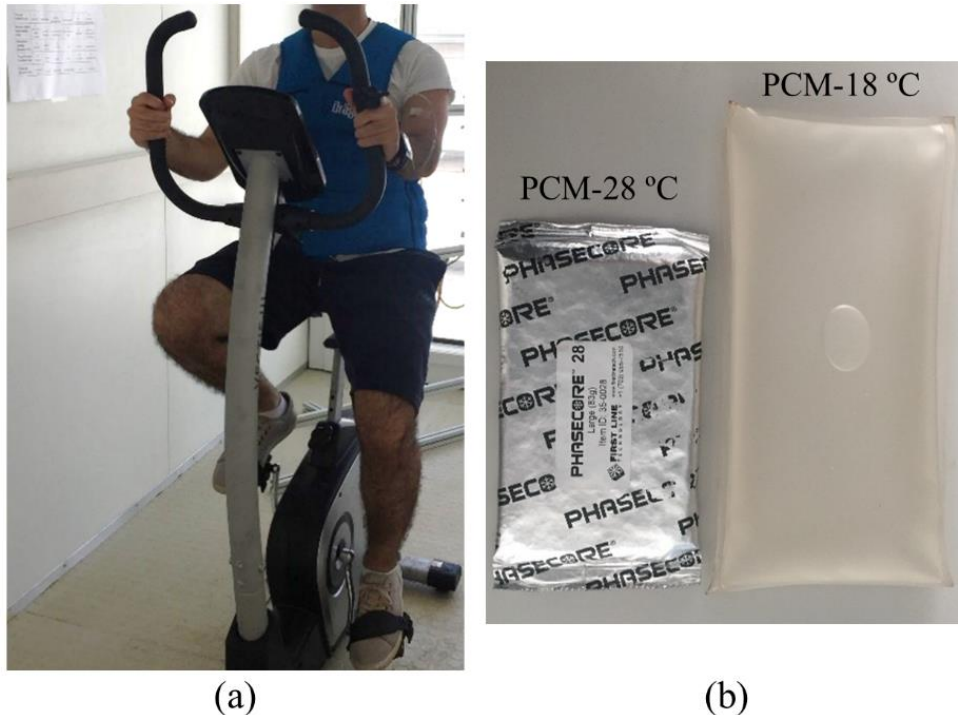


**Fig. 7:** Pictures showing (a) a participant at QU doing exercise while wearing a cooling vest and (b) PCM packets of 28 °C and PCM packets of 18 °C melting temperatures

All the subjects wore an ensemble consisting of similar 50 % cotton-50 % polyester t-shirts and light cotton shorts that were provided to them. For each garment piece, the measured clothing characteristics that include thickness, area density and dry and evaporative resistances are provided in Table 1 (ASTM F1291; ASTM F2370; ISO 5084:1996 and ISO 3801:1977). The cooling vest evaporative resistance and intrinsic insulation were found without the PCM packets, since the fabric-PCM model predicts the macroclimate temperature trapped inside the cooling vest, and does not take the overall vest resistance (vest with packets) as input. Participants wore their own socks (mainly cotton) and shoes (thin-soled with some woven fabric and knit shoes) and their



properties were estimated from standard data bases (Fu, 1995; McCullough et al., 1985 and McCullough, 1989).

**Table 1** Clothing characteristics used in experiments

<b>Clothing</b>	<b>Fiber content</b>	<b>Thickness (mm)</b>	<b>Area Density (g/m<sup>2</sup>)</b>	<b>Intrinsic insulation (m<sup>2</sup>·°C/W)</b>	<b>Evaporative resistance (m<sup>2</sup>·Pa/W)</b>
<b>Cooling vest</b>	100 % polyester	1.01 ± 0.01	824.00 ± 4.00	0.116 ± 0.030	29.50 ± 0.05
<b>T-shirt</b>	50 % cotton, 50 % polyester	0.56 ± 0.01	187.00 ± 1.00	0.042 ± 0.010	2.48 ± 0.02
<b>Shorts</b>	light cotton	0.91 ± 0.05	221.10 ± 9.90	0.014 ± 0.008	4.00 ± 0.30
<b>Socks*</b>	ankle-length & mainly cotton	2.87	386.70	0.004	13.60
<b>Shoes*</b>	thin-soled with some woven fabric and knit	3.50	900.00	0.004	52.00

\* Average data collected from Fu, 1995; McCullough et al., 1985 and McCullough, 1989

*Description of PCM packets and cooling vest cases:*

A polyester cooling vest that was commercially designed to hold up to 20 equally-sized PCM packets was used in this study. The vest had Velcro fasteners to ensure good fitting to the torso of the participants. Two types of PCM packets shown in Fig. 7 (b) were used in this study, having different melting temperatures of 18 °C and 28 °C and other thermo-physical properties as shown in Table 2 (Swedish Emergency & Disaster Equipment AB, 2017; All Safe Industries, 2017).

**Table 2** Thermo-physical properties of PCM packets (Swedish Emergency & Disaster Equipment AB, 2017; All Safe Industries, 2017)

PCM packet	Parameter (unit)	Value
<b>28 °C</b>	Length × Width × Thickness (cm)	11.8×6.8×0.875
	latent heat of fusion (kJ/kg)	159.0
	specific heat capacity (J/kg·K)	3.1
	mass (g)	87.5
<b>18 °C</b>	Length × Width × Thickness (cm)	15.2×6.7×1.3
	latent heat of fusion (kJ/kg)	113.0
	specific heat capacity (J/kg·K)	2.2
	mass (g)	155

The different experiments of this study consisted of subjects doing moderate activity for 50 minutes in a climatic chamber at 40 °C and 40% *RH*. The objective was to split the 50-min working period into two bouts at these environmental conditions, in order to resolve the problems with low PCM melting temperatures, as discussed in the introduction. The working duration was divided into two equally-timed 25-min bouts. In the first 25 min, the participant would have started from rest and would need a certain time to reach the required metabolic rate while his subjective votes are still acceptable. After the 25 min have passed, the participant would have started reaching uncomfortable sensation levels in the no cooling vest case.

In the two-bout cases, the vest used in the second bout would have a lower PCM melting temperature than the first one because the workers, by the end of the first bout, would have noticeable elevations in skin and core temperatures and discomfort levels (Gao et al., 2011). Consequently, a PCM melting temperature of 28 °C was proposed to be used in the first working bout and a PCM melting temperature of 18 °C was proposed to be used in the second working bout. The designation for using two

different melting temperatures for two bouts would be for example **V28** → **V18** where “28” would represent a melting temperature of 28 °C of bout 1 and “18” would be the melting temperature of 18 °C in bout 2.

Comparison of physiological and subjective results between using one cooling vest versus two with different PCM melting temperatures in the same working period was done. When performing the comparison, the cooling vests needed to have the same PCM coverage area, which was about 1600 cm<sup>2</sup> when using 20 packets with 28 °C melting temperature or when using 16 packets of the 18 °C melting temperature. Typically, the vests used for the whole working duration should have a higher PCM weight than those used in the two bouts for the same working period. However, since the packets were not custom-made, a difference in the weights of the vests existed, especially for those having packets with 18 °C melting temperature. The weight of the PCM packets affects the vest cooling duration, while the coverage area affects the vest cooling rate, which in turn affects subjective ratings of the participants, making it the most important factor to control in this study.

A total of four experiments were performed in this study; one without a cooling vest and the remaining with cooling vests, as described in Table 3. The cooling vest cases consisted of two cases with one cooling vest used for the whole working duration of 50 min at **All-V28** and **All-V18** and one case with two cooling vests used consecutively in the same working duration but divided into two equally-timed 25-min bouts (**V28** → **V18**). The PCM packets were cooled overnight to have an initial temperature of 16 °C at the start of all the corresponding experiments, so that all the packets were initially in a solid state.

**Table 3** Different PCM experiments tested on human subjects

<b>Experiment</b>	<b>PCM melting temperature in bout 1- bout 2 (°C)</b>	<b>Number of packets used</b>	<b>Total PCM weight (kg)</b>	<b>PCM coverage (cm<sup>2</sup>)</b>
<b>No vest</b>	-	0	0	0
<b>All-V28</b>	28 - 28	20	1.75	1600
<b>All-V18</b>	18 - 18	16	2.48	1632
<b>V28 → V18</b>	28 - 18	20 → 16	1.75 → 2.48	1600 → 1632

Experimental protocol:

Each experiment performed in this study lasted for 100 min and was conducted at the hot conditions of 40 °C and 40 % *RH* and air speed of 0.2 m/s.

After preparation and then resting at 25 °C and 50 % *RH* for a period of 45 minutes to attain a thermo-neutral state, the participant wearing the PCM cooling vest entered the climatic chamber and performed cycling for 50 minutes on a magnetic upright bike at about 3 MET with a workload of  $25 \pm 4$  Watts (Glass et al. 2007). In the two-bout cases, the participant performed cycling for 25 minutes while wearing the first vest and for another 25 min while wearing the second vest with lower PCM melting temperature. Tympanic temperature was selected to represent the core temperature readings and were taken by a nurse through the ear at the start and every 10 minutes throughout exercise, in order to halt the experiment if core temperature surpassed 38 °C. More frequent sampling was not recommended by the Institutional Review Board, since it might increase the risk of ear injury while taking measurements. Subjective votes were taken at the start and every 5 minutes throughout exercise. In the two-bout cases, the first cooling vest was weighed alone immediately after the first 25-min bout was over. The second vest was worn directly after removing the first one and it took about

half a minute to be done. After finishing the exercise, the cooling vest used in the single-bout cases and the second one used in the two-bout cases, the wet clothing, the participant after towel drying off the sweat remaining on his skin and the wet towel were weighed separately to find the body weight loss. Finally, the participant rested for 10 min.

A halt to the experiments was put if any of the possible situations transpired. The first was if the core temperature exceeded 38 °C (ISO 7243, 1989), the second was if the participant wished to halt the exercise at any time during the experiment. Nevertheless, no experiment was stopped in all the tested cases. Similar to the previously described experimental protocol, the cases without a cooling vest were conducted.

#### *Physiological and physical measurements:*

The weights were taken using a digital bench scale (Quartzell™ Bench Scale 3600SC, Avery Weigh-Tronix – USA, 1 gram resolution and accuracy  $\pm 0.01$  kg of 150 kg capacity). Skin temperatures of seven body segments at 11 locations (left upper arm, left and right chest, left and right abdomen, left and right upper back, left and right lower back, left thigh, and left calf) were measured every 5 minutes by taping iButton sensors (iButton® DS1922L, Maxim Integrated, CA, USA, 0.0625 °C resolution) using a surgical tape on the different segments. The iButton sensors have an average accuracy of  $\pm 0.09$  °C when used at the moderate conditions of  $34.9 \pm 0.1$  °C with a maximum deviation of 0.4 °C (Nakayoshi et al., 2014; van Marken Lichtenbelt et al., 2006). Moreover, a delay for correct temperature reading of about 2 minutes was considered, when the vests of bouts 1 and 2 were worn, in order to account for the thermal response time of the iButton sensors. In addition, the heart rate and core temperature,  $T_{cr}$ , were

measured every 5 and 10 minutes, respectively, via a wristband pulse oximeter (CMS-50F, accuracy  $\pm 2$  %) and an infrared tympanic thermometer, *IRTT*, (Braun ThermoScan® 7 IRT6520, Braun, Kronberg, Germany, accuracy  $\pm 0.2$  °C), respectively. Then, the change in core temperature from its initial state,  $\Delta T_{cr}$ , was found. In a recent study, good reliability of new generations of *IRTTs* in reflecting core temperature was found, if disposable shields are used and frequent cleaning is applied (Haugan et al., 2012). In addition, *IRTT* is easy to use and time efficient, more hygienic and acceptable to participants than rectal and was used in recent studies (Chudecka and Lubkowska, 2016; Haugan et al., 2012). In the current study, the results are used for validating the integrated bio-heat and fabric-PCM model and the same *IRTT* was used for all subjects. Thus, it was assumed that any potential measurement error was the same for all subjects, while applying all precautions recommended in taking the readings, as an indication for stopping the experiment.

The mean skin temperature,  $T_{sk,mean}$ , was evaluated using the formulation  $T_{sk,mean} = 0.3T_{chest} + 0.3T_{arm} + 0.2T_{thigh} + 0.2T_{leg}$  (Ramanathan, 1964). Then, the change in mean skin temperature from its initial state,  $\Delta T_{sk,mean}$ , was found. The torso skin temperature was evaluated by taking the average of 8 sensor readings distributed on the front and back torso, to accurately represent the parts that were either covered or not by the PCM packets. Body weight loss or sweat production was evaluated by the difference in the clothed subject weight before and after the exercise, after correcting it for any sweat absorbed in the clothing (Ilmarinen et al., 2004). Finally, the change in body heat storage,  $S$ , was found according to Chou et al. (2008) using the expression in equation (23) as an indication of the cooling performance of the vests and the estimated PCM weight needed in a specific cooling duration:

$$S = \frac{\Delta T_b \times m_b \times C_b}{t} \quad (23)$$

where  $m_b$  is the human body mass,  $C_b$  is the body specific heat and is equivalent to 3470 J/kg·°C,  $t$  is the working period, and  $\Delta T_b$  is the change in the mean body temperature from the start of the work period till the end defined as follows:

$$\Delta T_b = 0.8 \times \Delta T_{cr} + 0.2 \times \Delta T_{sk,mean} \quad (24)$$

Subjective votes and statistical analysis:

At the start and every 5 min throughout the experiment, the participant reported his subjective votes using the reference scales for overall thermal comfort,  $TC$ , (*0 neutral, 1 comfortable, 2 slightly uncomfortable, 3 uncomfortable, 4 very uncomfortable, 5 extremely uncomfortable*) and torso thermal sensation,  $TTS$ , (*0 neutral, 1 slightly warm, 2 warm, 3 hot, 4 very hot, 5 extremely hot*) (Reinertsen et al., 2008). The effect of wearing no vest, one cooling vest and two cooling vests for the same working duration was examined using paired samples t tests, with the statistical significance set at  $p < 0.05$ .

b. Validation with Placement of PCM Packets on Torso Segments that Trigger Comfort

Human subject experimentation:

The approvals of the Institutional Review Boards at the American University of Beirut and Qatar University allowed 6 healthy males to participate in the study. The sample size used in this study was found adequate for validating the predictions of the integrated model as was done with one human subject for validating a similar bio-heat model in the study of Pokorný et al. (2017). The participants had an average age of  $21.5 \pm 1.1$  years (mean  $\pm$  SD), height of  $1.75 \pm 0.05$  m and weight of  $75.5 \pm 7.7$  kg. Each subject participated in seven experiments, one without a cooling vest and six with a cooling vest with different PCM arrangement worn over the t-shirt. The participants

wore similar clothing garments described in *section a. Validation Applying Two-Bout Strategy*.

The integrated bio-heat and fabric-PCM model were validated against experimental data of human subjects performing cycling on a magnetic upright bike at about 3 MET in moderate environmental conditions of  $35\text{ }^{\circ}\text{C} \pm 0.5\text{ }^{\circ}\text{C}$  for an exercise period of 45 minutes. The subjects were wearing cooling vests with different placements of 14 PCM packets of  $28\text{ }^{\circ}\text{C}$  melting temperature or they were not wearing a vest. The number of PCM packets needed so that total melting of the packets did not occur was found by performing preliminary simulations such that the PCM melted fraction is above 0.85 for effective use of the PCMs. According to the preliminary simulations, 12 PCM packets would be needed to ensure almost complete melting in 45 minutes. However, 14 packets were selected by design for the tests to make sure that total melting does not happen during experiments and hence accounting for any possible deviation in the model from real situation.

Similar protocol, as described in *section a. Validation Applying Two-Bout Strategy*, was followed to record physiological and physical measurements and subjective ratings of the human subjects. More details can be found in Ouahrani et al. (2017)

*Description of PCM arrangements in cooling vest tested on human subjects:*

The PCM packets used were made up of a salt mixture of sodium sulfate and water known as Glauber's salt at melting temperature of  $28\text{ }^{\circ}\text{C}$ . The packets were cooled overnight to have an initial temperature of  $20\text{ }^{\circ}\text{C}$ . As mentioned earlier, a total number of 14 PCM packets are used in the vest for the experiments and validation of the integrated model. Given that the maximum number of packets that can be held on the



back or the front was 10, the choice of 14 packets still allowed a significant variation in coverage area by the PCM between the upper front (UF), lower front (LF) and back torso segments. Thus, the options of full 100% back/front coverage with partial front/back coverage were possible, in order to identify the optimal PCM placement on comfort.

**Table 4** PCM arrangements of the different experiments on the UF, LF and back

<b>PCM Arrangement</b>	<b>PCM on UF</b>	<b>PCM on LF</b>	<b>PCM on Back</b>	<b>Total PCM in Vest</b>
<b>No vest</b>	0	0	0	0
<b>4UF-0LF-10B</b>	4	0	10	14
<b>2UF-2LF-10B</b>	2	2	10	14
<b>0UF-4LF-10B</b>	0	4	10	14
<b>4UF-2LF-8B</b>	4	2	8	14
<b>4UF-4LF-6B</b>	4	4	6	14
<b>6UF-4LF-4B</b>	6	4	4	14

Seven different variations of the **14** PCM arrangements in the cooling vest were tested as described in Table 4 and are shown in the schematics of Fig. 8 (a-f). These arrangements were tested experimentally on participants wearing the vest. The commercially available vest can hold a maximum of 10 PCM packets on the back, 6 on the UF and 4 on the LF torso segments. Thus, the PCM arrangement with **4UF-0LF-10B** represented the case where **4** packets were placed on the UF torso segment, **0** on the LF and the remaining **10** packets were placed on the back, as shown in Fig. 8 (a). In arrangement **2UF-2LF-10B**, the number of packets on UF was decremented by **2** packets so that **2** packets were placed on UF, **2** on LF and the remaining **10** on the back, as shown in Fig. 8 (b). Thus, the effect of placing more packets on the UF or LF torso segments on comfort can be assessed. In arrangement **4UF-2LF-8B**, the number of

packets on UF was incremented by 2 while that at the back was decremented by 2, and so on for the remaining arrangements. Each PCM arrangement experimental test was repeated six times, in addition to the no PCM vest case.

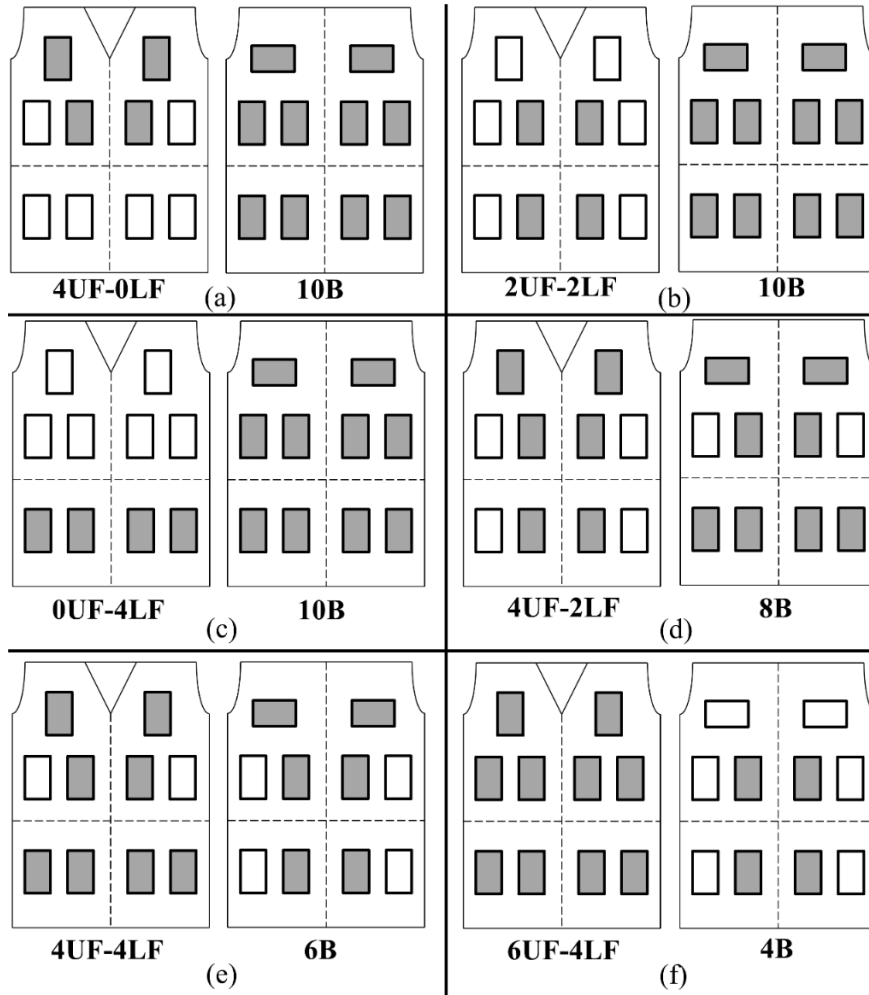


**Fig. 8:** Schematic showing the PCM placement cases (a) 4UF-0LF-10B, (b) 2UF-2LF-10B, (c) 0UF-4LF-10B, (d) 4UF-2LF-8B, (e) 4UF-4LF-6B and (f) 6UF-4LF-4B

## ***2. Testing on a Thermal Manikin and on Human Subjects of PCM Packets of Different Melting Temperatures Used in One Cooling Vest***

In the presence of two melting temperatures in the same vest, improvement in PCM vest cooling effect might be achieved by proper placement of packets with different melting temperatures on the upper and lower torso segments. Experimentation

on a thermal manikin will be first done to test the cooling power of the different PCM arrangements either with one or with two melting temperatures simultaneously and conclude the best arrangements among them. However, for complete vest assessment for comfort and cooling, experiments on human subjects are performed to obtain physiological and thermal response data and subjective comfort and sensation votes. Thus, testing different PCM arrangements in the vest on human subjects would provide closure on the selection of the optimal tested arrangement.

*Thermal manikin clothed with cooling vest at constant temperature mode:*

The aim of the manikin experiments is to investigate the significance of the arrangement on the cooling effect when using two different melting temperatures in the vest against using only one melting temperature. Random mixing between the two types of PCM packets in the vest will not be considered, however, the criteria will be placing each PCM type on either the upper or lower torso segments. Placing the packets with the higher melting temperature on the upper torso segments, might enhance the microclimate air flow rate and thus affect the vest cooling performance. It should be kept in mind that the total PCM coverage area in all the vests will be fixed and divided equally on the front and back torso segments, while varying the position of the two PCM types on the torso. Since the PCM vest covers only the torso segments of the thermal manikin, the shoulders, chest, abdomen and back segments were included in the assessment of the vest cooling effect by finding their average heat flux.

The cooling power of the PCM vest under four different PCM arrangements was initially measured on the 20-zone “Newton” thermal manikin shown in Fig. 9. A constant thermal manikin skin temperature at 35 °C was used to record the cooling power of the different PCM packets on the torso segments. The different cooling vest arrangements tested have the same PCM coverage area of 1,224 cm<sup>2</sup> and have either a

uniform melting temperature in the vest or two temperatures simultaneously. Table 5 shows the four different experiments done on the thermal manikin.

Many variables should be controlled when using two melting temperatures in the same vest. The choice of the coverage area and the number of packets in the vest for the different experiments is based on having enough packets to cover a good portion of the torso. The total coverage area in all the vests will be fixed at 1,224 cm<sup>2</sup> and divided equally on the front and back torso segments with 612 cm<sup>2</sup> covering each, while varying the position of the two PCM types (18 °C and 28 °C melting temperatures) on the torso (chest, abdomen, lower back and upper back). In the cases using two melting temperatures simultaneously, 6 packets of 18 °C melting temperature are equivalent in coverage area to 8 packets of 28 °C melting temperature. However, a maximum weight difference of 0.46 kg is present when considering all packet of 18 °C or all packets of 28 °C. The added weight, if worn by a human would have a slight effect on his metabolism; however, on a thermal manikin weight is irrelevant in this case.

The manikin was clothed with a long sleeved cotton shirt and trousers as shown in Fig. 9. The experiments were conducted in a climatic chamber at the moderate ambient temperature of  $32 \pm 0.5$  °C and  $45 \pm 3\%$  relative humidity. The thermal manikin divides the torso into 4 segments, which include the shoulders or upper back, chest, stomach or abdomen and back. The segmental heat fluxes were recorded every minute using the ThermDAC control software (Burke et al., 2009) and then used to find the average torso heat flux. The thermal manikin, which was present in the climatic chamber over the night, was turned on after the room conditions as well as the thermal manikin reached steady values of  $32 \pm 0.5$  °C (after about 3 hours). The manikin was turned on to reach a constant skin temperature of 35 °C and the cooling vest was put on once the skin temperature was attained (after about 45 min). The PCM packets at initial

temperature of 15 °C were placed inside the vest pockets adjacent to the upper and lower torso segments. The whole process of placing the packets in the vest and clothing the manikin took around two minutes and the duration of the experiment was 200 minutes. The experiments on the manikin were repeated twice and average values were used for analysis, were each experiment was conducted on a separate day.

**Table 5** Different PCM arrangements tested on thermal manikin

<b>PCM Arrangement</b>	<b>PCM coverage on front/back (cm<sup>2</sup>)</b>	<b>Number of 18 &amp; 28 °C packets used</b>	<b>Total PCM weight (kg)</b>
<b>28U-18L</b>	612/612	6 & 8	1.63
<b>18U-28L</b>	612/612	6 & 8	1.63
<b>28F-28B</b>	612/612	0 & 16	1.40
<b>18F-18B</b>	612/612	12 & 0	1.86



**Fig. 9:** Picture showing Newton thermal manikin clothed with the PCM cooling vest

Human subject experimentation:

Ethical approval to carry out the study on six male subjects was obtained from the Institutional Review Board at Qatar University. The average age of the participants was  $22.3 \pm 1.5$  years (mean  $\pm$  SD), the average height was  $1.73 \pm 0.05$  m and average weight was  $75.9 \pm 9.8$  kg. Fig. 10 (a) shows a picture at QU for one participant doing exercise while wearing a vest. Each participant was asked to do seven experiments at the same time of the day with at least two days between them; one without a PCM cooling vest and six with the vest but with different PCM arrangement at a randomized order. Similar protocol, as described in *section a. Validation Applying Two-Bout Strategy*, was followed to record physiological and physical measurements and subjective ratings of the human subjects.

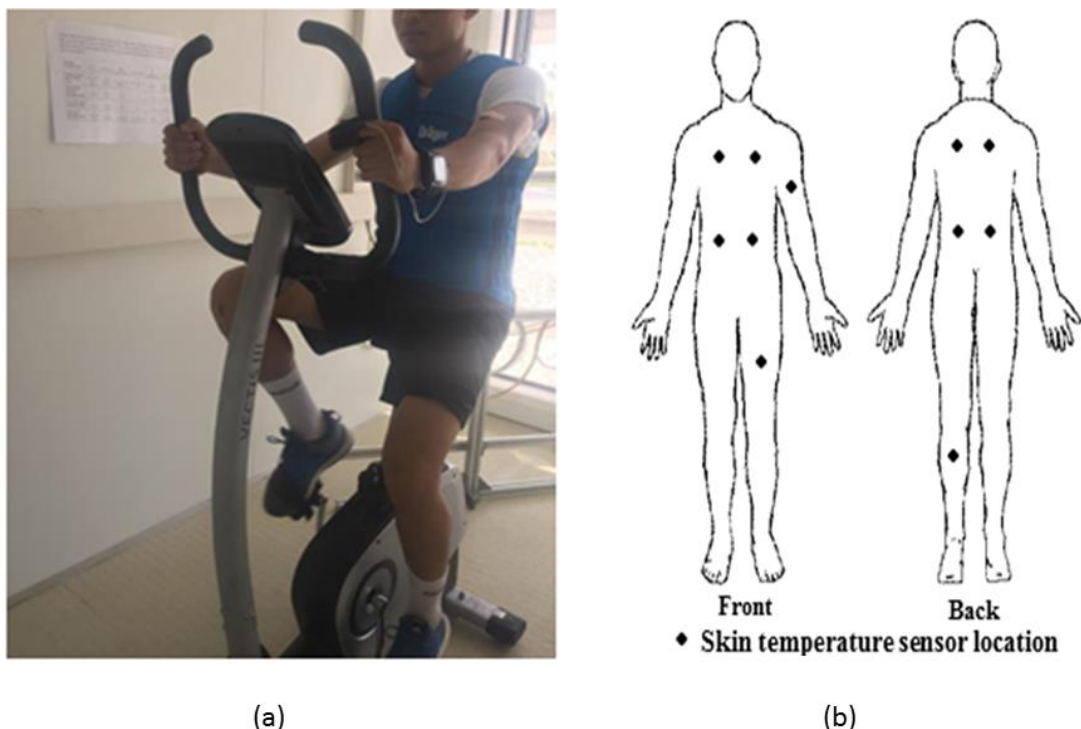


**Fig. 10:** Pictures showing (a) one participant doing exercise while wearing a vest at QU and (b) skin temperature sensor locations on body segments

**Table 6** Different PCM arrangements tested on human subjects

<b>PCM Arrangement</b>	<b>PCM coverage on front/back (cm<sup>2</sup>)</b>	<b>Number of 18°C and 28 °C packets used</b>	<b>Total PCM weight (kg)</b>
<b>No vest</b>	0	0 & 0	0
<b>28U-18L</b>	612/612	6 & 8	1.63
<b>18U-28L</b>	612/612	6 & 8	1.63
<b>28F-28B</b>	612/612	0 & 16	1.40
<b>18F-18B</b>	612/612	12 & 0	1.86
<b>28F-18B</b>	612/612	6 & 8	1.63
<b>18F-28B</b>	612/612	6 & 8	1.63

*Description of cooling vest arrangements tested on human subjects:*

The different PCM arrangements corresponding to the human subject testing are described in Table 6. Six different PCM arrangements and a no vest case will be tested while the subjects are doing moderate activity on a magnetic upright bike for 45 minutes in a climatic chamber at 35 °C and 50 % relative humidity. All the PCM packets were cooled overnight to have an initial temperature of 15 °C at the start of every experiment. The PCM melting temperatures are chosen such that a good temperature gradient exists between the skin and the PCM temperature as well as a substantial difference between the two melting temperatures themselves accompanied with high latent heats of fusion. The melting temperatures used in this study were 18 °C and 28 °C and their properties are described in Table 2. It should be noted that two additional vest cases were tested on the human subjects that were not tested on the manikin, which are 18F-28B and 28F-18B. The former two cases would result in the same heat flux if tested on the manikin, however, if tested on human subjects, then

physiology due to different segmental sensitivity to cooling may influence subjective votes and result in additional factors affecting the selection of the best cooling vest.

More details on the experimental methods can be found in Ouahrani et al. (2017).

### ***3. Validation of Fabric-PCM-Desiccant on a Wet Clothed Heated Cylinder***

Validation of the fabric-PCM-Desiccant model is done by conducting experiments on clothed heated cylinder with a solid desiccant packet placed in contact to the PCM packet on the inner side of the clothing. The data collected from the experiment, which include the microclimate and macroclimate air temperatures, the temperature variation of the PCM packet and the desiccant and the moisture content of the microclimate air layer are compared with their equivalent predicted by the model to validate it for certain environmental conditions, wind speed, clothing permeability and thermal properties and geometry. The thermal resistance between the PCM and the desiccant in the PCM-Desiccant packet is also found by using equation (14).

#### ***PCM-Desiccant packet:***

The PCM-Desiccant packet used in the experiments has dimensions of 118 mm  $\times$  50 mm  $\times$  15 mm and a total mass of the PCM and the solid desiccant of 100.47 grams, of which 15.64 grams are for the desiccant. The desiccant packet has dimensions of 80 mm  $\times$  29 mm  $\times$  7 mm and was not protruding out of the PCM packet. The material used for the PCM in the experiment constitutes of a salt mixture of sodium sulfate and water and has a melting temperature of 28 °C and a density of 1239 kg/m<sup>3</sup> (Gao et al., 2010; Swedish Emergency & Disaster Equipment AB, 2017). The desiccant used in the experiment is silica gel granules of Type A, with a bulk density of 750 kg/m<sup>3</sup> placed



inside a water vapor permeable membrane made up of polypropylene. The volume fraction of the desiccant in the PCM-Desiccant packet was 18 %, covering 39 % of the surface area of the PCM packet facing the microclimate air layer.

*Thermal resistance between PCM and desiccant:*

The total thermal resistance to conduction between the PCM and the desiccant packet is due to the adhesive tape that bonds the PCM packet to the desiccant one as well as the desiccant membrane that holds the desiccant. The adhesive is thermally conductive, with a thermal conductivity of 0.6 W/m·K and thickness of  $1.27 \times 10^{-4}$  m, to ensure good contact between the PCM and the desiccant without having air gaps in between. The desiccant membrane has a thermal conductivity of 0.2 W/m·K and thickness of  $1 \times 10^{-5}$  m. The thermal storage or capacity in the thermally conductive adhesive and the desiccant membrane is considered negligible. Thus the resultant total thermal resistance for conduction,  $R_{tot}$ , has a value of  $2.62 \times 10^{-4}$  m<sup>2</sup>·K/W or 0.11 K/W with a desiccant area of 23 cm<sup>2</sup>, which is required as input to the fabric-PCM-Desiccant model. The resistance to heat transfer between the PCM-Desiccant packet and the micro and macro climate air layers is represented by the reciprocal of the convective heat transfer coefficient.

*Experimental setup:*

The experiment is conducted on a wet clothed heated cylinder, similar to the one used in the study of Ghaddar et al. (2010), and placed in a climatic chamber with ambient conditions maintained at  $28 \pm 0.5$  °C and relative humidity of  $50 \pm 2$  % and wind speed at 0.3 m/s, as shown in the schematic in Fig. 11. Air was supplied from

grills placed at a height of 2 m from floor level in a climatic chamber of a height of 2.8 m. The wind speed was measured using 731A anemometer with an accuracy of 3%.

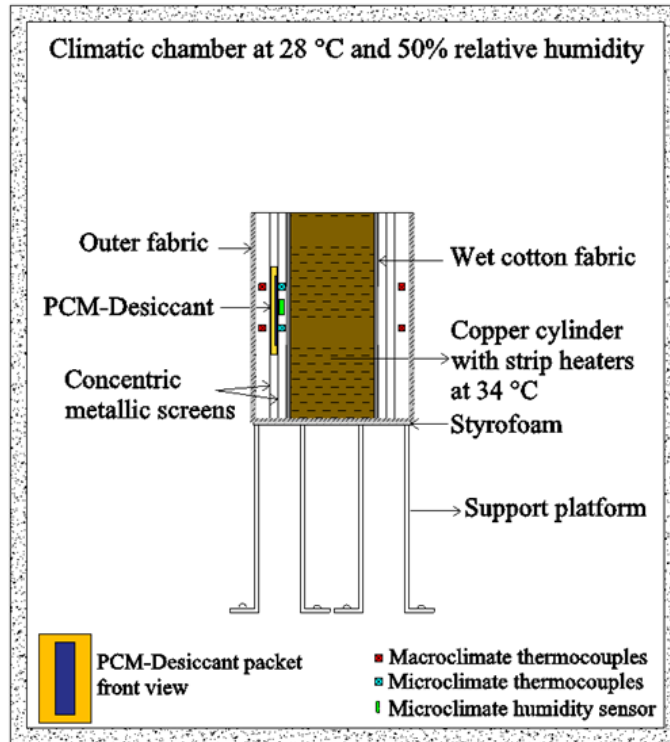


**Fig. 11:** Schematic of the experimental setup of the wet clothed inner heated cylinder

The heated cylinder used is made up of copper and has a diameter of 0.104 m and a length of 0.215 m. The copper cylinder is wrapped with Omega-KH-1012 highly conductive metallic resistance heaters to produce a constant heat flux condition per heater at the cylinder surface. Independent regulation of the heat fluxes from the different strip heaters is done to ensure a uniform mean steady surface temperature of  $34\text{ °C} \pm 0.5\text{ °C}$  for each strip heater. The copper heated cylinder is wrapped by a wet stretch fabric completely wetted before being placed around the heaters. It is ensured that no water is dripping from the wet stretch fabric and that no dry areas appear on its surface through monitoring the wet fabric temperature. After about 30 minutes, the wet fabric temperature reached a uniform mean steady temperature of  $33\text{ °C} \pm 0.5\text{ °C}$ . Then,

two concentric thin metallic screens (0.215 m long each) are used to guard the wet clothed heated cylinder and hold the PCM-Desiccant packet (inner and outer guards), as shown in Fig. 11. The diameters of the concentric inner and outer guards are 0.108 m and 0.128 m, respectively. A third 0.215 m long guard with a 0.14 m diameter, the outer fabric guard, made up of a metallic mesh is used to hold the outer fabric layer. The wet clothed cylinder and its guards are fixed on an insulated support platform made up of Styrofoam material at the bottom of the cylinder so that minimal heat and mass transfer take place at the bottom.

The cotton fabric used in the experiment is obtained from Testfabrics Inc. (Middlesex, NJ 08846) (Testfabrics, 2017), and is made of knitted cotton, style #473 of thickness of 1 mm. The permeability of the clothing is measured by SDL MO2IA air permeability tester with a percent deviation in repeated measurements of  $\pm 0.9\%$  and an accuracy of  $10^{-4} \text{ m}^3/(\text{m}^2 \cdot \text{s})$  and is found to be  $0.65 \text{ m}^3/(\text{m}^2 \cdot \text{s})$ . The tester is characterized by fast, simple, and accurate determination of the air permeability of all kinds of flat materials. The cotton fabric dry thermal resistance and evaporative resistance are measured using the sweating guarded hotplate (Model 306-200/400) and found to be  $0.023 \text{ m}^2 \cdot \text{K}/\text{W}$  and  $16.77 \text{ Pa} \cdot \text{m}^2/\text{W}$ , respectively, with an error less than 0.1 %.

Microclimate and macroclimate air layers are formed by arranging the outer clothed cylinder and the metallic guards around the clothed heated cylinder. The temperature of the microclimate air layer is measured via two T-type thermocouples placed on the metallic guards in the layer neighboring the PCM-Desiccant packet (Fig. 11). Furthermore, the temperature of the macroclimate air layer was measured using six T-type thermocouples placed at different positions in the layer neighboring the outer clothed cylinder. The humidity ratio of the microclimate air layer was measured using OM-EL-USB-2 sensor with an accuracy  $\pm 3\%$  in reading the relative humidity. In order

to measure the temperatures of the PCM and the desiccant, T-type thermocouple are also used and placed inside each one of them. The PCM and desiccant packets were well-sealed using epoxy to prevent any leakage. Regeneration of the solid desiccant to restore its adsorption capacity was done by placing it in a hot oven at 75 °C for six hours and then placed in a plastic bag to cool down in the ambient room air.

Experimental protocol:

At the start of the experiment, the heated vertical cylinder was turned on and kept for about 30 minutes to reach a steady wet fabric surface temperature of 33 °C ± 0.5 °C. After that, the PCM with the desiccant membrane packet, initially at 26 °C was brought and covered with a removable plastic cover. The regenerated solid desiccant, initially at 26 °C, was inserted in the desiccant membrane shielded with a plastic cover to avoid moisture transport to the desiccant while preparing the PCM-Desiccant packet. Then, after ensuring a uniform thickness of the desiccant layer, sealing the packet and removing the plastic cover, the PCM-Desiccant packet was inserted in its allocated position on the metallic guards. Thus the PCM-Desiccant packet together with the metallic guards and the outer clothed cylinder can be then placed around the heated cylinder. The previous step took about 2 minutes while data about the different parameters started logging. The thermocouples reading the microclimate and macroclimate temperatures and the PCM and desiccant temperatures were connected to OM-DAQPRO-3500 data logger set to take a reading every 10 seconds. Another experiment was also performed with a PCM packet (without the desiccant packet). The PCM packet had the same weight of about 85 grams compared to the weight of the PCM in the PCM-Desiccant packet.

## CHAPTER IV

### RESULTS AND DISCUSSIONS

In this chapter, the results and discussions of the human subject testing and validation of the integrated fabric-PCM and bio-heat model will be presented for: 1) applying the two-bout strategy and 2) placing PCM packets on torso segments that trigger comfort. Then, the results for the human subject and thermal manikin testing of the placement of PCM packets having different melting temperatures in one cooling vest will be discussed. Finally, the experimental results obtained on a wet clothed heated cylinder and those predicted by the fabric-PCM-Desiccant model will be presented.

#### **A. Integrated Fabric-PCM and Bio-Heat model simulations and Human Subject Testing**

##### ***1. Applying Two-Bout Strategy***

In this section, comparison of physiological data and subjective votes on sensation and comfort between the experimental and the integrated model results was done. Three reference cases existed; no vest and one vest with uniform packets of 28 °C and 18 °C melting temperatures (**All-V18** and **All-V28**). The remaining case considered wearing two cooling vests in a two-bout working duration (**V28** → **V18**).

##### **a. Physiological responses of skin and core temperatures, heart rate and sweat produced**

Comparison was done between model and experimental results of physiological data (torso skin temperature and sweat produced) for a hot environment (40 °C and 40 % *RH*), moderate activity level (3 MET) and a two-bout working duration

with transient variation of torso skin temperature. The simulation and experimental data (mean  $\pm$  SD) of local torso skin temperature during exercise for 50 min for the different cases are presented in Fig. 12 (a). Initially, the torso temperature was similar in all the cases, since the participants started from a thermo-neutral steady-state condition at 25 °C and 50 % *RH*. As it is expected, the no vest case had the highest temperature values throughout the 50 min continuous exercise reaching a maximum of 36.9 °C, as predicted by the model. In the presence of the cooling vests, the model was capable of predicting the drop in torso temperature upon wearing the vests in the first 5 min of exercise and after 25 min in the two-bout case, due to the relatively low PCM initial temperature of 16 °C. Good agreement between the model and experimental results was found for the transient temperature variation upon wearing the second cooling vest in **V28**  $\rightarrow$  **V18**.

In the first 25 min, the simulated torso temperature covered with 28 °C packets (cases **All-V28** and **V28**  $\rightarrow$  **V18**) had identical trends that started increasing after the initial drop to reach stable values in about 22 min of exercise. However, in case **All-V18**, the torso skin temperature kept on decreasing until reaching stable values in about 25 min due to the melting of the PCM packets. In the second 25-min bout, the simulated torso temperatures in **All-V18** and **V28**  $\rightarrow$  **V18** reached similar stable values in the last 10 min of exercise, with 0.66 °C maximum difference from experimental data. The reason behind this was that the packets were melting at a constant temperature with identical PCM coverage area. Similar reductions in local skin temperatures upon wearing cooling vests incorporating different melting temperatures were found in previous studies (Gao et al., 2012; House et al., 2012). Moreover, all vest cases showed an experimental ( $p < 0.02$ ) and simulated significant difference in torso skin temperature

from the no vest case at all times of exercise, except case **All-V28**. Total melting of any type of PCM packets used in the different experiments did not occur.

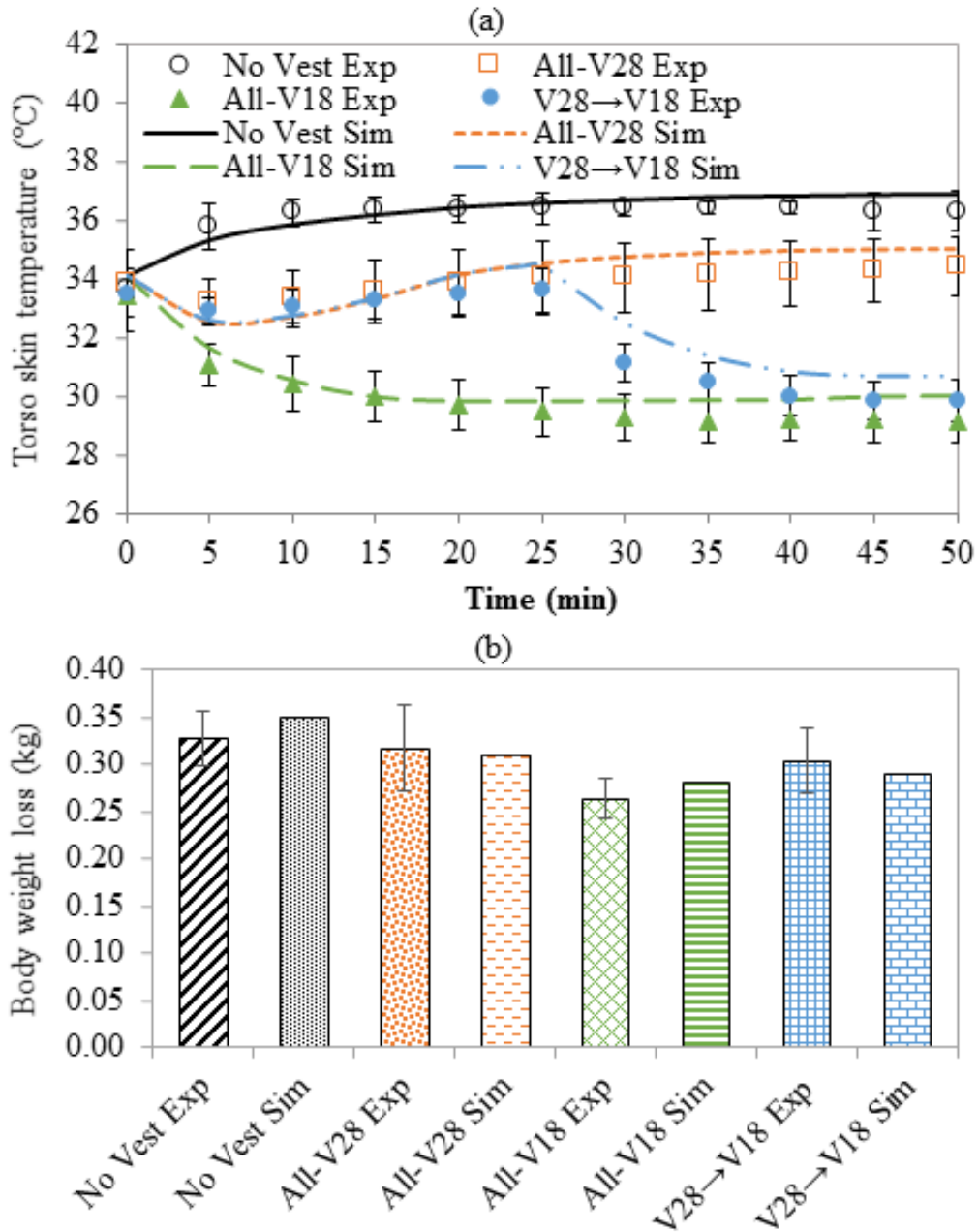


**Fig. 12:** Simulation and experimental data (mean  $\pm$  SD) of (a) local torso skin temperature during exercise for 50 min and (b) body weight loss after exercise for the different cases

The simulated and experimental (hatched bars) sweat produced or body weight loss for all the cases are shown in Fig. 12 (b). The maximum body weight loss was in the no vest case with a value of  $0.33 \pm 0.03$  kg, and it decreased slightly in cases **All-V28** and **V28**  $\rightarrow$  **V18**. Only case **All-V18** decreased significantly ( $p < 0.05$ ) the body weight loss from the no vest case to  $0.26 \pm 0.02$  kg. Similar results were predicted by the two-bout model, with 8 % maximum difference from mean experimental data. Typically, the results indicated that covering the torso with packets of lower melting temperatures led to higher suppression of sweat production, as previously found at similar activity levels and hot conditions (Gao et al., 2011; House et al., 2012).

At the hot condition of 40 °C, experimental heart rates in all cases had similar trends of variation, increasing initially from  $83 \pm 5$  bpm and reaching highest toward the end of exercise at about  $97 \pm 8$  bpm, as shown in Fig. 13 (a). No significant difference ( $p > 0.05$ ) at all times of exercise was found among any of the vest cases, which could be due to the light load. However, it could also be due to using 18 °C PCM packets as the lowest melting temperature, which would not show a significant effect on heart rate. In a similar study, House et al. (2012) performed experiments on human subjects doing stepping exercise in an environment at 40 °C and tested 4 cooling vests having PCMs of 0 °C, 10 °C, 20 °C and 30 °C melting temperatures. Their results showed a significant difference only with the vest filled with PCMs of 0 °C melting.

Results for the experimental change in mean skin,  $\Delta T_{skin,mean}$ , core temperatures, body temperatures from the start of the experiment for single-bout cases and for every bout of two-bout case (bout 1:  $T$  (at  $t = 25$  min) -  $T$  (at  $t = 0$  min) and bout 2:  $T$  (at  $t = 50$  min) -  $T$  (at  $t = 25$  min)) are presented in Table 7. In addition, the transient variation of simulated and experimental (mean  $\pm$  SD)  $T_{cr}$  and  $T_{skin,mean}$  are presented in Fig. 13 (b) and (c), respectively. Initially, the mean skin temperatures,  $T_{skin,mean}$ , and core



temperatures,  $T_{cr}$ , were at similar values in all the cases due to starting from a thermo-neutral state and were at  $33.33 \pm 0.5$  °C and  $37.04 \pm 0.2$  °C, respectively. No significant difference was found in  $\Delta T_{cr}$ , between any of the cases over the whole period or over about 1 or about 2 periods as can be seen from Fig. 13 (b) and Table 7. These results are similar to the findings of House et al. (2012) who also reported no significant differences in the rectal temperature between all the 4 cooling vests they tested.

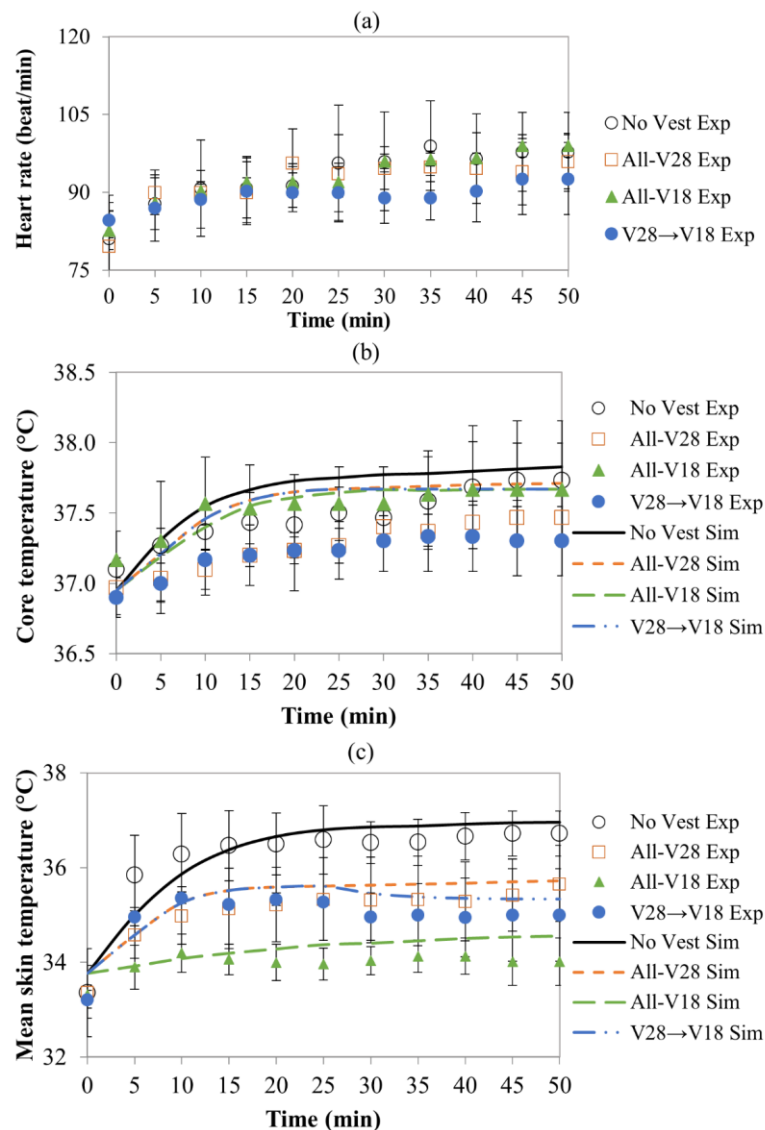


**Fig. 13:** Transient variation of the (a) experimental (mean  $\pm$  SD) heart rate and simulated and experimental (mean  $\pm$  SD) (b) core temperature and (c) mean skin temperature during 50 min exercise for the different cases

**Table 7** Change in mean skin, core and body temperatures from the start of the experiment for single-bout cases and for every bout of two-bout case (bout 1:  $T$  (at  $t=25$  min) -  $T$  (at  $t=0$  min) and bout 2:  $T$  (at  $t=50$  min) -  $T$  (at  $t=25$  min))

Case	$\Delta T_{skin,mean}$ (°C)		$\Delta T_{cr}$ (°C)		$\Delta T_b$ (°C)	
	Total period (bout 1+ bout 2)					
<b>No vest</b>	3.36 ± 0.9		0.7 ± 0.3		1.23 ± 0.3	
<b>All-V28</b>	2.29 ± 0.8		0.5 ± 0.2		0.86 ± 0.2	
<b>All-V18</b>	0.70 ± 0.5*		0.5 ± 0.4		0.54 ± 0.2*	
<b>V28 → V18</b>	1.78 ± 0.2*		0.4 ± 0.1		0.68 ± 0.1*	
	$\Delta T_{skin,mean}$ (°C) <b>bout 1</b>	$\Delta T_{skin,mean}$ (°C) <b>bout 2</b>	$\Delta T_{cr}$ (°C) <b>bout 1</b>	$\Delta T_{cr}$ (°C) <b>bout 2</b>	$\Delta T_b$ (°C) <b>bout 1</b>	$\Delta T_b$ (°C) <b>bout 2</b>
	2.06 ± 0.2*	-0.28 ± 0.2	0.3 ± 0.1	0.1 ± 0.1	0.66 ± 0.1*	0.02 ± 0.1

\* Significant statistical differences ( $p < 0.05$ ) between the vest case and the no vest one

Although the results show how the single-bout cases had similar trends of variation for  $T_{skin,mean}$ ,  $T_{cr}$  and  $T_b$ , however there were significant differences in  $T_{skin,mean}$  between **No vest** ( $3.36 \pm 0.9$  °C) and **All-V18** ( $0.70 \pm 0.5$  °C) and between **No vest** ( $3.36 \pm 0.9$  °C) and **V28→V18** ( $1.78 \pm 0.2$  °C), as shown in Table 7 and in Fig. 13 (c). The change in  $T_{skin,mean}$  during bout 2 of **V28→V18** was  $-0.28 \pm 0.2$  °C, which indicates a slight drop in mean skin temperature upon wearing the second cooling vest, as shown in Fig. 13 (c). This drop was not significant due to attainment of almost stable states for core and skin temperatures of the uncooled body segments, at the defined environmental conditions and activity level. The uncooled body segments constitute 70 % of the computed mean skin temperature (Ramanathan, 1964). In the single bout cases and after about 20 min of exercise,  $T_{skin,mean}$  reached values that varied slightly over the remaining 30 min of exercise (see Fig. 13 (c)). It is noted that  $T_{cr}$  in **All-V18** was the highest

among the vest cases due to starting from a slightly higher temperature at the start of exercise, however,  $\Delta T_{cr}$  was similar in the different vest cases but lower than the no vest case.

b. Thermal comfort and sensation

The simulation and experimental data (mean values  $\pm$  SD) of torso thermal sensation, *TTS* and overall thermal comfort, *TC*, during exercise for the different cases are shown in Fig. 14 (a) and Fig. 14 (b), respectively. An increasing trend was noticed in the no vest case with the poorest *TC* and highest *TTS* values among all the cases throughout exercise, reaching  $3.83 \pm 0.9$  (close to very uncomfortable) and  $3.67 \pm 0.7$  (close to very hot) at the end, respectively. The model predictions, at the hot ambient conditions and moderate activity level, were in good agreement with the experimental ones with an accuracy of  $\pm 0.55$  in *TTS* and  $\pm 0.58$  in *TC*.

It can be noticed from Fig. 14 (a) that in all the vest cases and irrespective of the PCM melting temperature, *TC* and *TTS* had similar values in the first 15 to 20 min of exercise, in both simulated and experimental results. This indicated that using packets of lower melting temperature at early periods of exercise is not necessary for improving *TC* and *TTS* levels. Participants in **All-V28** and **V28**  $\rightarrow$  **V18** voted for slightly uncomfortable and a warm sensation for the first 25 minutes, with similar model predictions of  $\pm 0.6$  as maximum deviation. Thus, in the upcoming 25-min period, there was a need to use the second cooling vest with lower PCM melting temperature of 18 °C to alleviate the uncomfortable and hot sensations.

Upon wearing the vest with lower melting temperature in the second bout, a drop in *TC* and *TTS* levels was noticed and detected by the integrated model as shown in Fig. 14. Thus, experimental and simulated *TC* and *TTS* levels toward the end of the 50-min exercise in the two-bout case were maintained at lower values than those with

single bout reaching slightly uncomfortable and slightly warm, respectively, with similar values to **All-V18**. **All-V18** had a significant difference ( $p < 0.05$ ) in *TC* and *TTS* from the no vest case at all times of exercise. In the two-bout case, there was a significant difference in experimental and simulation results from the no vest case in the last 10 min of exercise for *TC* and in the last 25 min for *TTS*.

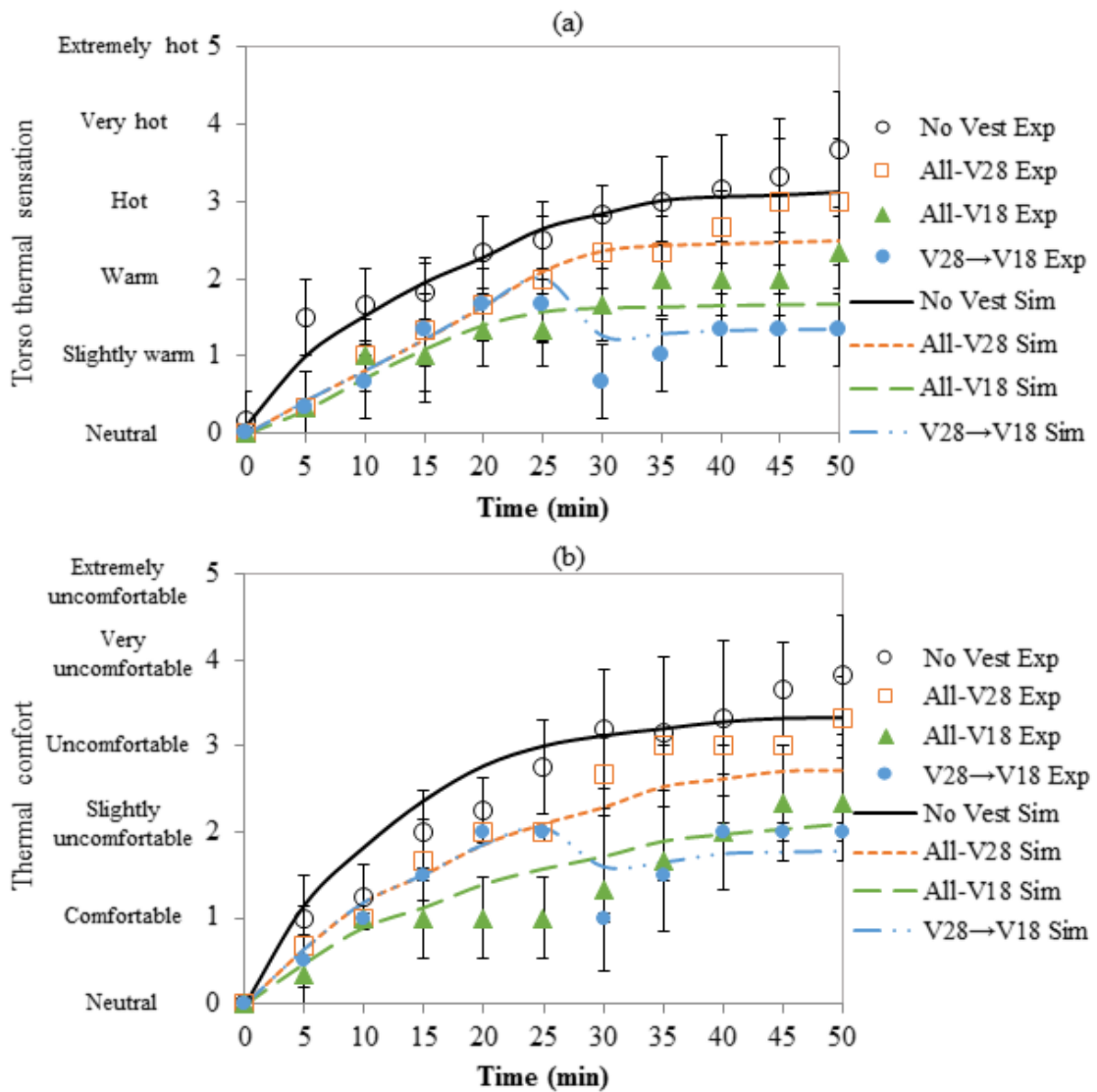


**Fig. 14:** Simulation and experimental data (mean values  $\pm$  SD) of (a) torso thermal sensation and (b) thermal comfort for the different cases during exercise

The results mentioned above demonstrated an acceptable accuracy of the integrated model at hot conditions and moderate activity level with maximum deviation

from experimental values of  $\pm 0.9$  °C, 8 %,  $\pm 0.6$  and  $\pm 0.6$  in torso skin temperature, body weight loss, thermal sensation and thermal comfort, respectively. The accuracy of the model was similar to those found by previous studies adopting a similar previous version of the bio-heat model and compared to published experimental data (Hamdan et al., 2016; Karaki et al., 2013; Salloum et al., 2007) In addition, other recently published models have similar accuracy in predicting the human thermal responses as in the study of Yang et al. (2014), where their model showed accurate predictions of skin and core temperatures in terms of their tendency and absolute values (maximum of 0.59 °C, 0.75 °C and 0.2 °C in mean skin, local skin and core temperatures, respectively). Moreover, the model was able to detect the transient skin temperature variations and subjective votes due to wearing the second cooling vest. Applying the two-bout strategy was effective in improving thermal comfort and sensations due to local torso cooling, even though no significant change in core temperature over the whole period was noticed or in mean skin temperature upon wearing the second cooling vest. The two-bout strategy was able to attain similar improvements in *TC* and *TTS* to the optimal single-bout case with the lowest melting temperature of 18 °C. Thus, the model can be utilized to find the PCM melting temperatures that could be used in the two bouts while providing similar comfort levels to the optimal single-bout case but at lower carried weight, energy use and material cost. The effect of the carried weight when performing cycling in the human subject experimentation was minimal since the subjects were not performing an activity while carrying their own weight as well as that of the vest. Nevertheless, any reduction in carried weight in activities that involve running, outdoor construction work, etc., would contribute to easier movement and lower metabolic cost.

Thus, the findings showed that applying the two-bout strategy can enhance the subjective votes of moderately active workers in very hot conditions. Wearing cooling

vests in the second bout of lower PCM melting temperatures than the first bout would allow maintaining acceptable levels of comfort and sensation till the end of the total working duration. That strategy allows for optimizing the weight of the vests used in the two bouts. Thus, the problems of extra carried weight that affects the metabolism and hindrance of movement when applying continuous cooling during work, especially work that involves walking or outdoor construction work, (Chan et al., 2013; House et al., 2012; Tyler et al., 2013) could be diminished by applying the two-bout strategy. All the stated enhancements result in improved work settings that enhance the productivity of workers and reduce time-consuming errors at the very hot environments and put forward the possibility of extending the limited continuous working durations. On the other hand, some cost due to using an additional vest would be present when applying the two-bout strategy and the use of different types of PCM packets. In addition, the PCM packets and vests that would be used in the second bout should be readily available in a regenerated state so that changing the vest is not a time-consuming process.

## ***2. Placement of PCM Packets on Torso Segments That Trigger Comfort***

In this section, the experimental human subject results will be analyzed and compared to those predicted by the integrated model to show the effect of PCM placement on torso segments that trigger comfort. Seven cases were considered; no vest and six vests with **14** uniform packets of 28 °C melting temperature distributed on the UF, LF and back torso segments.

### **a. Physiological responses of heart rate, skin and core temperatures and sweat produced**

The heart rate increased from an initial value at rest of about  $68 \pm 8$  bpm to reach  $126 \pm 6$  bpm at the end of the experiment in the no vest case,  $87 \pm 4$  bpm in arrangement **2UF-2LF-10B** and  $92 \pm 4$  bpm in arrangement **4UF-0LF-10B**. Only arrangements **4UF-0LF-10B** and **2UF-2LF-10B** were significantly different ( $p < 0.05$ ) from the no vest one.

The experimental and simulation results for the transient variation of the front and back torso skin temperatures are provided in Fig. 15(a) and Fig. 15(b), respectively, for the different experiments. In addition, Fig. 15(c) shows experimental and simulation results of the back skin temperature at the end of the experiment, in order to visualize the effect of PCM coverage on the back skin temperature. The local skin temperatures of the no vest case had an increasing trend reaching their highest values at the end of the experiment and was also predicted by the integrated model. On the other hand, the cooling vest cases showed a drop in the local torso skin temperatures in the first 10 min followed by an increase in the skin temperatures to reach their final states. Thus, the model captured the transient variation of the skin temperatures when either covered with PCM packets or not. In the no vest case, the front torso skin temperature reached a maximum value of  $36.13 \text{ }^\circ\text{C} \pm 0.24 \text{ }^\circ\text{C}$ , while that of the back torso segment reached  $34.89 \text{ }^\circ\text{C} \pm 0.43 \text{ }^\circ\text{C}$ .

Upon varying the arrangement of the PCM packets on the UF, LF and back, a difference was detected between the segmental skin temperatures as the PCM coverage area increases. For example, as the PCM coverage area increased on the back segment from 40 % in arrangement **6UF-4LF-4B** to 100 % in arrangement **2UF-2LF-10B**, the back skin temperature showed a linear drop and had a difference of  $3.21 \text{ }^\circ\text{C} \pm 0.49 \text{ }^\circ\text{C}$ , as shown in Fig. 15(c), while the front showed a drop of  $1.47 \text{ }^\circ\text{C} \pm 0.44 \text{ }^\circ\text{C}$ . This difference in skin temperatures, as the coverage area increased, was captured by the

integrated model to an acceptable degree of accuracy with maximum deviation throughout the exercise period of  $\pm 0.78$  °C and  $\pm 0.66$  °C in front and back skin temperatures, respectively. Moreover, the highest drop in back temperature from the no vest case was with arrangement **4UF-0LF-10B** that showed a  $3.87$  °C  $\pm 0.6$  °C temperature drop, while the model predicted accurately a drop of  $3.6$  °C.

The arrangements with fixed PCM coverage on the back while varying the coverage on UF and LF segments (**0UF-4LF-10B**, **2UF-2LF-10B** and **4UF-0LF-10B**) showed similar back skin temperatures, however, lower front skin temperatures were attained as the coverage area on the UF segment increased (Fig. 15(a)). During the full exercise period, the front skin temperature corresponding to arrangements **4UF-2LF-8B**, **4UF-4LF-6B** and **6UF-4LF-4B** were significantly lower ( $p < 0.05$ ) than the no vest arrangement except for the front skin temperature corresponding to arrangements **0UF-4LF-10B**, **2UF-2LF-10B** and **4UF-0LF-10B**. As for the back skin temperature, arrangements **0UF-4LF-10B**, **2UF-2LF-10B** and **4UF-0LF-10B** were the only configurations significantly different from the no vest case throughout the whole exercise period. The two arrangements **4UF-0LF-10B** and **6UF-4LF-4B** were the ones that resulted in the lowest back and front skin temperatures, respectively, after 45 minutes of exercise. It was noted that total melting of the packets did not occur with 14 PCM packets at moderate conditions of  $35$  °C and for a 45 min exercise period.

The experimental change in mean skin temperature,  $\Delta T_{skin,mean}$ , in all the cases had an increasing trend with time. The maximum  $\Delta T_{skin,mean}$  corresponded to the no vest arrangement  $3.48 \pm 0.5$  °C at the end of the experiment. In all the cooling vest cases, a drop in  $\Delta T_{skin,mean}$  from the no vest case was found, with a statistically significant difference from the no vest arrangement ( $p < 0.05$ ) in the last 15 min of exercise in all the cases. With respect to the change in the core temperature, similar trend of variation to



the mean skin temperature was found, however, no significant difference existed in  $\Delta T_{cr}$  at all times throughout the exercise between the different cases. Thus, the above results signified that a detectable difference was found between the different PCM arrangements, but mainly in local torso skin temperatures.

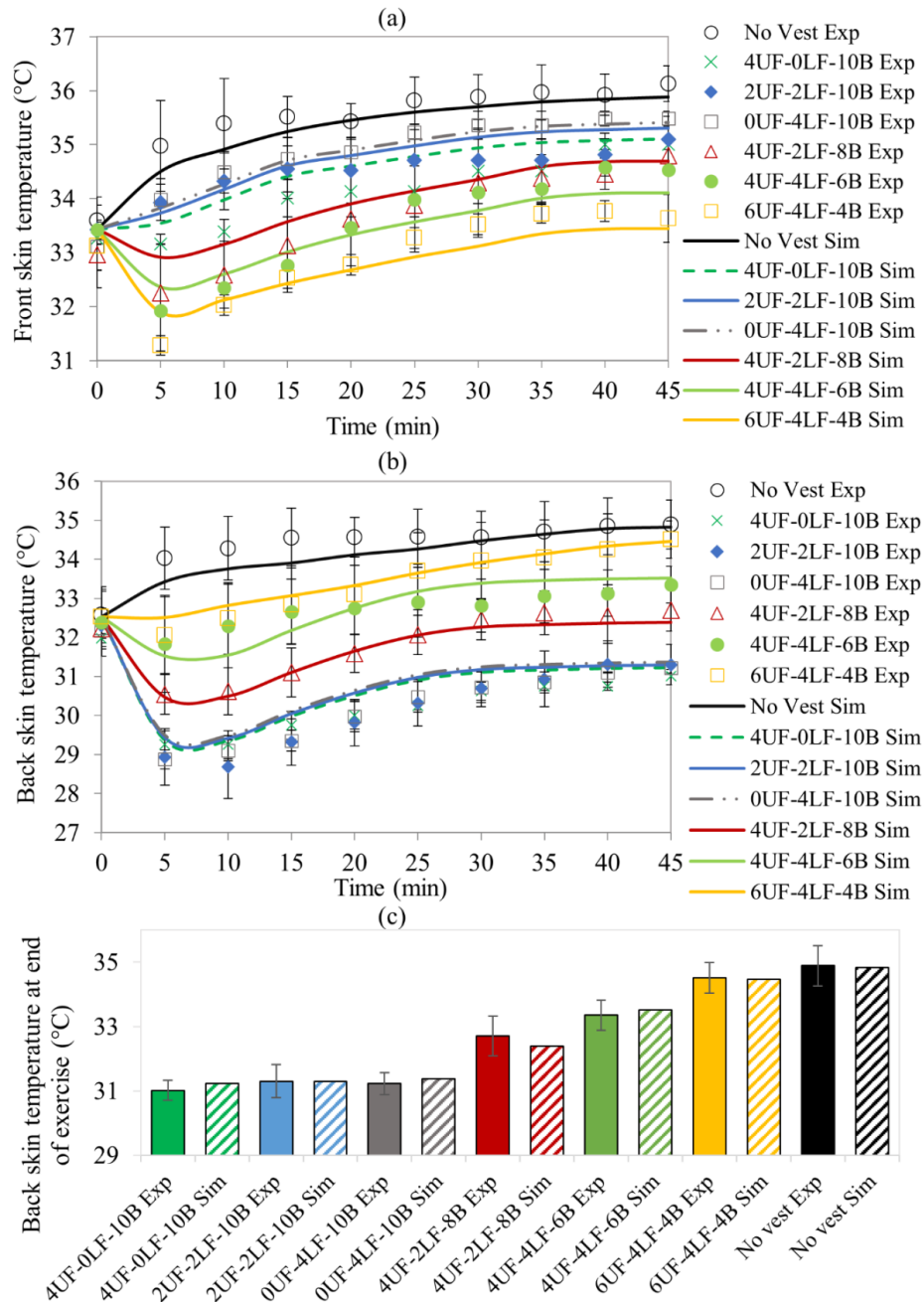


**Fig. 15:** Experimental (mean values  $\pm$  SD) and simulation results of (a) front local skin temperature, (b) back local skin temperature during 45 min exercise and (c) back skin temperature at the end of experiment for the different cases

The body weight loss or sweat production measured (solid fill bar) at the end of the 45 minutes exercise of the different experiments and for the predicted values by the model simulation (hatched bar) are shown in Fig. 16. The simulation results of the integrated model showed good agreement with the experimental ones, with a 14 % maximum error from the mean experimental values. In the presence of a cooling vest, the amount of sweat decreased as compared to the no vest that was at  $0.35 \pm 0.05$  kg. Only sweat produced in arrangements **4UF-0LF-10B**, **2UF-2LF-10B**, **0UF-4LF-10B** and **4UF-2LF-8B** was significantly different from the no vest case ( $p < 0.05$ ). Therefore, the back segment, as was previously found in literature, is a body region that suppresses sweat production when cooled (Cotter et al., 2005). The results were also in agreement with the conclusions of Choi et al. (2008), which indicated a reduction in total sweat rate when wearing a cooling vest while harvesting red pepper for two hours, drops in torso and mean skin temperatures and improved thermal sensation. Furthermore, Webster et al. (2005) observed enhanced thermal state and some reduction of core temperature increase in athletes running for 30 minutes at  $37^\circ\text{C}$  due to 35 minutes pre-cooling using an ice cooling vest.

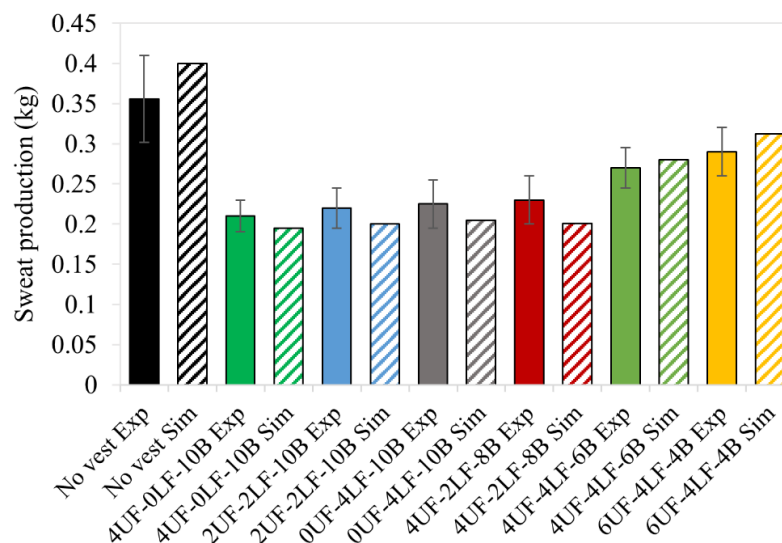


**Fig. 16:** Mean experimental values and SD (solid fill bars) and predicted values by simulation (hatched bars) of sweat production after exercise

## b. Thermal comfort and sensation

The mean experimental subjective ratings and simulation results of *TTS* and *TC* are shown in Fig. 17(a) and Fig. 17(b), respectively. In addition, Fig. 17(c) shows experimental and simulation results of *TC* at the end of exercise period, in order to visualize the effect of PCM coverage as it was varied on the torso segments. The ratings of *TTS* and *TC* kept on increasing in all the cases reaching the highest values of  $4.3 \pm 0.53$  (between very and extremely hot) and  $4.5 \pm 0.5$  (very uncomfortable), respectively, in the no vest case. When wearing the vest, the rate of increase of *TTS* and *TC* with time was lower than that of the no vest, which was also predicted by the simulation model. Variation of the PCM coverage area on the torso segments have led to a detectable difference in local skin temperatures and this was reflected in the *TTS* and *TC* experimental and model results. As the PCM coverage area increased from 40 % to 100 % on the back segment, while decreasing on the front, *TTS* linearly improved from  $4 \pm 0$  (very hot) to  $2 \pm 0.5$  (warm) (Fig. 17(a)) and *TC* almost linearly improved from  $3.67 \pm 0.6$  (uncomfortable) to  $1.75 \pm 0.5$  (slightly uncomfortable), as presented in Fig. 17(b) and Fig. 17(c). This difference in ratings was captured by the model predictions, where *TTS* and *TC* improved from 3.71 (hot) to 2.42 (warm) and from 3.5 (uncomfortable) to 2.15 (slightly uncomfortable) with maximum deviations from mean experimental data of  $\pm 0.7$  and  $\pm 0.8$ , respectively. During all the exercise period, improvements in *TTS* and *TC* were upmost with **4UF-0LF-10B**, followed by **2UF-2LF-10B** and **0UF-4LF-10B**, and all were significantly lower than the no vest case ( $p < 0.05$ ).

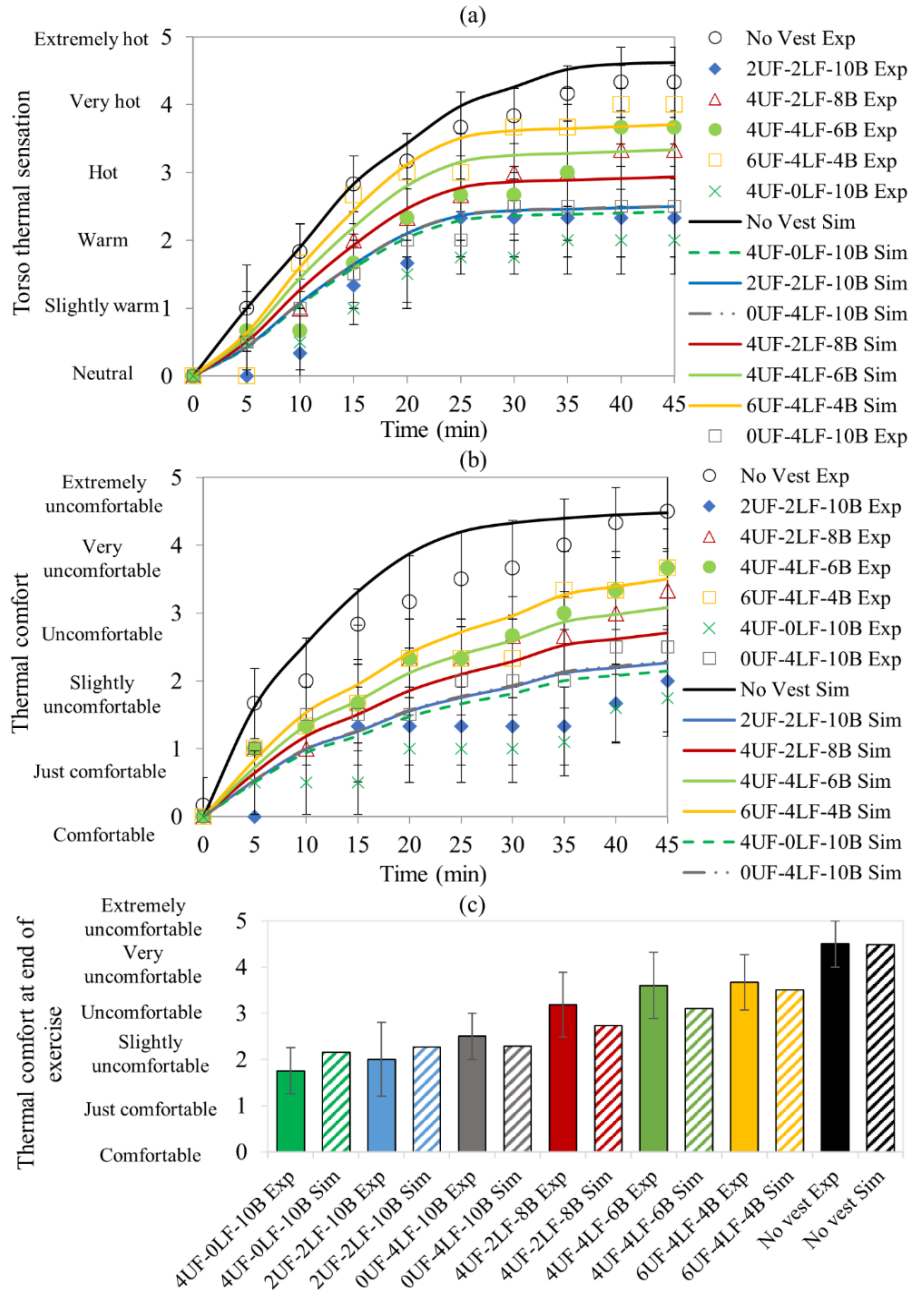


**Fig. 17:** Experimental (mean values  $\pm$  SD) and simulation results of (a) torso thermal sensation, (b) thermal comfort during exercise and (c) thermal comfort at end of exercise

However, it was noticed among those cases that as the PCM coverage area was increased on the UF segments while decreasing it on the LF and fixing it on the back, *TC* and *TTS* were improved. *TC* corresponding to arrangements **4UF-2LF-8B**, **4UF-4LF-6B** and **6UF-4LF-4B** was significantly different ( $p < 0.05$ ) in the last 15 minutes of exercise from the no vest case but there was no significant difference in *TTS*. Thus, as

the PCM coverage area increased on the back, improvements in overall comfort and torso sensation were significant. In addition, placing more packets on the UF segment showed improved *TC* over more coverage on the LF segment, while having full coverage on the back.

The above results were predicted with good accuracy by the integrated model, having a maximum difference from experimental data of  $\pm 0.78$  °C, 14 % and  $\pm 0.8$  in local skin temperatures, sweat rate and thermal comfort and sensation, respectively. The accuracy of the model was similar to that of previous studies utilizing similar bio-heat models (Karaki et al., 2013). The extent of comfort improvement can be evaluated by the difference between the two arrangements with highest and lowest PCM coverage area on the back and vice versa on the UF and LF segments. These two arrangements had no significant difference in sweat rate, mean skin and core temperatures, however, the model detected a difference by 1.66 °C and 3.23 °C in local back and front skin temperatures, respectively. This difference in skin temperatures was reflected in *TTS* and *TC* results with a magnitude of improvement by 1.29 and 1.35, respectively, as the coverage area increased on the back while the remaining packets covered the UF segment. From the findings of this study, it can be concluded that after the back and in order to have highest improvement in comfort, the UF torso segment should be first covered with PCM packets followed by the LF one. In addition, the results prove the robustness of the model for use in determining improvements in thermal and comfort states of an active human wearing cooling vest in presence of PCM asymmetry between UF, LF and back segments.

The findings of the simulated cases agree with the experimental ones, which showed that with a limited number of PCM packets, placing more packets on the back segment, followed by the UF and then LF segments, is an effective approach when body

cooling is needed, while asymmetry exists between front and back. The integrated model was capable of detecting the difference in comfort and sensation of an active human, upon varying the PCM arrangement on the UF, LF and back segments. It was also concluded in this study that increasing the PCM packets on the UF segment while decreasing them on the LF segment and fixing the packets on the back showed larger improvements in *TC*. In previous studies on the relative importance of different body regions for thermal comfort of humans (Nakamura et al., 2013; Nakamura et al., 2008), local cooling of the abdomen (LF) did not show significant improvement in thermal comfort, while local cooling of the upper and lower back segments did. In this study, the improvement in *TC* was more noticeable when the lower PCM melting temperatures used at the hot environment, were placed on the UF and not on the LF. This could be contributed to the body morphology of male subjects that were the focus of the study. Zhang et al. (2004) found that when the body was warm, cooling the UF segment would provide higher comfort than cooling the LF segment.

## **B. Testing on a Thermal Manikin and on Human Subjects of PCM Packets of Different Melting Temperatures Used in one Cooling Vest**

In this section, cooling vests that incorporate PCM packets of two different melting temperatures, simultaneously, with different arrangements are considered. Experiments were first done on a thermal manikin and then on human subjects to draw conclusions on thermal comfort and sensation votes.

### **1. Results of manikin testing**

After applying the constant skin temperature mode at 35 °C on the thermal manikin, the average torso heat flux was recorded for 200 minutes after clothing the

manikin with the cooling vest. Table 8 presents the average torso heat fluxes with their standard deviations recorded at the start and after steady state was attained for the different vests. The results indicated highest values of heat flux at the beginning of the experiments to reach after that stable levels due to the fixed temperature of the PCM packets while melting. Among the four experiments, the highest heat fluxes recorded are those of experiment **18F-18B** since all the segments were covered with packets of the lower melting temperature of 18 °C. It should be noted that during all the experiments, total melting of either the 28 °C or 18 °C packets did not happen after 200 minutes have passed. After attaining steady state in experiment **18F-18B**, the average torso heat flux was  $30 \pm 1.9 \text{ W/m}^2$ , which was the highest value recorded among the different experiments. However, it was noticed that the steady average torso heat flux of **28U-18L** was lower than that of **18F-18B** by about 27 % but higher than **28F-28B** by about 83 % due to mixing of two PCM types in the same vest. When comparing the results of experiment **28U-18L** and **18U-28L**, it was noticed that **28U-18L** had higher heat losses by about 16 % with a maximum deviation of 5 %. Thus, placing the PCM packets with the lower melting temperature on the lower torso segments resulted in better cooling effect on the torso. The reason behind that could be attributed to the effect of enhancing the microclimate air flow rate by placing the higher PCM temperature on the upper side. In other words, having the higher PCM temperature on the upper torso induces better circulation of microclimate air so that the hotter air rises upward and out of the vest more efficiently. The higher PCM temperature would result with a higher micro and macro climate air temperature in the vest at the upper segments, inducing upward air flow in the vest air gap.

**Table 8** Results of the thermal manikin experiments

<b>Experiment</b>	<b>28U-18L</b>	<b>18U-28L</b>	<b>28F-28B</b>	<b>18F-18B</b>
<b>Average torso heat flux at the start <math>\pm</math> SD (W/m<sup>2</sup>)</b>	65 $\pm$ 0.6	53 $\pm$ 0.7	51 $\pm$ 1.2	65 $\pm$ 2.1
<b>Average torso heat flux at steady state <math>\pm</math> SD (W/m<sup>2</sup>)</b>	22 $\pm$ 0.4	19 $\pm$ 0.5	12 $\pm$ 1.4	30 $\pm$ 1.9

The improvement in cooling effect on the manikin when placing the higher PCM temperature on the upper torso justifies the need to test it further on human subjects and check if similar conclusions can be drawn on thermal comfort and sensation votes. Manikin testing provided information about the heat losses from the torso without physiology being considered in the assessment and without subjective comfort and sensation votes. In addition, the issue if total melting of one packet happened is not present since total melting of either the 28 °C or 18 °C packets did not happen after 200 minutes have passed.

## ***2. Results of human subject experiments***

In order to analyze the skin temperature variations and psychological responses of the participants, the different PCM packets should be during their melting periods when their temperatures are fixed and not in their initial transient period. The transient period is defined as the time the temperatures of the packets need to increase from their initial state at 15 °C to their melting temperatures (either 18 °C or 28 °C). It should be noted that when packets of melting temperature 18 °C and 28 °C are considered simultaneously, the 18 °C packets has a shorter transient period than the 28 °C ones. After that, the packets are in their melting state at a stable temperature till the end of the exercise period of 45 min.



Comparisons of the different cases are done with respect to the three reference cases: i) the no vest case; ii) the uniform melting temperature PCM arrangement **18F-18B**; and iii) and the uniform melting temperature PCM arrangement **28F-28B**. The remaining arrangements are divided into (a) front and back cases (**18F-28B** and **28F-18B**) and (b) upper and lower cases (**18U-28L** and **28U-18L**) to ease the comparison.

a. PCM different states during exercise

The experimental results for PCM initial and final temperatures (mean  $\pm$  SD) and the time melting started for the different vest arrangements are presented in Table 9. In all the cases, a similar trend of variation was found, where the PCM temperatures increased from their initial values of about 15 °C to reach a stable temperature after some time indicating the start of melting. Moreover and in all the cases, the PCM temperatures remained stable near their melting temperature till the end of the exercise indicating that they were still in the melting phase and did not completely melt. It can be concluded from Table 9 that the transition period for the PCM packets to increase from their initial temperature to their melting one at 28 °C was about  $9 \pm 0.8$  min to  $16 \pm 0.3$  min and those with melting temperature of 18 °C, their transition period was about  $4 \pm 0.6$  min to  $7 \pm 0.7$  min only.

The variations in the start of melting between the different cases with the same type of PCM could be related to the higher temperature gradient between the skin temperatures and the PCM temperature; the higher the gradient is the earlier the melting starts. Thus, typically the packets with 28 °C melting temperature need more time to reach their melting phase but that was limited to the first 15 min of exercise. It was noted that the final temperature of the 18 °C and 28 °C packets was not at their exact melting temperatures (reported by the manufacturer) even though they were in their

melting phase and that could be due to having different types of additives in one packet rather than having a pure substance (Hamdan et al., 2016; Zalba et al., 2003). The remaining 30 min of exercise was the main focus to analyze the results of the skin temperatures and subjective votes in the following sections.

**Table 9** Experimental results for PCM initial and final states (mean  $\pm$  SD) during exercise and the time melting started for the different PCM arrangements

Case/ Arrangement	PCM Location on Torso	$T_{initial}$ ( $^{\circ}\text{C}$ )	$T_{final}$ ( $^{\circ}\text{C}$ )	Start of melting (min)
<b>28F-28B</b>	Front	$14.8 \pm 1.1$	$29.3 \pm 0.6$	$10 \pm 0.6$
	Back	$14.5 \pm 0.8$	$29.6 \pm 0.5$	$13 \pm 0.4$
<b>28F-18B</b>	Front	$15.2 \pm 1.9$	$29.2 \pm 0.9$	$10 \pm 0.8$
	Back	$15.6 \pm 1.0$	$19.6 \pm 1.0$	$5 \pm 0.6$
<b>18F-28B</b>	Front	$15.9 \pm 0.8$	$18.9 \pm 0.3$	$5 \pm 0.5$
	Back	$15.5 \pm 0.6$	$29.7 \pm 0.2$	$16 \pm 0.3$
<b>18F-18B</b>	Front	$15.1 \pm 2.0$	$18.6 \pm 0.3$	$6 \pm 0.3$
	Back	$14.9 \pm 1.5$	$19.0 \pm 0.5$	$7 \pm 0.7$
<b>28U-18L</b>	Upper	$15.3 \pm 1.9$	$29.9 \pm 0.9$	$9 \pm 0.8$
	Lower	$14.9 \pm 2.0$	$19.1 \pm 1.0$	$4 \pm 0.6$
<b>18U-28L</b>	Upper	$15.4 \pm 0.8$	$19.4 \pm 1.2$	$6 \pm 0.5$
	Lower	$15.7 \pm 2.0$	$29.3 \pm 1.0$	$10 \pm 0.9$

b. Heart rate and local skin temperatures

During the 45 minutes of exercise in the warm conditions of  $35^{\circ}\text{C}$ , the variation of the mean heart rate for the different cases is shown in Fig. 18. At the onset of the exercise, the initial value of the heart rate for all participants was about  $76 \pm 10$  bpm. Then, the heart rate had an increasing trend up to the end of the PCM transient period (about 15 min) in all the vest cases. During the PCM melting period, the heart rate has almost stabilized till the end of the 45 min of exercise. The corresponding stable

heart rates for PCM arrangements **28F-28B**, **28F-18B**, **18F-28B**, **18F-18B**, **28U-18L** and **18U-28L** were  $93.5 \pm 15$  bpm,  $89 \pm 15$  bpm,  $92 \pm 15$  bpm,  $95 \pm 13$  bpm,  $99 \pm 4$  bpm and  $95 \pm 9$  bpm, respectively. However, in the no vest case, the heart rate kept on increasing till it reached  $105 \pm 22$  bpm at the end of exercise. Moreover, no significant difference ( $p>0.05$ ) was found between the no vest case and all the other cases or among any of the vest cases at all times of exercise.

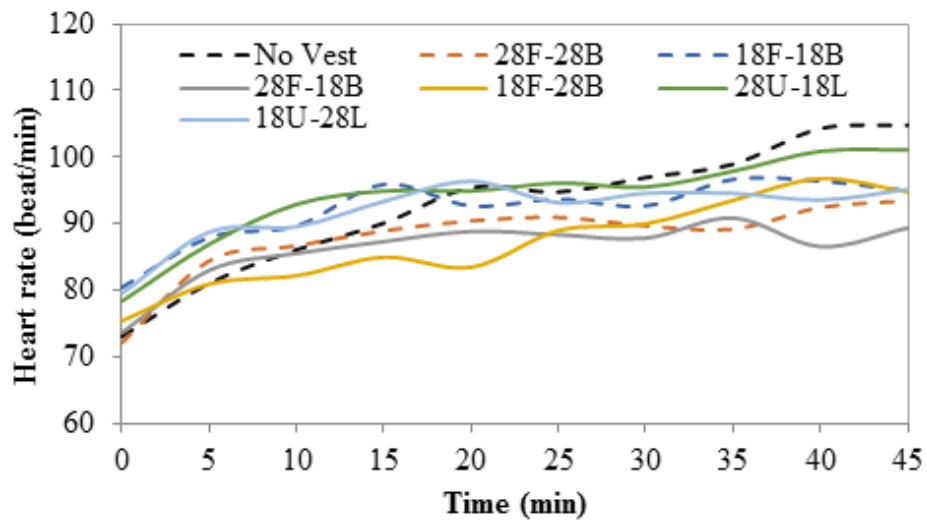


**Fig. 18:** Mean values of heart rate during 45 minutes exercise (dotted lines represent the reference cases of no vest and vests with uniform packets of 28 °C and 18 °C melting temperature)

The variations of the frontal and back local skin temperatures during the 45 min exercise are shown in Fig. 19 and Fig. 20, respectively, for the different cases. It can be noticed that in the no vest case, the local skin temperatures of the front and the back kept on increasing from their initial thermo-neutral state till their final states of  $35.34 \pm 0.5$  °C and  $35.1 \pm 1$  °C, respectively, at the end of exercise. Under the influence of the cooling vest in the remaining cases, a different trend of variation was noticed. At the time the cooling vests with 28 °C packets covering the front or back were worn, the skin temperatures had an initial drop due to the relatively lower PCM initial temperature

of 15 °C. After about 15 min of exercise, the PCM packets entered their melting phase and the skin temperatures started increasing to reach stable values. However, for the cooling vests having 18 °C packets covering the front or the back, there was a drop in skin temperature during the transient period of the PCMs to reach after that almost stable values till the end of exercise.

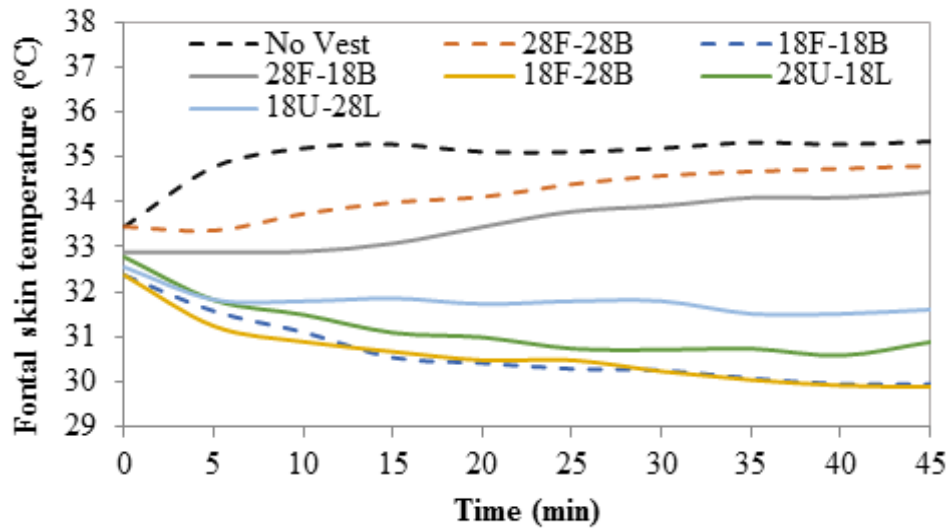


**Fig. 19:** Frontal local skin temperature for the different cases during exercise for 45 min (dotted lines represent the reference cases of no vest and vests with uniform packets of 28 °C and 18 °C melting temperature)

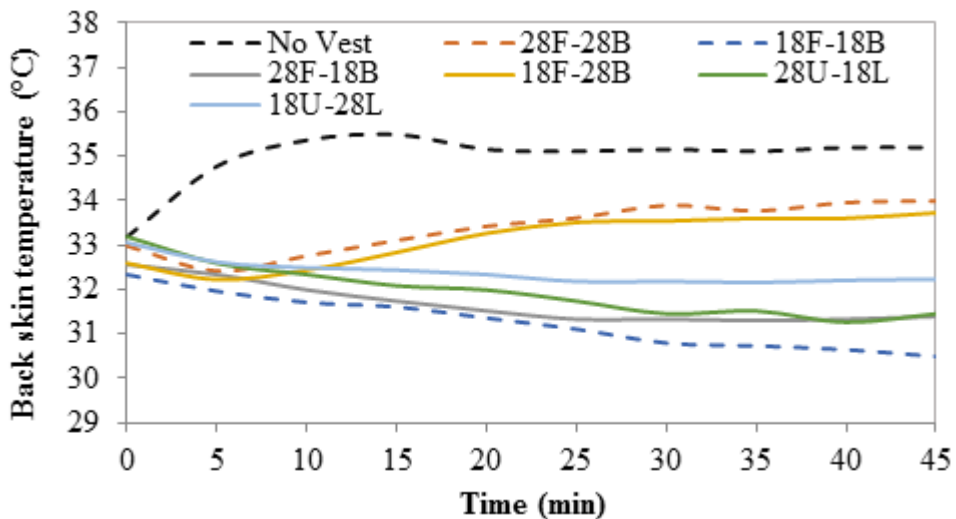


**Fig. 20:** Back local skin temperature for the different cases during exercise for 45 min (dotted lines represent the reference cases of no vest and vests with uniform packets of 28 °C and 18 °C melting temperature)

Uniform melting temperature vest arrangements **28F-28B** and **18F-18B** showed the highest and lowest local skin temperatures among the different vest cases, respectively. After the end of the PCM transient period in about  $13 \pm 0.4$  min and  $7 \pm 0.7$  min in cases **28F-28B** and **18F-18B**, respectively, the front skin temperature became stable at  $34.79 \pm 1.2$  °C and  $29.89 \pm 1.1$  °C, respectively, while those of the back became stable at  $33.99 \pm 0.9$  °C and  $30.48 \pm 1.9$  °C, respectively. Note that the front skin temperature is consistently higher than the back skin temperature for vest using uniform melting temperature for all PCM packets in the vest.

The cases that showed a significant difference ( $p < 0.05$ ) from the no vest case in frontal skin temperature at all times during exercise were **18F-28B**, **18F-18B**, **28U-18L** and **18U-28L**. Moreover, cases **18F-28B**, **18F-18B**, **28U-18L** and **18U-28L** showed a significant difference ( $p < 0.05$ ) from the no vest case at all times in back skin temperature. In case **28F-18B**, there was a significant difference from the no vest case in the last 30 minutes of exercise only in back skin temperature.

c. Mean skin and core temperatures and body weight loss

The experimental results of the change in mean skin, core and body temperatures from initial state (mean  $\pm$  SD) and heat storage reported every 15 min during the 45 min of exercise for the different cases are shown in Table 10. In general, the temperatures of the different cases kept on increasing with time from their initial value reaching a maximum value at the end of exercise. The cooling vests reduced the rate of increase of the different temperatures in comparison to the no vest case, however, at different significance levels.

Cooling vest **18F-18B**, while the PCM packets are in their melting phase, recorded significantly lower  $\Delta T_{skin,mean}$ ,  $\Delta T_{cr}$ , and  $\Delta T_b$  than the no vest case by 1.66 °C, 0.37 °C and 0.65 °C, respectively, at the end of exercise. In addition, arrangements **28F-**

**18B** and **28U-18L** showed significant reductions in the different temperatures by the end of the exercise. Thus, it could be noticed that no significant difference in  $T_{skin,mean}$  was present in the former cases, where the 18 °C packets were placed on the lower torso segments. In the last 15 min of exercise, all cases except **28F-28B** and **18U-28L** had significantly lower  $T_b$  (Colin et al., 1971; House et al., 2012) from the no vest case.

**Table 10** Change in mean skin, core and body temperatures from initial state (mean  $\pm$  SD) and heat storage reported every 15 min during exercise for the different cases

Time (min)	Case/Arrangement	$\Delta T_{skin,mean}$ (°C)	$\Delta T_{cr}$ (°C)	$\Delta T_b$ (°C)	Calculated S (W)
0	All cases	0.00 $\pm$ 0.0	0.00 $\pm$ 0.0	0.00 $\pm$ 0.0	0
15	No vest	+2.63 $\pm$ 1.0	+0.30 $\pm$ 0.2	+0.78 $\pm$ 0.2	229
	<b>28F-28B</b>	+3.08 $\pm$ 0.9	+0.15 $\pm$ 0.2	+0.74 $\pm$ 0.3	217
	<b>28F-18B</b>	+2.10 $\pm$ 0.9*	+0.05 $\pm$ 0.1	+0.46 $\pm$ 0.1*	135
	<b>18F-28B</b>	+2.35 $\pm$ 0.8	+0.05 $\pm$ 0.2	+0.51 $\pm$ 0.1*	149
	<b>18F-18B</b>	+1.44 $\pm$ 1.0*	+0.10 $\pm$ 0.1	+0.36 $\pm$ 0.2*	105
	<b>28U-18L</b>	+1.30 $\pm$ 0.6*	+0.10 $\pm$ 0.1	+0.34 $\pm$ 0.1*	100
	<b>18U-28L</b>	+1.29 $\pm$ 1.2	+0.32 $\pm$ 0.2	+0.52 $\pm$ 0.5	152
30	No vest	+2.57 $\pm$ 0.4	+0.37 $\pm$ 0.2	+0.83 $\pm$ 0.2	122
	<b>28F-28B</b>	+3.37 $\pm$ 0.9	+0.20 $\pm$ 0.1	+0.84 $\pm$ 0.3	123
	<b>28F-18B</b>	+2.12 $\pm$ 0.9	+0.10 $\pm$ 0.1*	+0.50 $\pm$ 0.2	73
	<b>18F-28B</b>	+2.39 $\pm$ 1.1	+0.20 $\pm$ 0.2	+0.63 $\pm$ 0.3	92
	<b>18F-18B</b>	+1.48 $\pm$ 0.8*	+0.12 $\pm$ 0.1*	+0.39 $\pm$ 0.2*	57
	<b>28U-18L</b>	+1.50 $\pm$ 0.5*	+0.14 $\pm$ 0.1	+0.41 $\pm$ 0.1*	72
	<b>18U-28L</b>	+1.25 $\pm$ 1.1*	+0.38 $\pm$ 0.2	+0.56 $\pm$ 0.3	82
45	No vest	+2.74 $\pm$ 0.4	+0.57 $\pm$ 0.2	+1.02 $\pm$ 0.2	100
	<b>28F-28B</b>	+3.50 $\pm$ 0.7	+0.22 $\pm$ 0.2*	+0.88 $\pm$ 0.3	86
	<b>28F-18B</b>	+2.16 $\pm$ 0.7*	+0.12 $\pm$ 0.1*	+0.53 $\pm$ 0.1*	52
	<b>18F-28B</b>	+2.40 $\pm$ 1.0	+0.25 $\pm$ 0.2*	+0.68 $\pm$ 0.3*	66
	<b>18F-18B</b>	+1.08 $\pm$ 0.8*	+0.20 $\pm$ 0.1*	+0.37 $\pm$ 0.2*	36
	<b>28U-18L</b>	+1.58 $\pm$ 0.4*	+0.26 $\pm$ 0.1*	+0.52 $\pm$ 0.1*	51
	<b>18U-28L</b>	+1.29 $\pm$ 0.9*	+0.40 $\pm$ 0.2	+0.58 $\pm$ 0.4	57

\* Significant statistical differences ( $p < 0.05$ ) between the vest case and the no vest one

The results for the calculated change in body heat storage (House et al., 2012; Zander et al., 2015),  $S$ , show that the no vest case at the end of exercise had the highest value among the different cases at 100 W, which is justified since no cooling is applied. The arrangements that showed a significant decrease in heat stored after 45 min of exercise were **18F-18B**, followed by **28U-18L**, **28F-18B** and **18U-28L**.

Body weight loss or sweat production, shown in Fig. 21, was measured for the different experiments at the end of the 45 minutes of exercise. The body weight loss was maximum in the no vest case with  $0.29 \pm .03$  kg, and it decreased under the influence of the cooling vest. Following the no vest case, the sweat rates in descending order for cases **28U-18L**, **18F-28B**, **28F-28B**, **18U-28L**, **28F-18B** and **18F-18B** were  $0.28 \pm .05$  kg,  $0.275 \pm .05$  kg,  $0.27 \pm .02$  kg,  $0.26 \pm .06$  kg,  $0.25 \pm .04$  kg and  $0.22 \pm .05$  kg, respectively. All the vest cases showed no statistical significant difference ( $p > 0.05$ ) in the sweat produced from the no vest case except **18F-18B**. In addition, there was no statistical significant difference between the vest cases.

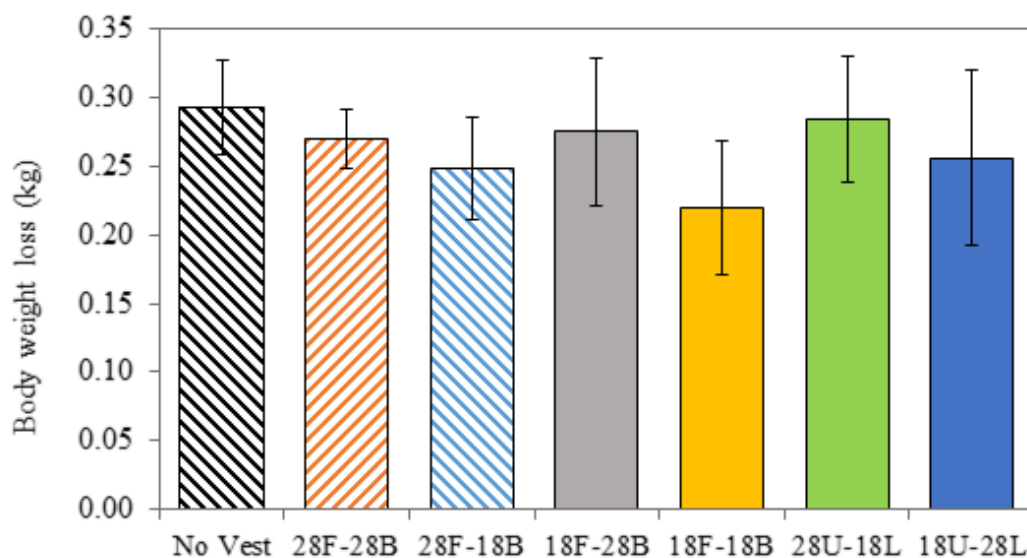


**Fig. 21:** Sweat production or body weight loss after exercise (Mean values and SD) (with hatched columns representing the reference cases of no vest and vests with uniform packets of 28 °C and 18 °C melting temperature)

d. Thermal comfort and sensation

The experimental mean ratings of overall thermal comfort, *TC*, and torso thermal sensation, *TTS*, during exercise for the different cases are presented in Fig. 22, and Fig. 23, respectively, while focusing on the comparison between (a) front and back cases and (b) upper and lower cases.

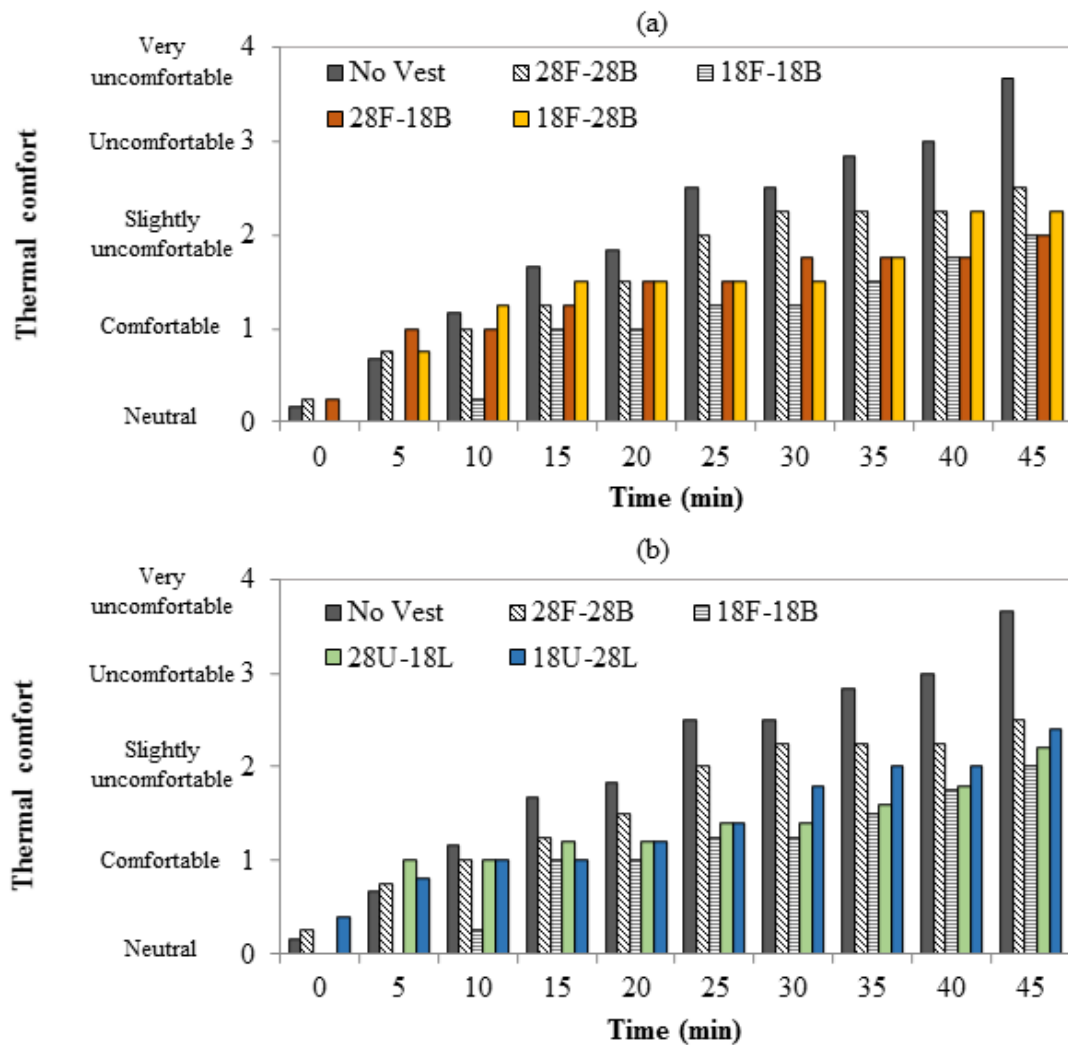


**Fig. 22:** Experimental mean ratings of overall thermal comfort showing (a) front and back cases & (b) upper and lower cases (hatched columns represent reference cases of no vest and vests with uniform packets of 28 °C and 18 °C melting temperature)



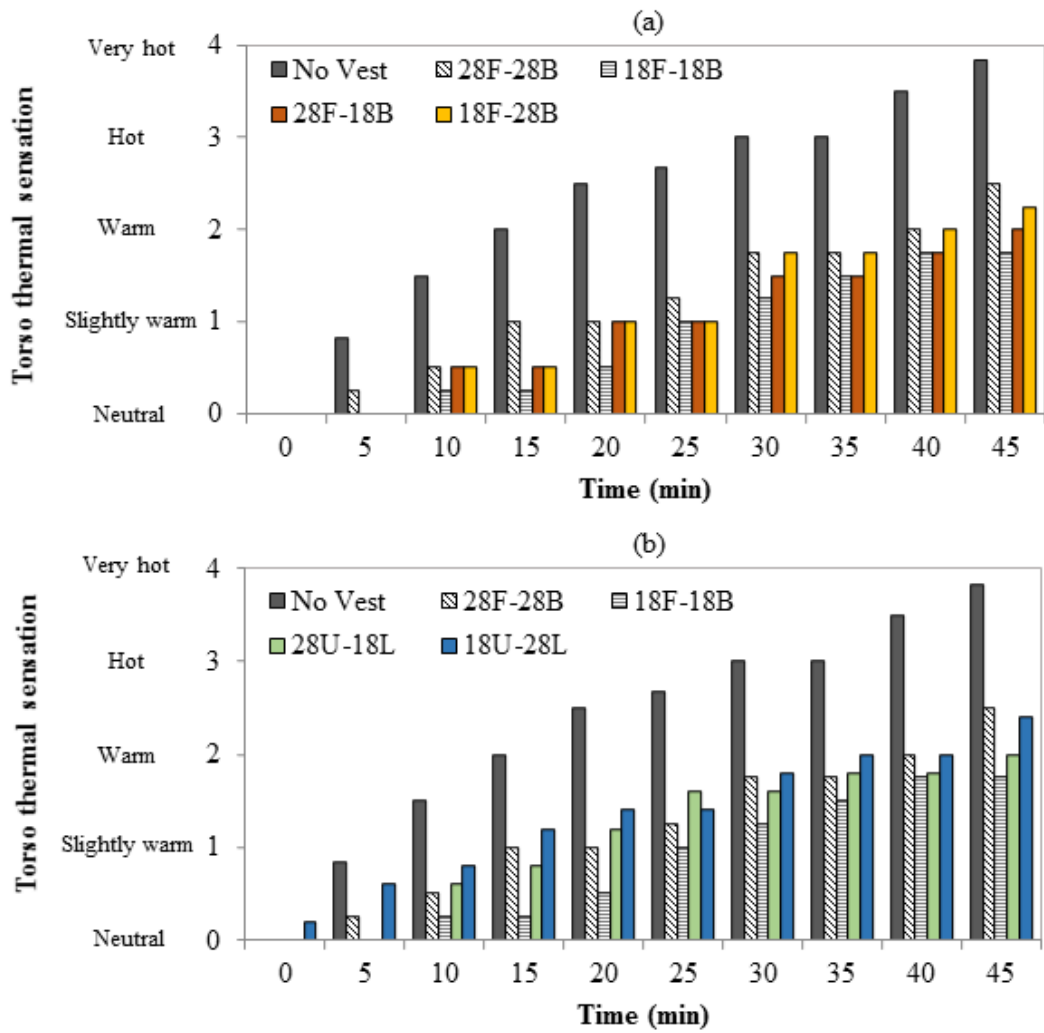


**Fig. 23:** Experimental mean ratings of torso thermal sensation during exercise showing (a) front and back cases & (b) upper and lower cases (hatched columns represent reference cases of no vest and vests with uniform packets of 28 °C and 18 °C melting temperature)

In the case where no vest is worn, *TC* and *TTS* had similar increasing trends throughout the exercise period and reached the highest values of  $3.67 \pm 0.8$  and  $3.83 \pm 0.9$ , respectively, among the different cases at the end of exercise with an uncomfortable *TC* level and a hot *TTS* (Table 6). In general, it was noticed in all the vest cases that the rate of increase of the *TC* level was slower than the no vest case and reached stable values in the last 15 min of exercise due to the packets being in their melting phase at an almost constant temperature. The different PCM arrangements were able to lower *TC* and *TTS* from the no vest case, however, not all cases showed a statistically significant

difference from the no vest case at all times of exercise. Arrangement **28F-28B** reduced the *TC* and *TTS* to  $2.5 \pm 1.2$  (slightly uncomfortable) and  $2.5 \pm 1$  (warm), respectively, in comparison to the no vest case at the end of exercise with no significant difference at all times during exercise. However, arrangement **18F-18B** showed a significant difference from the no vest case at all times reaching *TC* and *TTS* values of  $2 \pm 0$  (slightly uncomfortable) and  $1.75 \pm 0.5$  (slightly warm), respectively, at the end of exercise. Moreover, in the last 30 min, the *TC* for arrangements **28F-18B** and **28U-18L** showed significant differences from the no vest reaching  $2 \pm 0.8$  (slightly uncomfortable) and  $2.2 \pm 0.8$  (slightly uncomfortable) at the end of exercise, respectively. Similarly, *TTS* for arrangements **28F-18B** and **28U-18L** showed significant differences from the no vest at all times with values of  $2 \pm 0.8$  (warm) and  $2 \pm 0.7$  (warm) at the end of exercise, respectively. Thus, placing the 18 °C packets on the back segment resulted in slightly better *TC* levels, but similar *TTS*, than placing them on the lower torso segments. In addition, *TC* for case **18F-18B** was very similar to that of **28F-18B**, where two types of PCM packets were used.

#### e. Discussion

Many researches have concluded that providing a greater body cooling area would be more effective in reducing heat strain for humans (Choi et al., 2008; Gao et al., 2010). However, in some applications like outdoor construction or field work, whole body cooling is not feasible, consumes a lot of energy and unnecessary as targeting certain body areas may result with the desired cooling effect (Young et al., 1987). Moreover, local cooling would contribute to energy savings in an increasingly energy

demanding air conditioning systems in the presence of global warming (Pallubinsky et al., 2016).

In the current study, the cooling effect of the PCM vests was evaluated via both thermal manikin and human subject testing. One of the common uses of thermal manikins is to find the clothing thermal properties (Holmér and Nilsson, 1995). In the current study, the thermal manikin was used to assess the heat fluxes of different cooling vest cases. The results of the manikin experiments using two types of PCM packets of different melting points showed that an improvement in cooling effect with more heat losses can be achieved if the PCM packets with the higher melting temperature of 28 °C are placed on the upper torso segments, while placing the 18 °C packets on the lower torso segments. The improvement in cooling effect could be due to enhancing the microclimate air flow rate by placing the higher PCM temperature on the upper side, inducing better circulation of microclimate air so that the hotter air rises upward and out of the vest efficiently. However, further assessment was needed to include physiology and subjective votes through human testing.

The selection of the best cooling vest depends on how much heat is absorbed by the PCM and on how the participants perceive it. In cases of uniform melting PCM vest of **18F-18B** and **28F-28B**, there was no specific PCM arrangement to specify which resulted in significant improvement in sensation, but rather only the assessment of how much heat was absorbed by the packets. In the remaining cases (**18F-28B**, **28F-18B**, **28U-18L** and **18U-28L**), the arrangement of the packets was a factor that determined which torso segment is more sensitive to cooling and triggers better comfort and sensation than others. With further analysis on the results of human subject testing, the arrangement **18F-18B** significantly lowered the local skin temperatures of the frontal and back torso segments by a maximum of  $5.45 \pm 1$  °C and  $4.62 \pm 1.6$  °C,

respectively. The findings confirm with what previous studies have concluded on reductions in local torso skin temperatures by about 3-5 °C in the presence of cooling vests (Choi et al., 2008; Gao et al., 2012; House et al., 2012).

The change in mean body temperature, found through the changes in mean skin and core temperatures, was significantly reduced in the last 15 min of exercise in most cooling vest cases. Thus, a significant cooling effect evaluated at the end of exercise (House et al., 2012; Zander et al., 2015) was found in cases 18F-18B, 28U-18L, **28F-18B** and **18U-28L** with 64 W, 49 W, 48 W and 43 W of cooling, respectively. The uniform low melting temperature PCM vest case **18F-18B** absorbed the highest amount of heat from the participants. In addition, it was found that placing the 18 °C packets on the back segment resulted in a similar cooling effect to placing them on the lower front and back torso segments when using two PCM types.

A reduction in sweat rate was observed in this study with the presence of a cooling vest, which is consistent with findings in previous experiments (Choi et al., 2008; Chou et al., 2008; Gao et al., 2011; House et al., 2012). However, only arrangement **18F-18B** significantly reduced the body weight loss by about 24 % from the no vest case at 35 °C ambient temperature. Similarly, in the study of Choi et al. (2008), the sweat rate was reduced due to the cooling vest by 20 % in comparison to the no vest case at 33 °C ambient temperature. It was also noted in previous studies that the torso areas that contain high distribution of sweat glands are the chest and upper back (Arens and Zhang, 2006; Herrmann et al., 1952; Randall, 1946). Thus, placing the PCM packets with the lower melting temperature of 18 °C on the chest and upper back segments suppressed sweat production in arrangements **18F-18B**, **18U-28L** and **28F-18B**.

Both overall thermal comfort and torso thermal sensation were improved by wearing the PCM cooling vests and reached stable values in the last 15 min of exercise, but not all arrangements showed major changes from the no vest case. Moreover, participants of arrangement **28F-18B** had similar *TC* levels to **18F-18B** and slightly higher *TTS* values, which shows that cooling the back segment is an effective way to improve *TC* levels. When considering two PCM melting points in the same vest, placing the packets with lower melting temperature on the back segment (**28F-18B**) resulted in similar *TC* levels to placing them on the lower front and back torso segments (**28U-18L**). The findings agree with previous conclusions, which stated that placing the PCM packets on the back improved thermal sensation votes (Reinertsen et al., 2008).

In this study, the proposed cooling vest with two PCM melting temperatures (18 °C and 28°C) was tested at moderate ambient conditions and for a limited exercise period of 45 min. It is expected that at the same ambient conditions and for longer working durations, for example two hours, the proposed system would allow for reductions in vest weight to be carried by the workers. It is estimated that with arrangement **18F-18B**, about 3.31 kg of the 18 °C packets would be needed to remove 52 W of body stored heat in two hours. However, using two PCM types (18 °C and 28 °C) in the same vest with equal coverage area of each type would require a total PCM weight of 2.77 kg. Thus, using arrangement **28F-18B** or **28U-18L** would result in a vest 16 % lighter than **18F-18B** with similar improvement in thermal comfort and sensation levels. However, such improvements need further investigation on human subjects doing a heavier activity level and in hotter environments. In addition, when considering the effect of wearing either cooling vest **28F-18B** or **28U-18L** for a period of two hours, the weight distribution on the torso would be a factor that affects the comfort of the wearer. Previous studies reported that carrying the external load on the front and the

back torso segments is the most physiologically efficient method than carrying the load on the back (Datta and Ramanathan, 2000; Lloyd and Cooke, 2000). Thus, arrangement **28U-18L** would result in the best arrangement choice in providing comfort for a working period of two hours.

Therefore, it can be concluded from the reduction in heat storage and improvement in comfort and sensation levels that using two PCM melting temperatures in one cooling vest can be implemented for a prolonged working duration. In addition, the proposed method was successful in making use of the advantages of both high and low melting temperature PCMs; the ones with high latent heat of fusion and lower energy use for regeneration and the one with lower melting temperature. It is recommended to select the arrangement that places the packets with lower melting temperatures on the lower front and back torso segments as a first option, followed by the arrangement that places them on the back torso segment, as in arrangements **28U-18L** and **28F-18B** in this study.

### **C. Fabric-PCM-Desiccant on a Wet Clothed Heated Cylinder**

In this section, a comparison is done between the results of the two experiments conducted on clothed wet heated cylinder and (i) using only a PCM packet and (ii) using a PCM-Desiccant packet. The reason for doing the two experiments is to compare the conditions of the microclimate air (temperature and humidity content) and PCM temperature when a solid desiccant is used. The main inputs to the fabric-PCM-Desiccant model are the PCM melting temperature, ambient conditions, PCM-Desiccant mass and surface area, PCM-Desiccant thermal properties, and the total thermal resistance between the PCM and the desiccant.

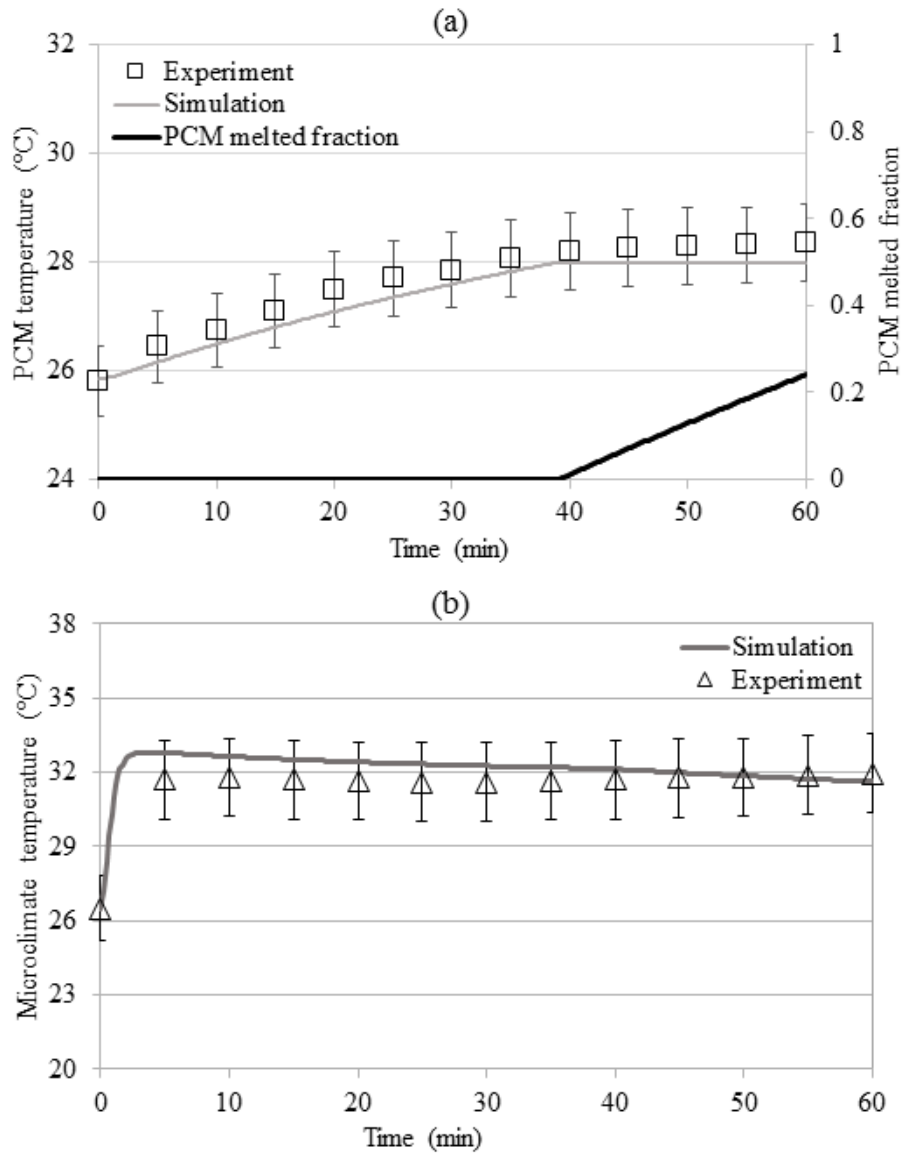


**Fig. 24:** Plots showing the variation with time of the (a) experimental and simulation results of the PCM temperature and simulated PCM melted fraction and (b) the microclimate air temperature corresponding to the experiment on the PCM packet only

Fig. 24 shows the comparison between the measured and the predicted PCM and microclimate air temperatures as well as the simulated PCM melted fraction in the case when no desiccant is used. The experimental PCM temperature rises from its initial condition at about 26 °C after it gains heat to reach its melting temperature of 28 °C after 35 min. The initial condition of the PCM packet is taken as input to the model and the results showed a later start of melting (after about 39 min). The predicted melted

fraction of the PCM packet was about 0.25 after 60 minutes have passed. The microclimate temperature shows a sharp increase in the first few minutes due to subjecting the microclimate air to a high temperature of 34 °C of the heated cylinder. After 15 minutes have passed, the microclimate temperature reached a stable value of about 32 °C. The recorded humidity ratio of the microclimate air at the beginning of the experiment was 16.8 g/kg dry air and reached a value of 21.23 g/kg dry air at the end of the experiment. The results show a good agreement between the measured and the predicted temperatures, where the maximum relative error is 3% and 4% for the PCM and microclimate air temperatures, respectively. The under-estimation of the fabric-PCM model of the PCM temperature could be related to the fact that the PCM did not show a constant melting temperature at 28 °C in the experiment, but rather a higher one.

Fig. 25 shows the comparison between the experimental and the simulation results of the PCM and solid desiccant temperatures as well as the simulated PCM melted fraction in the case when a PCM-Desiccant packet is used. The PCM temperature rises from its initial condition at about 26 °C to reach its melting temperature of 28 °C after 22 min while the model predicts a slightly later start of melting after about 24 min. The predicted melted fraction of the PCM packet was about 0.5 after 60 minutes have passed. The results indicate that a faster start of PCM melting by about 15 minutes was observed due to the presence of the solid desiccant in contact with the PCM, which justifies also the higher melted fraction of the PCM. A higher desiccant temperature than that of the PCM is evident during the time when the PCM is in the transient phase in the first 24 minutes. The desiccant temperature showed higher values than that of the PCM due to the thermal contact resistance between the PCM and the desiccant, in addition to the adsorption process that releases heat of adsorption.



Consequently, the maximum relative error in predicting the PCM and desiccant temperatures is 3% and 4%, respectively.

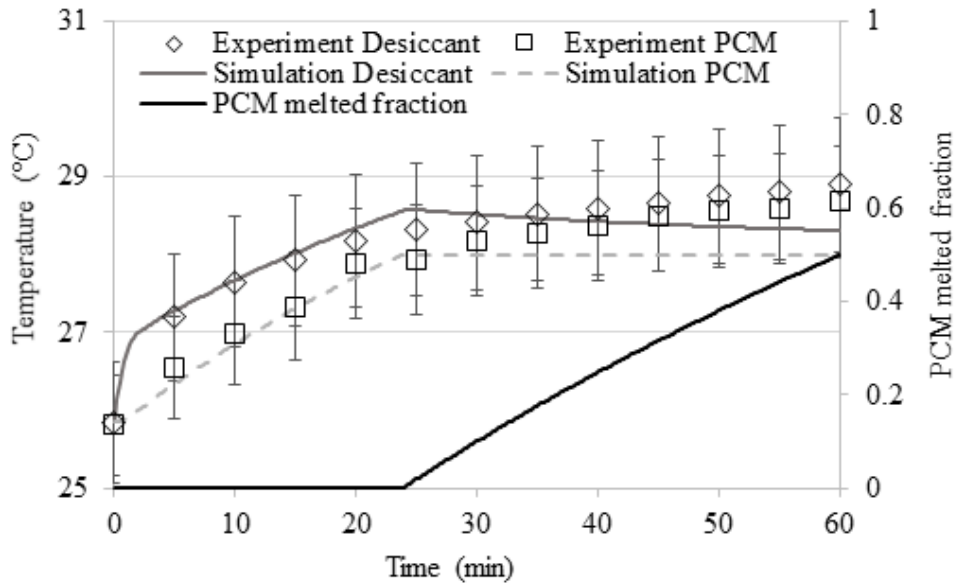


**Fig. 25:** Plot showing the variation with time of experimental and simulation results of the PCM and desiccant temperature as well as the PCM melted fraction corresponding to the experiment on the PCM-Desiccant packet

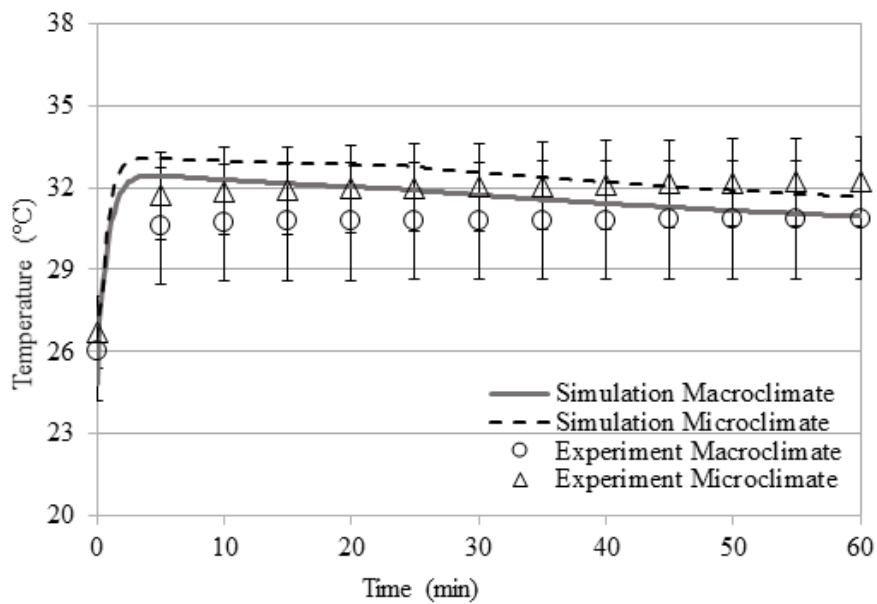


**Fig. 26:** Plot showing the variation with time of experimental and simulation results of the microclimate and macroclimate temperatures corresponding to the experiment on the PCM-Desiccant packet

Fig. 26 shows the comparison between the measured and predicted results of the microclimate and macroclimate air temperatures in the case when a PCM-Desiccant packet is used. Both measured temperatures had a similar trend similar throughout the duration of the experiment. A sharp increase in the temperatures occurred in the first few minutes due to the exposure to the relatively high surface temperature of the heated cylinder and the temperatures started stabilizing after 20 minutes of the experiment have passed. However, the microclimate air temperature had higher values than the macroclimate one due to the exposure to the heated cylinder maintained at a surface temperature of 34 °C. The recorded humidity ratio started initially at 16.9 g/kg dry air and ended at 19.74 g/kg dry air. Thus, comparing the humidity ratio of the two experiment cases, it can be deduced that the presence of the desiccant caused a reduction in the humidity content of the microclimate air as desired. Good agreement was found between the measured and the predicted results with a maximum relative error of 5% and 7% corresponding to microclimate and macroclimate temperatures, respectively. Comparing the microclimate temperature in the case when a PCM-Desiccant packet was used to that when only a PCM packet was used, it can be deduced that higher values by an average of about 0.6 °C were attained when using the PCM-Desiccant packet. Thus, the presence of the desiccant increased the microclimate temperature to reach higher values than those reached when no desiccant was used.

Fig. 27 shows the comparison between the measured and predicted results of the microclimate relative humidity for the two cases: (i) using only a PCM packet with no desiccant and (ii) using a PCM-Desiccant packet throughout the experiment. The trend of the relative humidity showed a slight decrease with time, accompanied with an increase in the moisture content of the microclimate air. The results also show a higher reduction in the relative humidity when a desiccant was added to the PCM packet,

where a sharp decrease was noticed in the first 10 minutes of the experiment. The relative humidity at the end of the experiment when no desiccant was used reached about 70% and about 65% when a desiccant was used. The corresponding humidity ratio of the microclimate air at the end of the experiment, where no desiccant was used, was 21.23 g/kg dry air and 19.74 g/kg dry air when a PCM-Desiccant packet was used. Thus, the desiccant caused a reduction in the humidity content of the microclimate air as desired.

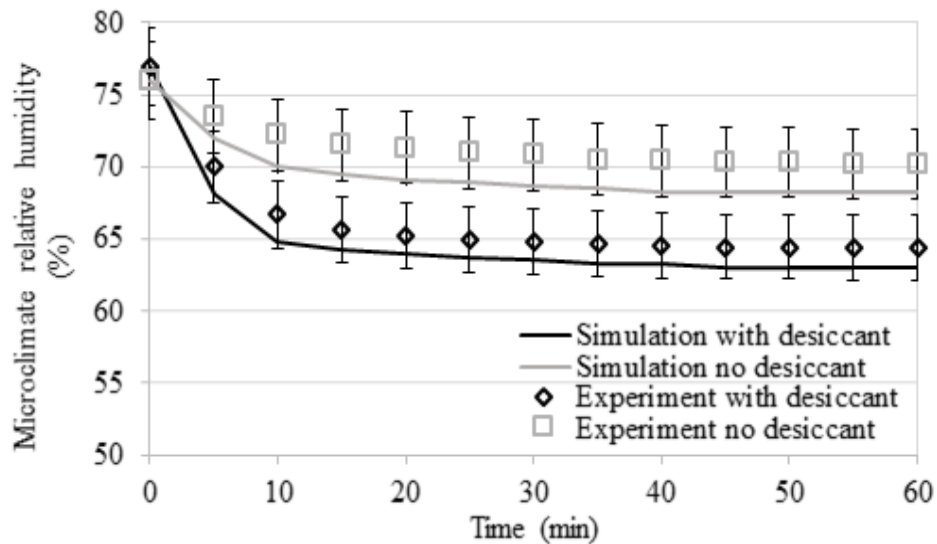


**Fig. 27:** Plot showing the time variation of the experimental and predicted microclimate air relative humidity when using only the PCM packet and when using the PCM-Desiccant packet

The analysis of the experimental and predicted results shows that the problem of blockage of water vapor transport associated with the PCM packets can be solved. Using a PCM-Desiccant packet to provide a dryer microclimate region would improve the performance of cooling vests by increasing the coverage area of the PCM on the skin without causing undesired moisture accumulation and discomfort for the wearer, especially in hot environments (Reinertsen et al., 2008). The proposed PCM-Desiccant packet can be used to improve the performance of the cooling vest and widen the region

of its applicability without the risk of condensation. Thus, the combined PCM-Desiccant packet can be utilized for providing a similar performance to a PCM only cooling vest by possibly adding a number of PCM packets with a slightly higher mass in the vest. Another possibility could be by introducing a combination of PCM-Desiccant packets and PCM only packets to maintain acceptable performance in hot humid environment through controlling both temperature and humidity within the trunk microclimate. These design possibilities could be addressed in future work for optimizing a PCM-Desiccant cooling vest for best combination, weight, and duration of melting.

## CHAPTER V

### CONCLUSIONS AND RECOMMENDATIONS

Modeling and experimentation have been adopted in this work to investigate the effect of applying different strategies using personal cooling vests, that incorporate phase change material, on physiological and subjective aspects of active humans. In order to enhance the cooling effect of PCM vests and comfort of workers the following strategies were implemented: 1) targeting torso sensitive areas that trigger comfort; 2) using two PCM melting temperatures in one cooling vest and the possibility of reducing vest weight, 3) applying a two-bout strategy while reducing energy use, carried weight and material cost and 4) introducing a PCM-Desiccant packet to overcome the hindrance of moisture transport by the PCM packets in the cooling vest.

A bio-heat model that can predict human thermal responses was integrated with a fabric-PCM model for the PCM cooling vest. The fabric-PCM model has been developed using energy and mass balance equations for the different vest and air layers in the vest as well as the PCM packets during transient changes and during melting. The cooling vest targets the torso segments of the human body. The bio-heat model adopted in this study decomposes the torso into 4 segments and each segment into two nodes (left and right). The fabric-PCM model was integrated with each torso segment to reflect the effect on their corresponding physiological responses. Moreover, overall thermal comfort and torso thermal sensation were predicted using the model of Zhang et al. (2004).

Experimental and simulation results showed that the two-bout strategy was able to attain similar improvements in *TC* and *TTS* to the single-bout case. The integrated model was validated using experiments on active human subjects doing

exercise in a hot environment at 40 °C for a duration of 50 min. The model showed maximum deviation from experimental values by  $\pm 0.9$  °C, 8 % and  $\pm 0.6$  in torso skin temperature, body weight loss and thermal sensation and comfort, respectively. The issue of extra carried weight, that affects ease of movement when applying continuous cooling during certain types of activities, could be reduced by applying the two-bout strategy. Thus, lower PCM weight, material cost and energy use are made possible by the proposed strategy.

The importance of PCM arrangement in a cooling vest on improving comfort and thermal responses of active human at different working durations and climates was assessed. Experiments were done on six male subjects, which included cycling on a bike at 3 MET for 45 minutes at a moderate environment of 35°C and 50% relative humidity. The experimental findings were used to validate the integrated bio-heat and fabric-PCM model which proved its capability in detecting a difference in thermal responses and comfort sensations upon varying the PCM arrangement of a fixed number of packets on the torso segments; UF, LF and back. The findings showed that local cooling of the torso when full coverage is not needed and with a limited number of PCM packets, placing more packets on the back, followed by the UF and then LF, would show the optimal improvement in thermal comfort. Cooling the LF segment did not show significant improvement in comfort over cooling the UF segment. Moreover, in situations where a backpack, for example, is carried, placing PCM packets on the back would achieve the desired cooling effect as targeting this body region improves comfort.

The cooling performance of PCM cooling vests having one or two PCM melting temperatures in the same vest simultaneously was assessed. The main findings showed that using a PCM cooling vest that covers only the torso was effective in

reducing local skin temperatures by a maximum of  $5.45 \pm 1$  °C, body heat storage by a maximum of 64 W as well as improving subjective thermal comfort and sensation votes of subjects performing moderate work at 35 °C. Placing the PCM packets with the lower melting temperature of 18 °C on the chest and upper back segments suppressed sweat production. Reduction in sweat rate was observed in the presence of all tested cooling vests, but significant reduction was found when 18 °C PCM packets covered both frontal and back torso segments. This reduction leads to reduced water loss and thus lower dehydration and the need for fresh water intake. Moreover, similar improvements in thermal comfort and sensation levels to **18F-18B** would be obtained with arrangements **28F-18B** and **28U-18L** with vest weights 16 % lighter than that of **18F-18B**. Better cooling effect was found when covering the upper torso segments (chest and upper back) with PCM packets having a higher melting temperature than those covering the lower torso segments (abdomen and lower back) in both thermal manikin and human subject experiments. Thus, for a prolonged working duration, it is recommended to select the arrangement that places the lower melting temperature packets on the lower front and back torso segments as a first option, followed by the arrangement that places them on the back.

A novel idea was proposed, modeled and validated experimentally to find the state of the microclimate air and its moisture content under the influence of using a PCM-Desiccant packet. The idea entailed using a solid desiccant in addition to a PCM packet to maintain dry skin and macroclimate air layers, prevent condensation and enhance sweat evaporation from the skin. Experiments were conducted on a clothed wet heated cylinder with two cases considered to show the effect of adding the desiccant to the PCM packet. Microclimate air temperatures and relative humidity as well as PCM and desiccant temperatures were measured experimentally and predicted by the

developed fabric-PCM-Desiccant model with a maximum relative error of 7%. The results showed a desired effect, which is the decrease in the humidity content of the microclimate air from 21.23 g/kg dry air to 19.74 g/kg dry air in the presence of the solid desiccant. Moreover, higher microclimate temperature by 0.6 °C was attained when using the PCM-Desiccant packet instead of the PCM packet.

The findings of the study could be extended to consider individual differences such as gender and age when applying the different strategies, however, adjustments to the bio-heat model would be needed as well as further experiments to validate the model. Individual differences could be related to the body composition, such as lean body mass and fat mass, in addition to distribution and intensity of sweat production on front and back torso segments. The findings of this study need to be assessed if they can be applied in applications such as firefighting, where improving comfort does not put the humans under risk or mask the warning signals of the body. Moreover, future work could address optimized design of PCM-Desiccant cooling vest for best combination and placement of PCM-Desiccant and PCM packets taking into consideration human thermal response to local cooling and dryness. The placement of the desiccant, either in contact with the skin or exposed to the microclimate air between the skin and the desiccant, might affect the human wetness and thermal sensations differently.



## BIBLIOGRAPHY

- Al Assaad, D., Ghali, K., Ghaddar, N., & Habchi, C. (2017). Mixing ventilation coupled with personalized sinusoidal ventilation: Optimal frequency and flow rate for acceptable air quality. *Energy and Buildings*, 154, 569-580.
- Al-Othmani, M., Ghaddar, N., & Ghali, K. (2008). A multi-segmented human bioheat model for transient and asymmetric radiative environments. *International Journal of Heat and Mass Transfer*, 51(23), 5522-5533.
- All Safe Industries, Available at: <http://www.allsafeindustries.com/store/p/5914-Mesh-Cooling-Vest.aspx> (accessed 21 July 2017).
- Arens, E. A., & Zhang, H. (2006). The skin's role in human thermoregulation and comfort. Center for the Built Environment.
- ASTM F1291-15 (2015). Standard test method for measuring the thermal insulation of clothing using a heated manikin, ASTM International, West Conshohocken, PA. <http://dx.doi.org/10.1520/F1291-15>.
- ASTM F2370-16 (2016). Standard test method for measuring the evaporative resistance of clothing using a sweating manikin, ASTM International, West Conshohocken, PA. <https://doi.org/10.1520/F2370-16>
- Avolio, A. P. (1980). Multi-branched model of the human arterial system. *Medical and Biological Engineering and Computing*, 18(6), 709-718.
- Barr, D., Gregson, W., & Reilly, T. (2010). The thermal ergonomics of firefighting reviewed. *Applied ergonomics*, 41(1), 161-172.
- Bates, G. P., & Schneider, J. (2008). Hydration status and physiological workload of UAE construction workers: A prospective longitudinal observational study. *Journal of Occupational Medicine and Toxicology*, 3(1), 21.
- Bejan, A. (1994). Convection heat transfer. John Wiley & sons.
- Bendkowska, W., Kłonowska, M., Kopias, K., & Bogdan, A. (2010). Thermal manikin evaluation of PCM cooling vests. *Fibres & Textiles in Eastern Europe*, (1 (78)), 70-74.
- Bongers, C. C., Thijssen, D. H., Veltmeijer, M. T., Hopman, M. T., & Eijsvogels, T. M. (2014). Precooling and percooling (cooling during exercise) both improve performance in the heat: a meta-analytical review. *Br J Sports Med*, bjsports-2013.
- Burke, R., Curran, A., & Hepokoski, M. (2009). Integrating an active physiological and comfort model to the Newton sweating thermal manikin. In *Proceedings of the 13th International Conference on Environmental Ergonomics (ICEE)*. University of Wollongong, Wollongong (pp. 313-317).
- Chan, A. P., Yang, Y., Song, W. F., & Wong, D. P. (2017). Hybrid cooling vest for cooling between exercise bouts in the heat: Effects and practical considerations. *Journal of thermal biology*, 63, 1-9.
- Chan, A. P., Chan, A. P., Yi, W., Yi, W., Wong, F. K., & Wong, F. K. (2016). Evaluating the effectiveness and practicality of a cooling vest across four industries in Hong Kong. *Facilities*, 34(9/10), 511-534.

- Chan, A. P. C., Yang, Y., Wong, D. P., Lam, E. W. M., & Li, Y. (2013). Factors affecting horticultural and cleaning workers' preference on cooling vests. *Building and environment*, 66, 181-189.
- Chan, A. P., Wong, F. K., Wong, D. P., Lam, E. W., & Yi, W. (2012). Determining an optimal recovery time after exercising to exhaustion in a controlled climatic environment: Application to construction works. *Building and Environment*, 56, 28-37.
- Choi, J. W., Kim, M. J., & Lee, J. Y. (2008). Alleviation of Heat Strain by Cooling Different Body Areas during Red Pepper Harvest Work at WBGT 33 °C. *Industrial health*, 46(6), 620-628.
- Chou, C., Tochihara, Y., & Kim, T. (2008). Physiological and subjective responses to cooling devices on firefighting protective clothing. *European journal of applied physiology*, 104(2), 369-374.
- Chudecka, M., & Lubkowska, A. (2016). Thermal imaging of body surface temperature distribution in women with anorexia nervosa. *European Eating Disorders Review*, 24(1), 57-61.
- Climator Sweden AB, Available at: <http://climator.com/produktdatablad/> (accessed 18 July 2017).
- Colin, J., Timbal, J., Houdas, Y., Boutelier, C., & Guieu, J. D. (1971). Computation of mean body temperature from rectal and skin temperatures. *Journal of Applied Physiology*, 31(3), 484-489.
- Cotter, J. D., & Taylor, N. A. (2005). The distribution of cutaneous sudomotor and alliesthesial thermosensitivity in mildly heat - stressed humans: an open-loop approach. *The Journal of physiology*, 565(1), 335-345.
- Danielsson, U. (1996). Convection coefficients in clothing air layers. Doctoral Thesis. The Royal Institute of Technology, Stockholm, Sweden.
- Datta, S. R., & Ramanathan, N. L. (1971). Ergonomic comparison of seven modes of carrying loads on the horizontal plane. *Ergonomics*, 14(2), 269-278.
- Dorman, L. E., & Havenith, G. (2007). Effects of simulated clothing weight distribution on metabolic rate.
- Dorman, L. E., & Havenith, G. (2009). The effects of protective clothing on energy consumption during different activities. *European journal of applied physiology*, 105(3), 463-470.
- Dotti, F., Ferri, A., Moncalero, M., & Colonna, M. (2016). Thermo-physiological comfort of soft-shell back protectors under controlled environmental conditions. *Applied ergonomics*, 56, 144-152.
- Elson, J., & Eckels, S. (2015). An objective method for screening and selecting personal cooling systems based on cooling properties. *Applied ergonomics*, 48, 33-41.
- Farid, M. M., Khudhair, A. M., Razack, S. A. K., & Al-Hallaj, S. (2004). A review on phase change energy storage: materials and applications. *Energy conversion and management*, 45(9), 1597-1615.

- Fiala, D., Havenith, G., Bröde, P., Kampmann, B., & Jendritzky, G. (2012). UTCI-Fiala multi-node model of human heat transfer and temperature regulation. *International journal of biometeorology*, 56(3), 429-441.
- Fu, G. (1995). A transient, 3-D mathematical thermal model for the clothed human. KSU, Dissertation.
- Gao, C., Kuklane, K., Wang, F., & Holmér, I. (2012). Personal cooling with phase change materials to improve thermal comfort from a heat wave perspective. *Indoor air*, 22(6), 523-530.
- Gao, C., Kuklane, K., & Holmér, I. (2011). Cooling vests with phase change materials: the effects of melting temperature on heat strain alleviation in an extremely hot environment. *European journal of applied physiology*, 111(6), 1207-1216.
- Gao, C., Kuklane, K., & Holmér, I. (2010). Cooling vests with phase change material packs: the effects of temperature gradient, mass and covering area. *Ergonomics*, 53(5), 716-723.
- Ghaddar, N., Ghali, K., & Chehaitly, S. (2011). Assessing thermal comfort of active people in transitional spaces in presence of air movement. *Energy and Buildings*, 43(10), 2832-2842.
- Ghaddar, N., Ghali, K., & Othmani, M. (2010). Effect of moisture transport on mixed convection in vertical annulus of a heated clothed vertical wet cylinder in uniform cross wind. In *Proceedings of 14th international heat transfer conference (IHTC14)* (pp. 7-13).
- Ghali, K., Othmani, M., Jreije, B., & Ghaddar, N. (2009). Simplified heat transport model of a wind-permeable clothed cylinder subject to swinging motion. *Textile Research Journal*, 79(11), 1043-1055.
- Givoni, B., & Goldman, R. F. (1971). Predicting metabolic energy cost. *Journal of Applied Physiology*, 30(3), 429-433.
- Glass, S., Dwyer, G. B., & American College of Sports Medicine (Eds.). (2007). *ACSM'S metabolic calculations handbook*. Lippincott Williams & Wilkins.
- Haldane, J. S. (1905). The influence of high air temperatures No. I. *Epidemiology & Infection*, 5(4), 494-513.
- Hamdan, H., Ghaddar, N., Ouahrani, D., Ghali, K., & Itani, M. (2016). PCM cooling vest for improving thermal comfort in hot environment. *International Journal of Thermal Sciences*, 102, 154-167.
- Hatoum, O., Ghaddar, N., Ghali, K., & Ismail, N. (2017). Experimental and numerical study of back-cooling car-seat system using embedded heat pipes to improve passenger's comfort. *Energy Conversion and Management*, 144, 123-131.
- Haugan, B., Langerud, A. K., Kalvøy, H., Frøslie, K. F., Riise, E., & Kapstad, H. (2012). Can we trust the new generation of infrared tympanic thermometers in clinical practice?. *Journal of clinical nursing*, 22(5-6), 698-709.
- Havenith, G., Fogarty, A., Bartlett, R., Smith, C. J., & Ventenat, V. (2008). Male and female upper body sweat distribution during running measured with technical absorbents. *European journal of applied physiology*, 104(2), 245-255.
- He, Y., Li, N., He, M., & He, D. (2017). Using radiant cooling desk for maintaining comfort in hot environment. *Energy and Buildings*, 145, 144-154.

- Hearle, J. W., & Morton, W. E. (2008). *Physical properties of textile fibres*. Elsevier.
- Heller, M. A., & Schiff, W. (1991). Conclusions: The future of touch. *The psychology of touch*, 327-337.
- Herrmann, F., Prose, P. H., Sulzberger, M. B., Mandol, L., Medoff, G., & Roth, L. (1952). Studies on sweating: V. Studies of quantity and distribution of thermogenic sweat delivery to the skin. *Journal of Investigative Dermatology*, 18(1), 71-86.
- Holmér, I., Kuklane, K., & Gao, C. (2006). Test of firefighter's turnout gear in hot and humid air exposure. *International journal of occupational safety and ergonomics*, 12(3), 297-305.
- Holmér, I., & Nilsson, H. (1995). Heated manikins as a tool for evaluating clothing. *The Annals of Occupational Hygiene*, 39(6), 809-818.
- Holopainen, R. (2012). *A human thermal model for improved thermal comfort*. VTT Technical Research Centre of Finland.
- House, J. R., Lunt, H. C., Taylor, R., Milligan, G., Lyons, J. A., & House, C. M. (2012). The impact of a phase-change cooling vest on heat strain and the effect of different cooling pack melting temperatures. *European journal of applied physiology*, 113(5), 1223-1231.
- Houshyar, S., Padhye, R., Troynikov, O., Nayak, R., & Ranjan, S. (2015). Evaluation and improvement of thermo-physiological comfort properties of firefighters' protective clothing containing super absorbent materials. *The Journal of The Textile Institute*, 106(12), 1394-1402.
- Huizenga, C., Hui, Z., & Arens, E. (2001). A model of human physiology and comfort for assessing complex thermal environments. *Building and Environment*, 36(6), 691-699.
- Hyland, R. W., & Wexler, A. (1983). Formulations for the thermodynamic properties of the saturated phases of H<sub>2</sub>O from 173.15 K to 473.15 K. *ASHRAE transactions*, 89, 500-519.
- Ilmarinen, R., Lindholm, H., Koivistoinen, K., & Helistén, P. (2004). Physiological evaluation of chemical protective suit systems (CPSS) in hot conditions. *International Journal of Occupational Safety and Ergonomics*, 10(3), 215-226.
- Itani, M., Ghaddar, N., Ghali, K., Ouahrani, D., & Chakroun, W. (2017a). Cooling vest with optimized PCM arrangement targeting torso sensitive areas that trigger comfort when cooled for improving human comfort in hot conditions. *Energy and Buildings*, 139, 417-425.
- Itani, M., Ghaddar, N., & Ghali, K. (2017b). Innovative PCM-desiccant packet to provide dry microclimate and improve performance of cooling vest in hot environment. *Energy Conversion and Management*, 140, 218-227.
- Itani, M., Ghaddar, N., Ouahrani, D., Ghali, K., & Khater, B. (2017c). An Optimal Two-Bout Strategy with Phase Change Material Cooling Vests to Improve Comfort in Hot Environment. *Journal of Thermal Biology*, 72, 10-25.
- Itani, M., Ouahrani, D., Ghaddar, N., Ghali, K., & Chakroun, W. (2016). The effect of PCM placement on torso cooling vest for an active human in hot environment. *Building and Environment*, 107, 29-42.

- ISO 5151 (2010). Non-ducted air conditioners and heat pumps - Testing and rating for performance ISO 5151:2010(E), International Standards Organization, Geneva, Switzerland, 2010.
- ISO 5084 (1996). Textiles–determination of thickness of textiles and textile products.
- ISO 7143 (1989). Hot environments, Estimation of heat stress on working man, based on the WBGT-index (wet bulb globe temperature) ISO 7243:1989. ISO Geneva, Switzerland.
- ISO 3801 (1977). Textiles–woven fabrics – determination of mass per unit length and mass per unit area.
- Jones, B. W., Ogawa, Y. (1993). Transient interaction between the human and the thermal environment. *ASHRAE Trans.*, 98(1), 189-195.
- Kampmann, B., & Bröde, P. (2015). Metabolic costs of physiological heat stress responses-Q 10 coefficients relating oxygen consumption to body temperature. In *Extreme Physiology & Medicine*, 4, A103. BioMed Central.
- Karaki, W., Ghaddar, N., Ghali, K., Kuklane, K., Holmér, I., & Vanggaard, L. (2013). Human thermal response with improved AVA modeling of the digits. *International Journal of Thermal Sciences*, 67, 41-52.
- Kjellstrom, T., Kovats, R. S., Lloyd, S. J., Holt, T., & Tol, R. S. (2009). The direct impact of climate change on regional labor productivity. *Archives of Environmental & Occupational Health*, 64(4), 217-227.
- Kosonen, R., & Tan, F. (2004). Assessment of productivity loss in air-conditioned buildings using PMV index. *Energy and Buildings*, 36(10), 987-993.
- Lai, D., Wei, F., Lu, Y., & Wang, F. (2017). Evaluation of a hybrid personal cooling system using a manikin operated in constant temperature mode and thermoregulatory model control mode in warm conditions. *Textile Research Journal*, 87(1), 46-56.
- Lloyd, R., & Cooke, C. B. (2000). The oxygen consumption with unloaded walking and load carriage using two different backpack designs. *European Journal of Applied Physiology*, 81(6), 486-492.
- Lundgren, K., Kuklane, K., Gao, C., & Holmer, I. (2013). Effects of heat stress on working populations when facing climate change. *Industrial health*, 51(1), 3-15.
- Marks, S. B. (1983). The effect of crystal size on the thermal energy storage capacity of thickened Glauber's salt. *Solar Energy*, 30(1), 45-49.
- Marks, S. B. (1982). U.S. Patent No. 4,349,446. Washington, DC: U.S. Patent and Trademark Office.
- Marks, S. (1980). An investigation of the thermal energy storage capacity of Glauber's salt with respect to thermal cycling. *Solar Energy*, 25(3), 255-258.
- McCullough, E. A. (1989). A data base for determining the evaporative resistance of clothing. *ASHRAE Trans.*, 95, 316-328.
- McCullough, E. A., Jones, B. W., & Huck, J. (1985). A comprehensive data base for estimating clothing insulation. *Ashrae Trans*, 91(2), 29-47.

- McNall, P. E., Jaax, J., Rohles, F. H., Nevins, R. G., & Springer, W. (1967). Thermal comfort (thermally neutral) conditions for three levels of activity. *ASHRAE transactions*, 73(1), 1-3.
- Miller, V. S., & Bates, G. P. (2007). The thermal work limit is a simple reliable heat index for the protection of workers in thermally stressful environments. *Annals of occupational hygiene*, 51(6), 553-561.
- Mondal, S. (2008). Phase change materials for smart textiles—An overview. *Applied Thermal Engineering*, 28(11), 1536-1550.
- Nakamura, M., Yoda, T., Crawshaw, L. I., Kasuga, M., Uchida, Y., Tokizawa, K., Nagashima, K., & Kanosue, K. (2013). Relative importance of different surface regions for thermal comfort in humans. *European journal of applied physiology*, 113(1), 63-76.
- Nakamura, M., Yoda, T., Crawshaw, L. I., Yasuhara, S., Saito, Y., Kasuga, M., Nagashima, K., & Kanosue, K. (2008). Regional differences in temperature sensation and thermal comfort in humans. *Journal of applied physiology*, 105(6), 1897-1906.
- Nakayoshi, M., Kanda, M., Shi, R., & de Dear, R. (2014). Outdoor thermal physiology along human pathways: a study using a wearable measurement system. *International journal of biometeorology*, 59(5), 503-515.
- Ouahrani, D., Itani, M., Ghaddar, N., Ghali, K., & Khater, B. (2017). Experimental study on using PCMs of different melting temperatures in one cooling vest to reduce its weight and improve comfort. *Energy and Buildings*, 155, 533-545.
- Pallubinsky, H., Schellen, L., Rieswijk, T. A., Breukel, C. M. G. A. M., Kingma, B. R. M., & van Marken Lichtenbelt, W. D. (2016). Local cooling in a warm environment. *Energy and Buildings*, 113, 15-22.
- Pan, N., & Gibson, P. (Eds.). (2006). *Thermal and moisture transport in fibrous materials*. Woodhead Publishing.
- Pesaran, A. A., & Mills, A. F. (1987). Moisture transport in silica gel packed beds—I. Theoretical study. *International Journal of Heat and Mass Transfer*, 30(6), 1037-1049.
- Pokorný, J., Fišer, J., Fojtlín, M., Kopečková, B., Toma, R., Slabotínský, J., & Jícha, M. (2017). Verification of Fiala-based human thermophysiological model and its application to protective clothing under high metabolic rates. *Building and Environment*, 126, 13-26.
- Ramanathan, N. L. (1964). A new weighting system for mean surface temperature of the human body. *Journal of applied physiology*, 19(3), 531-533.
- Randall, W. C. (1946). Quantitation and regional distribution of sweat glands in man. *Journal of Clinical Investigation*, 25(5), 761.
- Reinertsen, R. E., Færevik, H., Holbø, K., Nesbakken, R., Reitan, J., Røyset, A., & Suong Le Thi, M. (2008). Optimizing the performance of phase-change materials in personal protective clothing systems. *International Journal of Occupational Safety and Ergonomics*, 14(1), 43-53.
- Rubitherm Technologies GmbH, Available at: <https://www.rubitherm.eu/en/productCategories.html> (accessed 18 July 2017).

- Salloum, M., Ghaddar, N., & Ghali, K. (2007). A new transient bioheat model of the human body and its integration to clothing models. *International journal of thermal sciences*, 46(4), 371-384.
- Sarier, N., & Onder, E. (2012). Organic phase change materials and their textile applications: an overview. *Thermochimica Acta*, 540, 7-60.
- Schlader, Z. J., Stannard, S. R., & Mündel, T. (2010). Human thermoregulatory behavior during rest and exercise—a prospective review. *Physiology & behavior*, 99(3), 269-275.
- Sharma, S. D., & Sagara, K. (2005). Latent heat storage materials and systems: a review. *International Journal of Green Energy*, 2(1), 1-56.
- Smith, C. J., & Havenith, G. (2011). Body mapping of sweating patterns in male athletes in mild exercise-induced hyperthermia. *European journal of applied physiology*, 111(7), 1391-1404.
- Snook, S. H., & Ciriello, V. M. (1974). The effects of heat stress on manual handling tasks. *The American Industrial Hygiene Association Journal*, 35(11), 681-685.
- Song, W., & Wang, F. (2016). The hybrid personal cooling system (PCS) could effectively reduce the heat strain while exercising in a hot and moderate humid environment. *Ergonomics*, 59(8), 1009-1018.
- Stevens, J. C. (1979). Variation of cold sensitivity over the body surface. *Sensory processes*, 3(4), 317.
- Swedish Emergency & Disaster Equipment AB, Available at: <http://www.swedeproducts.se/econtent/140> (accessed 21 July 2017).
- Teappcm, Available at: <http://www.teappcm.com/> (accessed 18 July 2017).
- Testfabrics.  
<http://www.testfabrics.com/products.php?catID1=TWpBPQ&%3BcatID2=1>  
 (accessed 04 January 2017).
- Tyler, C. J., Sunderland, C., & Cheung, S. S. (2013). The effect of cooling prior to and during exercise on exercise performance and capacity in the heat: a meta-analysis. *Br J Sports Med*, bjsports-2012.
- van Marken Lichtenbelt, W. D., Daanen, H. A., Wouters, L., Fronczek, R., Raymann, R. J., Severens, N. M., & Van Someren, E. J. (2006). Evaluation of wireless determination of skin temperature using iButtons. *Physiology & behavior*, 88(4), 489-497.
- Wang, H., & Hu, S. (2016). Experimental study on thermal sensation of people in moderate activities. *Building and Environment*, 100, 127-134.
- Webster, J., Holland, E. J., Sleivert, G., Laing, R. M., & Niven, B. E. (2005). A light-weight cooling vest enhances performance of athletes in the heat. *Ergonomics*, 48(7), 821-837.
- Weng, W. G., Han, X. F., & Fu, M. (2014). An extended multi-segmented human bioheat model for high temperature environments. *International Journal of Heat and Mass Transfer*, 75, 504-513.
- Wong, D. P. L., Chung, J. W. Y., Chan, A. P. C., Wong, F. K. W., & Yi, W. (2014). Comparing the physiological and perceptual responses of construction workers

- (bar benders and bar fixers) in a hot environment. *Applied ergonomics*, 45(6), 1705-1711.
- Yang, J., Weng, W., & Zhang, B. (2014). Experimental and numerical study of physiological responses in hot environments. *Journal of thermal biology*, 45, 54-61.
- Yazdi, M. M., Sheikhzadeh, M., & Chavoshi, S. E. (2015). Modeling the performance of a PCM cooling vest considering its side effects. *International Journal of Clothing Science and Technology*, 27(4), 573-586.
- Yazdi, M. M., & Sheikhzadeh, M. (2014). Personal cooling garments: a review. *The Journal of The Textile Institute*, 105(12), 1231-1250.
- Yi, W., Zhao, Y., Chan, A. P., & Lam, E. W. (2017). Optimal cooling intervention for construction workers in a hot and humid environment. *Building and Environment*, 118, 91-100.
- Yi, W., & Chan, A. P. (2013). Optimizing work–rest schedule for construction rebar workers in hot and humid environment. *Building and environment*, 61, 104-113.
- Young, A. J., Sawka, M. N., Epstein, Y., Decristofano, B. A. R. R. Y., & Pandolf, K. B. (1987). Cooling different body surfaces during upper and lower body exercise. *Journal of Applied Physiology*, 63(3), 1218-1223.
- Zalba, B., Marín, J. M., Cabeza, L. F., & Mehling, H. (2003). Review on thermal energy storage with phase change: materials, heat transfer analysis and applications. *Applied thermal engineering*, 23(3), 251-283.
- Zander, K. K., Botzen, W. J., Oppermann, E., Kjellstrom, T., & Garnett, S. T. (2015). Heat stress causes substantial labour productivity loss in Australia. *Nature Climate Change*, 5(7), 647-651.
- Zhang, H., Arens, E., Huizenga, C., & Han, T. (2010). Thermal sensation and comfort models for non-uniform and transient environments, part III: Whole-body sensation and comfort. *Building and Environment*, 45(2), 399-410.
- Zhang, H., Huizenga, C., Arens, E., & Wang, D. (2004). Thermal sensation and comfort in transient non-uniform thermal environments. *European journal of applied physiology*, 92(6), 728-733.
- Zhang, H. (2003). Human thermal sensation and comfort in transient and non-uniform thermal environments. Center for the built environment.
- Zhao, M., Gao, C., Wang, F., Kuklane, K., Holmér, I., & Li, J. (2012). The torso cooling of vests incorporated with phase change materials: a sweat evaporation perspective. *Textile Research Journal*, 83(4), 418-425.



